Overview of the MOSAiC expedition: Ecosystem

Allison A. Fong, Clara J. M. Hoppe*, Nicole Aberle, Carin J. Ashjian, Philipp Assmy, Youcheng Bai, Dorothee C. E. Bakker, John Paul Balmonte, Kevin R. Barry, Stefan Bertilsson, William Boulton, Jeff Bowman, Deborah Bozzato, Gunnar Bratbak, Moritz Buck, Robert G. Campbell, Giulia Castellani, Emelia J. Chamberlain, Jianfang Chen, Melissa Chierici, Astrid Cornils, Jessie M. Creamean, Ellen Damm, Klaus Dethloff, Elise S. Droste, Oliver Ebenhöh, Sarah Lena Eggers, Anja Engel, Hauke Flores, Agneta Fransson, Stefan Frickenhaus, Jessie Gardner, Cecilia E. Gelfman, Mats A. Granskog, Martin Graeve, Charlotte Havermans, Céline Heuzé, Nicole Hildebrandt, Thomas C. J. Hill, Mario Hoppema, Antonia Immerz, Haiyan Jin, Boris Koch, Xianyu Kong, Alexandra Kraberg, Musheng Lan, Benjamin A. Lange, Aud Larsen, Benoit Lebreton, Eva Leu, Brice Loose, Wieslaw Maslowski, Camille Mavis, Katja Metfies, Thomas Mock, Oliver Müller, Marcel Nicolaus, Barbara Niehoff, Daiki Nomura, Eva-Maria Nöthig, Marc Oggier, Ellen Oldenburg, Lasse Mork Olsen, Ilka Peeken, Donald K. Perovich, Ovidiu Popa, Benjamin Rabe, Jian Ren, Markus Rex, Anette Rinke, Sebastian Rokitta, Björn Rost, Serdar Sakinan, Evgenii Salganik, Fokje L. Schaafsma, Hendrik Schäfer, Katrin Schmidt, Katyanne M. Shoemaker, Matthew D. Shupe, Pauline Snoeijs-Leijonmalm, Jacqueline Stefels, Anders Svenson, Ran Tao, Sinhué Torres-Valdés, Anders Torstensson, Andrew Toseland Adam Ulfsbo, Maria A. Van Leeuwe, Martina Vortkamp, Alison L. Webb, Rolf R. Gradinger

see Author Information table for author affiliations, ORCID IDs etc.

* corresponding author (email: Clara.Hoppe@awi.de)

This manuscript is a non-peer reviewed preprint submitted to EarthArXiv. It has been submitted for publication to Elementa: Science of the Anthropocene and is currently under consideration.

Full Name	Email	ORCID	Affiliation
Fong, Allison A.	allison.fong@awi.de	0000-0002-3779-9624	Alfred-Wegener-Institute - Helmholtzzentrum für Polar- und Meeresforschung
Hoppe, Clara Jule Marie	choppe@awi.de	0000-0002-2509-0546	Alfred-Wegener-Institute - Helmholtzzentrum für Polar- und Meeresforschung
Aberle, Nicole	nicole.aberle-malzahn@ntnu.no	0000-0003-3254-5710	Department of Biology, Norwegian University of Science and Technology (NTNU), Trondheim, Norway
Ashjian, Carin J.	cashjian@whoi.edu	0000-0002-7894-1519	Woods Hole Oceanographic Institution, USA
Assmy, Philipp	philipp.assmy@npolar.no	0000-0002-8241-7541	Norwegian Polar Institute, Fram Centre, Tromsø, Norway
Bai, Youcheng	ycbai@sio.org.cn	0000-0003-1116-7319	Key Laboratory of Marine Ecosystem Dynamics, Second Institute of Oceanography, Ministry of Natural Resources, Hangzhou, China
Bakker, Dorothee C. E.	d.bakker@uea.ac.uk	0000-0001-9234-5337	Centre for Ocean and Atmospheric Sciences, University of East Anglia, Norwich, UK
Balmonte, John Paul	jpb422@lehigh.edu	0000-0001-5571-4893	Stockholm University, Department of Ecology, Environment and Plant Sciences, Stockholm, Sweden
Barry, Kevin R.	kevin.barry@colostate.edu	0000-0002-1896-1921	Department of Atmospheric Science, Colorado State University
Bertilsson, Stefan	stefan.bertilsson@slu.se	0000-0002-4265-1835	Swedish University of Agricultural Sciences, Department of Aquatic Sciences and Assessment, Uppsala, Sweden
Boulton, William	W.Boulton@uea.ac.uk	0000-0002-8258-4673	School of Computing Sciences, University of East Anglia, Norwich, United Kingdom
Bowman, Jeff	jsbowman@ucsd.edu	0000-0002-8811-6280	Scripps Institution of Oceanography, University of California San Diego, USA
Bozzato, Deborah	d.bozzato@rug.nl	0000-0002-6004-1096	Groningen Institute for Evolutionary Life Sciences, University of Groningen, Groningen, The Netherlands
Bratbak, Gunnar	gunnar.bratbak@uib.no	0000-0001-8388-4945	University of Bergen, Department of Biological Sciences, Bergen, Norway
Buck, Moritz	moritz.buck@slu.se	0000-0001-6632-5324	Swedish University of Agricultural Sciences, Department of Aquatic Sciences and Assessment, Uppsala, Sweden
Campbell, Robert G.	rgcampbell@uri.edu	0000-0002-3710-9750	University of Rhode Island, Graduate School of Oceanography, USA
Castellani, Giulia	giulia.castellani@awi.de	0000-0001-6151-015X	Alfred-Wegener-Institute - Helmholtzzentrum für Polar- und Meeresforschung
Chamberlain, Emelia J.	echamber@ucsd.edu	0000-0003-2218-3488	Scripps Institution of Oceanography, University of California San Diego, USA
Chen, Jianfang	jfchen@sio.org.cn	0000-0002-6521-0266	Key Laboratory of Marine Ecosystem Dynamics, Second Institute of Oceanography, Ministry of Natural Resources, Hangzhou, China
Chierici,Melissa	melissa.chierici@hi.no	0000-0003-0222-2101	Institute of Marine Research, Tromsø, Norway
Cornils, Astrid	astrid.cornils@awi.de	0000-0003-4536-9015	Alfred-Wegener-Institut Helmholtz-Zentrum für Polar- und Meeresforschung
Creamean, Jessie M.	jessie.creamean@colostate.edu	0000-0003-3819-5600	Department of Atmospheric Science, Colorado State University
Damm, Ellen	ellen.damm@awi.de	0000-0002-1487-1283	Alfred-Wegener-Institut Helmholtz-Zentrum für Polar- und Meeresforschung
Dethloff, Klaus	Klaus.Dethloff@awi.de	0000-0003-4162-148X	Alfred-Wegener-Institut Helmholtz-Zentrum für Polar- und Meeresforschung
Droste, Elise S.	elise.droste@awi.de	0000-0002-3467-0083	Centre for Ocean and Atmospheric Sciences, School of Environmental Sciences, University of East Anglia, Norwich, UK
Ebenhöh, Oliver	oliver.ebenhoeh@hhu.de	0000-0002-7229-7398	Institute of Quantitative and Theoretical Biology, Heinrich-Heine University Düsseldorf, Düsseldorf, Germany
Eggers, Sarah Lena	lena.eggers@awi.de	0000-0001-6094-3201	Stockholm University, Department of Ecology, Environment and Plant Sciences, Stockholm, Sweden
Engel, Anja	aengel@geomar.de	0000-0002-1042-1955	GEOMAR Helmholtz Centre for Ocean Research, Kiel, Germany
Flores, Hauke	hauke.flores@awi.de	0000-0003-1617-5449	Alfred-Wegener-Institute - Helmholtzzentrum für Polar- und Meeresforschung
Fransson, Agneta	agneta.fransson@npolar.no	0000-0003-1403-2110	Norwegian Polar Institute, Fram Centre, Tromsø, Norway
Frickenhaus, Stephan	Stephan.Frickenhaus@awi.de	0000-0002-0356-9791	Alfred-Wegener-Institut Helmholtz-Zentrum für Polar- und Meeresforschung
Gardner, Jessie	jessiegardner001@gmail.com	0000-0003-1730-023X	UiT The Arctic University of Norway
Gelfman, Cecilia E.	cgelfman@uri.edu	0000-0002-3523-5702	University of Rhode Island, Graduate School of Oceanography, USA
Granskog, Mats A.	mats.granskog@npolar.no	0000-0002-5035-4347	Norwegian Polar Institute, Fram Centre, Tromsø, Norway
Graeve, Martin	martin.graeve@awi.de	0000-0002-2294-1915	Alfred-Wegener-Institute - Helmholtzzentrum für Polar- und Meeresforschung
Havermans, Charlotte	Charlotte.Havermans@awi.de	0000-0002-1126-4074	Alfred-Wegener-Institute - Helmholtzzentrum für Polar- und Meeresforschung
Heuzé, Céline	celine.heuze@gu.se	0000-0002-8850-5868	Department of Earth Sciences, University of Gothenburg, Gothenburg, Sweden
Hildebrandt, Nicole	Nicole.Hildebrandt@awi.de	0000-0003-0555-3096	Alfred-Wegener-Institute - Helmholtzzentrum für Polar- und Meeresforschung
Hill, Thomas C. J.	thomas.hill@colostate.edu	0000-0002-5293-3959	Department of Atmospheric Science, Colorado State University

Hoppema, Mario	Mario.Hoppema@awi.de	0000-0002-2326-619X	Alfred-Wegener-Institut Helmholtz-Zentrum für Polar- und Meeresforschung, Bremerhaven
Immerz, Antonia	antonia.immerz@gmx.de	0000-0002-9859-3558	Alfred-Wegener-Institute - Helmholtzzentrum für Polar- und Meeresforschung
Jin, Haiyan	jinhaiyan@sio.org.cn	0000-0002-4965-2830	Key Laboratory of Marine Ecosystem Dynamics, Second Institute of Oceanography, Ministry of Natural Resources, Hangzhou, China
Koch, Boris	boris.koch@awi.de	0000-0002-8453-731X	Alfred-Wegener-Institute - Helmholtzzentrum für Polar- und Meeresforschung
Kong, Xianyu	xianyu.kong@awi.de	0000-0002-7366-5180	Alfred-Wegener-Institute - Helmholtzzentrum für Polar- und Meeresforschung
Kraberg, Alexandra	Alexandra.Kraberg@awi.de	0000-0003-2571-2074	Alfred-Wegener-Institute - Helmholtzzentrum für Polar- und Meeresforschung
Lan, Musheng	lanmusheng@pric.org.cn		Polar Research Institute of China, Shanghai
Lange, Benjamin A.	blange.sea.ice@gmail.com	0000-0003-4534-8978	Norwegian Polar Institute, Fram Centre, Tromsø, Norway
Larsen, Aud	aula@norceresearch.no	0000-0001-6927-5537	Environment and Climate Division, NORCE Norwegian Research Centre, 5008 Bergen, Norway
Lebreton, Benoit	benoit.lebreton@univ-lr.fr	0000-0001-8802-2287	Joint Research Unit Littoral, Environment and Societies (CNRS - University of La Rochelle)
Leu, Eva	eva.leu@akvaplan.niva.no	0000-0002-5328-3396	Akvaplan-niva, Tromsø, Norway
Loose, Brice	bloose@uri.edu	0000-0002-3002-4113	University of Rhode Island, Graduate School of Oceanography, USA
Maslowski, Wieslaw	maslowsk@nps.edu	0000-0002-5790-9229	Naval Postgrduate School
Mavis, Camille	camille.mavis@colostate.edu		Department of Atmospheric Science, Colorado State University
Metfies, Katja	Katja.Metfies@awi.de	0000-0003-3073-8033	Alfred-Wegener-Institute - Helmholtzzentrum für Polar- und Meeresforschung
Mock, Thomas	T.Mock@uea.ac.uk	0000-0001-9604-0362	School of Environmental Sciences, University of East Anglia, Norwich, United Kingdom
Müller, Oliver	oliver.muller@uib.no	0000-0001-5405-052X	University of Bergen, Department of Biological Sciences, Bergen, Norway
Nicolaus, Marcel	marcel.nicolaus@awi.de	0000-0003-0903-1746	Alfred-Wegener-Institut Helmholtz-Zentrum für Polar- und Meeresforschung
Niehoff, Barbara	barbara.niehoff@awi.de	0000-0002-7483-9373	Alfred-Wegener-Institut Helmholz center for Polar and Marine Research
Nomura, Daiki	daiki.nomura@fish.hokudai.ac.jp	0000-0003-3047-4023	Hokkaido Univeristy, Hakodate, Japan
Nöthig, Eva-Maria	eva-maria.noethig@awi.de	0000-0002-7527-7827	Alfred-Wegener-Institut Helmholtz-Zentrum für Polar- und Meeresforschung, Bremerhaven
Marc Oggier	moggier@alaska.edu	0000-0003-4679-1103	International Arctic Research Center, University of Alaska Fairbanks
Oldenburg, Ellen	ellen.oldenburg@hhu.de	0000-0002-0993-9247	Institute of Quantitative and Theoretical Biology, Heinrich-Heine University Düsseldorf, Düsseldorf, Germany
Olsen, Lasse Mork	lasse@aqua-kompetanse.no	0000-0003-1328-2687	University of Bergen, Department of Bioscience, Bergen, Norway
Peeken, Ilka	ilka.peeken@awi.de	0000-0003-1531-1664	Alfred-Wegener-Institute - Helmholtzzentrum für Polar- und Meeresforschung
Perovich, Donald K.	donald.k.perovich@dartmouth.ed	0000-0002-0576-0864	Dartmouth College, Hanover, NH, USA
Popa, Ovidiu	ovidiu.popa@hhu.de	0000-0003-4470-0378	Institute of Quantitative and Theoretical Biology, Heinrich-Heine University Düsseldorf, Düsseldorf, Germany
Rabe, Benjamin	benjamin.rabe@awi.de	0000-0001-5794-9856	Alfred-Wegener-Institut Helmholtz-Zentrum für Polar- und Meeresforschung
Ren, Jian	jian.ren@sio.org.cn	0000-0002-1889-5661	Key Laboratory of Marine Ecosystem Dynamics, Second Institute of Oceanography, Ministry of Natural Resources, Hangzhou, China
Rex, Markus	markus.rex@awi.de	0000-0001-7847-8221	Alfred-Wegener-Institut, Helmholtz-Zentrum für Polar- und Meeresforschung, Potsdam, Germany & University of Potsdam, Potsdam, Germany
Rinke, Anette	annette.rinke@awi.de	0000-0002-6685-9219	Alfred-Wegener-Institut, Helmholtz-Zentrum für Polar- und Meeresforschung, Potsdam, Germany
Rokitta, Sebastian	sebastian.rokitta@awi.de	0000-0002-7540-9033	Alfred-Wegener-Institute - Helmholtzzentrum für Polar- und Meeresforschung
Rost, Björn	bjoern.rost@awi.de	0000-0001-5452-5505	Alfred-Wegener-Institute - Helmholtzzentrum für Polar- und Meeresforschung
Sakinan, Serdar	serdar.sakinan@wur.nl	0000-0002-5651-2836	Wageningen Marine Research, IJmuiden, The Netherlands
Salganik, Evgenii	evgenii.salganik@npolar.no	0000-0001-8383-7815	Norwegian Polar Institute, Fram Centre, Tromsø, Norway
Schaafsma, Fokje L.	fokje.schaafsma@wur.nl	0000-0002-8945-2868	Wageningen Marine Research, Ankerpark 27, 1781 AG Den Helder, The Netherlands
Schäfer, H.	H.Schaefer@warwick.ac.uk	0000-0001-8450-7893	University of Warwick, School of Life Sciences
Schmidt, Katrin	katrin7schmidt@gmail.com	0000-0002-6488-623X	University of Plymouth, School of Geography, Earth and Environmental Sciences
Shoemaker, Katyanne M.	katyanne.shoemaker@noaa.gov	0000-0002-5129-2387	University of Rhode Island, Graduate School of Oceanography, USA

Shupe, Matthew D.	matthew.shupe@noaa.gov	0000-0002-0973-9982	Cooperative Institute for Research in Environmental Sciences, University of Colorado Boulder & NOAA Physical Sciences Laboratory, Boulder, CO; USA
Snoeijs-Leijonmalm, Pauline	pauline.snoeijs-leijonmalm@su.se	0000-0002-4544-2668	Stockholm University, Department of Ecology, Environment and Plant Sciences, Stockholm, Sweden
Stefels, J	j.stefels@rug.nl	0000-0001-9491-1611	University of Groningen, Groningen Institute of Evolutionary Life Sciences (GELifeS), Groningen, the Netherlands
Svenson, Anders	anders.svenson@slu.se		Swedish University of Agricultural Sciences, Lysekil, Sweden
Tao, Ran	ran.tao@awi.de	0000-0002-6690-9212	Alfred-Wegener-Institute - Helmholtzzentrum für Polar- und Meeresforschung
Torres-Valdés, Sinhué	sinhue.torres-valdes@awi.de	0000-0003-2749-4170	Alfred-Wegener-Institute - Helmholtzzentrum für Polar- und Meeresforschung
Torstensson, Anders	torstensson.anders@gmail.com	0000-0002-8283-656X	Stockholm University, Department of Ecology, Environment and Plant Sciences, Stockholm, Sweden
Toseland, Andrew	A.Toseland@uea.ac.uk	0000-0002-6513-956X	School of Environmental Sciences, University of East Anglia, Norwich, United Kingdom
Ulfsbo, Adam	adam.ulfsbo@gu.se	0000-0001-7550-7381	Department of Marine Sciences, University of Gothenburg, Gothenburg, Sweden
Van Leeuwe, Maria A.	m.a.van.leeuwe@rug.nl	0000-0002-9572-4700	University of Groningen, Groningen Institute of Evolutionary Life Sciences (GELifeS), Groningen, the Netherlands
Vortkamp, Martina	Martina.Vortkamp@awi.de		Alfred-Wegener-Institute - Helmholtzzentrum für Polar- und Meeresforschung
Webb, Alison Louise	alison.webb@york.ac.uk	0000-0003-1762-2060	University of Warwick, School of Life Sciences
Gradinger, Rolf R.	rolf.gradinger@uit.no	0000-0001-6035-3957	UiT The Arctic University of Norway

ABSTRACT

An international and interdisciplinary sea ice drift expedition, the 'The Multidisciplinary drifting Observatory for the Study of Arctic Climate' (MOSAiC), was conducted from October 2019 to September 2020. The aim of MOSAiC was to study the interconnected physical, chemical and biological characteristics and processes from the atmosphere to the deep sea of the central Arctic system. The ecosystem team addressed current knowledge gaps and explored unknown biological properties over a complete seasonal cycle focusing on three major research areas: biodiversity, biogeochemical cycles and linkages to the environment. In addition to the coverage of core properties along a complete seasonal cycle, dedicated projects covered specific processes and habitats, or organisms on higher taxonomic or temporal resolution. A wide range of sampling approaches from sampling, sea ice coring, lead sampling to CTD rosette-based water sampling, plankton nets, ROVs and acoustic buoys was applied to address the science objectives. Further, a wide range of process-related measurements to address e.g. productivity patterns, seasonal migrations and diversity shifts were conducted both in situ and onboard *RV Polarstern*. This paper provides a detailed overview of the sampling approaches used to address the three main science objectives. It highlights the core sampling program and provides examples of two habitat- or process-specific projects. First results presented include high biological activities in winter time and the discovery of biological hotspots in underexplored habitats. The unique interconnectivity of the coordinated sampling efforts also revealed insights into cross-disciplinary interactions like the impact of biota on Arctic cloud formation. This overview further presents both lessons learned from conducting such a demanding field campaign and an outlook on spin-off projects to be conducted over the next years.

1. INTRODUCTION

1.1. Motivation

The Multidisciplinary drifting Observatory for the Study of Arctic Climate (MOSAiC) expedition provides unique scientific opportunities to fundamentally understand the interlinked physical, chemical, and biological systems in the central Arctic Ocean. The science program was shaped over nearly a decade and provides a foundation to create new and important knowledge regarding the functioning of the Arctic ecosystem within the context of the coupled Arctic climate system. Five closely cooperating science teams were formed to develop and execute the integrated science plan, focusing on atmosphere, sea ice, ocean, ecosystem and biogeochemistry. This paper provides an overview of the multiple facets of ecosystem-related research to highlight the interlinked research activities at multiple trophic levels in relation to the environment. Within the MOSAiC ecosystem team (termed *ECO team* in the following), a total of 25 institutions across 15 nations contributed to generating the field observations and measurements as part of the research program. Similar overviews are available for other MOSAiC research topics, currently for sea ice physics, physical oceanography, and various aspects of the atmosphere (Nicolaus et al., 2022b; Rabe et al., 2022; Shupe et al., 2022), while an overview on biogeochemical research not covered in this article is forthcoming.

The integrated ecological observations and knowledge generated by the ECO team was specifically aimed at understanding seasonally-resolved processes on different scales. These are critical for future predictions related to climate change impacts on the Arctic system, including alterations to ecosystem structure and functioning (Intergovernmental Panel on Climate Change (IPCC), 2023). While the research is ongoing, new projects are emerging based on insights, data and collaborations.

Section 1 of this paper outlines the main ecological research objectives addressed via the MOSAiC ecosystem research, followed in the second section by a more detailed description of the scientific approaches and methods being used. The coordinated ecological research also included biogeochemical variables (e.g. macronutrient concentrations, seawater and ice carbonate chemistry, dissolved organic carbon) due to their close links to ecosystem processes. Example data sets provided in section 3 demonstrate what to expect in the forthcoming peer-reviewed publications. Lastly, section 4 provides insights into “lessons learned” and challenges when planning such a yearlong expedition and point towards some of the expected impacts that could arise from the compiled knowledge over the years to come.

1.2. The Central Arctic Ecosystem and its links to the environment

The Arctic Ocean harbors unique and diverse biological communities in all available habitats: sea ice, snow, seawater, atmosphere, and sediments. Although the Arctic Ocean was once considered a relatively species-poor region with limited biological activity, research in recent decades has revised this paradigm (Bluhm et al., 2011). For example, it is now known that there is high biodiversity in all habitats and high biological activity year-round, including in the winter season (Berge et al., 2015; Hobbs et al., 2020). Furthermore, the Arctic ecosystem is not easily generalized due to the particularly high spatio-temporal variability in biological, chemical, and physical processes (Bluhm et al., 2015). Arctic marine ecosystems have regionally varying complex community structures and activity patterns, largely driven by differences in abiotic factors like water temperature, depth, salinity, light, inorganic nutrients, and sea ice properties (Balmonte et al., 2018; Bluhm et al., 2018, 2015; Clement Kinney et al., 2023; Ershova et al., 2021; Polyakov et al., 2020). Other efforts to explore ecosystem-level research in the central Arctic include SHEBA (e.g., Ashjian et al., 2003; Sherr et al., 2003), the Circumpolar Flaw Lead study (Barber et al., 2015), N-ICE2015 (Assmy et al., 2017; Granskog et al., 2018), the Synoptic Arctic Survey (Snoeijs-Leijonmalm et al., 2022), Tara Arctic (Ibarbalz et al., 2023; Royo-Llonch et al., 2021), and the Russian ice drift studies (Melnikov, 1980). Yet, despite these valuable efforts, the seasonal cycle in the central Arctic remains understudied because the region is difficult to access in winter with thick and extensive sea ice cover and harsh conditions for work in the field. Remote sensing of biological properties is also limited by the ice-covered, seasonally dark and often cloud-covered Arctic (Babin et al., 2015). New comprehensive time series data are further needed to construct numerical models and test mechanistic hypotheses within the context of Earth System Models (e.g., CMIP5 and CMIP6 for the IPCC AR5 and 6, respectively; IPCC, 2023). Representations of the marine ecosystem are lacking or less advanced than other components of the Earth system within large-scale models. Therefore, MOSAiC research is a critically needed evaluation of the current state of the Arctic marine ecosystem, required to adjust our understanding to new ecosystem components, and improve our understanding of basic biological processes to enhance predictions of future system status.

The central deep Arctic Ocean is divided into four abyssal plains separated by the Lomonosov, Gakkel, and Alpha ridges. Even so, the upper water column (~ 1000 m) is contiguous with two major ice drift and ocean circulation patterns: the Transpolar Drift (TPD) System and the Beaufort Gyre. The MOSAiC field campaign was established on a sea-ice floe at the Siberian edge of the Amundsen Basin (Figure 1), close to the origin of the TPD. During the campaign, the floe drifted in the TPD across the central Arctic towards Fram Strait. Details regarding the sea ice conditions during MOSAiC are provided by Krumpen et al. (2020) and Nicolaus et al. (2022b). The hydrography in the central Arctic Ocean is characterized by a strong, permanent vertical salinity gradient (halocline). The upper surface mixed layer in the Amundsen Basin is characterized by low salinity and largely cold waters, being affected by river discharge, ice melt / freeze processes and Pacific inflow inside the

TPD (Rabe et al., 2022; Rudels and Carmack, 2022; Schulz et al., 2023a). South of the Amundsen Basin, as separated by the Gakkel ridge, surface waters of the Nansen Basin (Figure 1) are less influenced by the TPD. Here surface waters carry a stronger signal of Atlantic sourced water masses (Schulz et al., 2023b). Below the surface mixed layer lay warmer and more saline waters of Atlantic origin. The core of the Atlantic Water is warmest and saltiest north of Svalbard and close to the Barents-Kara Sea slope. In addition, modelling studies suggest that Atlantic water can advect biomass from phytoplankton blooms developed in open waters upstream under the sea ice into the eastern Arctic (In addition, modelling studies suggest that Atlantic water can advect biomass from phytoplankton blooms developed in open waters upstream under the sea ice into the eastern Arctic (Clement Kinney et al., 2023). It is modified once it enters the basins and circulates around the Arctic, mainly along the shelf slopes as a deep circulation loop (Rudels and Carmack, 2022), and over time, becomes colder, fresher, and is subducted deeper in the water column. The influence of these major water sources (i.e. TPD- vs Atlantic-influenced) on the central Arctic Ocean depends on circulation dynamics, which control the proportion, layering, and mixing of different source waters and their respective nutrient inventories. In surface waters of the central Arctic, nutrient concentrations are variable, but low relative to the Arctic shelf regions and deeper water masses (Bluhm et al., 2015; Randelhoff et al., 2020).

The strong vertical gradients in nutrient concentrations, and factors such as irradiance and other ocean physico-chemical parameters, structure the pelagic realm. Highly diverse communities of phytoplankton and sea ice algae (Poulin et al., 2011) contribute to the primary production in the central Arctic (Gosselin et al., 1997; Wiedmann et al., 2020). Both ice and pelagic algae have developed several successful strategies to overcome months without sufficient light for photosynthesis (Johnsen et al., 2020) and rapidly utilize the light returning after the Polar night (Hoppe, 2022; Kvernvik et al., 2018). Still, the overwintering strategies and modes of nutrition of several key groups and species remain poorly understood. Also, lower trophic herbivores and omnivores, like sea ice meiofauna (Ehrlich et al., 2020; Patrohay et al., 2022) or pelagic zooplankton (Ershova et al., 2021; Hop et al., 2021), have evolved life cycles and physiological adaptations that allow them to survive and successfully compete under these extreme conditions in the ice-covered central Arctic Ocean. The microbial network, involving diverse bacterial and archaeal communities (Boetius et al., 2015), drives the remineralization of organic matter in ice and water (Balmonte et al., 2018; Laurion et al., 1995; Wietz et al., 2021), which is a key process for supplying nutrients for algal growth. However, heterotrophic bacteria and algae can also compete for inorganic nitrogen resources (Fouilland et al., 2007).

Sea ice provides a unique habitat for diverse biota ranging from viruses to marine mammals and birds. It sustains its own food web driven by the productivity of sea ice algae, which has been reported to contribute up to 55% of total primary production in ice covered areas (Gosselin et al., 1997; Wiedmann et al., 2020). This production is channeled through ice-associated herbivores including copepods and amphipods, and fish (specifically Arctic/polar cod, *Boreogadus saida*). In fact, trophic marker studies have demonstrated that a substantial part of the organic matter from sea ice algae culminates in apex species like ringed and bearded seals, or Arctic birds (e.g. Carlyle et al., 2022; Kohlbach et al., 2016; Kunisch et al., 2021). Diversity in sea ice systems is high, including viruses, bacteria, over 1000 species of unicellular algae and protozoa (Poulin et al., 2011), and about 100 associated metazoan taxa living in the ice brine channel system or the bottom of the ice (Bluhm et al., 2018 and references within). Summer melt ponds and low-salinity meltwater accumulated in leads and under the ice are examples of unique habitats that can form, disappear, and be replenished again multiple times over relatively short time scales during parts of a seasonal cycle (Smith et al., 2023). Similarly, also under ice productivity can be high in ice covered regions: a recent high resolution biophysical modeling study has found that 63% of the total primary production in the central Arctic occurs in waters with ≥50% sea ice cover, and 41% of the total primary production in areas with ≥85% cover (Clement Kinney et al., 2020). While considerable information exists for some regions, seasons, and taxa, the majority of biological components in the ice and ocean have not been identified and quantified through a complete annual cycle, particularly in the high Arctic. Filling this knowledge gap by investigating the full range of trophic components from bacteria to metazoans and exploring their unknown connections has been an ambitious and challenging goal of MOSAiC ecosystem research.

The activities of and interactions between different taxonomic, functional, and trophic groups change in space and time. In the Arctic, the strong seasonality and high interannual variability in environmental conditions such as temperature, nutrient availability, and irradiance drive the ecosystem state, phenology, and functions (Ardyna and Arrigo, 2020; Kosobokova and Hirche, 2000; Leu et al., 2015). Climate change has already substantially altered the Arctic marine system through increased fractions of first-year ice, stronger and warmer inflow from the Atlantic and Pacific Oceans, freshening of the surface waters, later sea ice formation and earlier onset of melt (Ingvaldsen et al., 2021; Polyakov et al., 2020) with associated biological system responses. For instance, under-ice phytoplankton blooms, algal infiltration communities at the snow-ice interface, and shifts in biodiversity due to borealization are increasingly observed (Ardyna et al., 2020; Fernández-Méndez et al., 2018; Ingvaldsen et al., 2021). Different sensitivities to climate change drivers by various ecosystem components may cause mismatches between trophic levels, such as algae blooms occurring earlier than the zooplankton life stages depending on them as food (Søreide et al., 2010). Also, the shift from a dominance of a multi-year ice (MYI) or second-year ice (SYI) to a first-year ice (FYI) regime will likely impact sea ice biota; however, evidence for change is patchy due to the limited availability of sufficiently long time-series data (Campbell et al., 2022). Comparisons between FYI and MYI diversity of sea ice protists indicate substantially lower (by 39%) diversity in FYI compared to MYI (Hop et al., 2020). The diversity and presence of sea ice meiofauna taxa has also decreased, including the nearly complete absence of flatworms and nematodes in recent studies (Ehrlich et al., 2020). MYI might also act as a seed bank for sea ice algae and fauna for adjacent newly forming and growing FYI (Olsen et al., 2017). Sea ice biogeochemical cycles could be impacted, as FYI is typically saltier, with higher brine volume fractions creating more habitable space, and permeability resulting in higher fluxes within the ice, and increased nutrient supply (Tedesco et al., 2019). Beyond these structural and functional changes in the sea ice ecosystem itself, an alteration of the relative contribution of sea ice algae versus phytoplankton to overall annual primary production also has consequences for other ecosystem components, including through the often tight sympagic-pelagic and sympagic-benthic coupling processes (Rybakova et al., 2019; Wang et al., 2015; Wiedmann et al., 2020).

Biological processes in ice and seawater are not only relevant for the marine ecosystem, but impact the entire Arctic System. These processes are linked to physical processes in the atmosphere, ice, and ocean through various coupled processes and feedback mechanisms (Figure 2). Whereas the strong interdependence between the seasonally changing sea ice properties and ocean-atmosphere physics is widely recognized (Shupe et al., 2022), the tightly coupled interaction between the sea ice and the biology and chemistry of the ocean underneath is not well understood and, as a consequence, often neglected in numerical models. Biological activity affects the cycling and transformation of inorganic molecules and organic matter, and exerts strong controls on the cycling of climate-active gases such as carbon dioxide (CO_2), methane (CH_4), nitrous oxide (N_2O), and dimethyl sulfide (DMS) in the ocean and ice, as well as across the atmosphere-ice-ocean interfaces (Falkowski et al., 1998). For example, CO_2 concentrations are controlled by a range of chemical and biological processes including organic production, remineralization, gas exchange, and inorganic calcium carbonate precipitation within sea ice and dissolution in sea ice meltwater (Angelopoulos et al., 2022; Fransson et al., 2011; Miller et al., 2011; Nomura et al., 2018; Rysgaard et al., 2012, 2007) leading to seasonally varying air-sea-ice CO_2 exchange (e.g., Fransson et al., 2013; Mo et al., 2022). Seasonal sea ice melt decreases the partial pressure of CO_2 (pCO_2) of the stratified Arctic surface waters through dilution, ikaite dissolution, and supporting phytoplankton blooms near the surface (Fransson et al., 2017). In recent years, enhanced sea ice melt has exposed these low pCO_2 surface waters to high atmospheric pCO_2 levels, thereby promoting CO_2 uptake from the atmosphere (Qi et al., 2022). Over longer periods of time, the enhanced CO_2 uptake decreases the surface waters' pH buffering capacity and promoting vulnerability to ocean acidification (Qi et al., 2022). At the same time, the associated decreased buffer capacity for CO_2 promotes ocean acidification. Storm events in different seasons can impact air-sea CO_2 exchange by altering the surface layer pCO_2 through wind-induced mixing with subsurface water and by creating leads where direct air-sea gas exchange can occur (Fransson et al., 2017). For sea ice itself, rising temperatures and younger sea ice promote an increase in the brine volume fraction, which in turn enhances the transfer of gases and substances across gas-water interfaces within sea ice and between the sea ice and atmosphere (Nomura et al., 2018).

Marine biological processes can impact climate relevant processes through linkages beyond production cycles of climate-relevant gases. Biogenic compounds that become aerosol particles can become airborne through the air-water interfaces of the Arctic and serve as cloud condensation nuclei (CCN) and ice nucleating particles (INPs) in the atmosphere, affecting clouds and the radiative balance of the system (Creamean et al., 2022). This, in turn, may feedback on productivity through modulation of the light available to fuel primary production (Kauko et al., 2017). High standing stocks of organisms in the sea ice and water column also change the energy budget and heat uptake of these components as they increase the absorption of shortwave radiation, thereby affecting the freeze and melt cycles of their own habitat (Taskjelle et al., 2017; Zeebe et al., 1996). Also, sea ice microstructural properties relevant for gas exchange can be modified through ice algal production of extracellular polymeric substances (Krembs et al., 2011).

1.3. The mission of MOSAiC ecosystem studies

The MOSAiC sampling program used existing knowledge on ecosystem-relevant processes and components to fill major gaps in current knowledge and explore so far unknown links. The integrated MOSAiC ecosystem research program combined year-round consistent measurements of specific core properties (Table 1) with embedded individual research projects (supplementary Table S1) and opportunistic sampling. The core program included an extensive suite of biological and chemical components sampled from the water column, and undeformed level FYI and SYI. The aim of the core measurement program was to provide a consistent and continuous backbone of key measurements over the drift period, which would allow to link different integrative and complementary process studies. The project-specific measurements either provided higher temporal or spatial resolution beyond the weekly sampling program, or focused on processes or habitats that were not part of the core parameter time-series. Our investigations relied on a combination of traditional tools and more recently developed technologies and cross-cutting approaches. This combined approach facilitated linkages to previous studies, while providing new knowledge into the seasonality of high Arctic biological and biogeochemical processes at unprecedented temporal resolution. The work of the ECO team is focused on three fundamental and essential research questions: 1) Which species are present in the Arctic Ocean (WHO, i.e. Biodiversity)? 2) How do fluxes of energy and matter flow through food webs and habitats (HOW, i.e. Ecosystem functioning)? And 3) Why do physical and chemical parameters exert control on species distribution and activities and vice versa (WHY, i.e. linkages with the environment)?

Biodiversity: The program was designed to capture a full seasonal sampling of ice and seawater habitats, including the dark season, with a wide range of established and innovative tools to achieve the most complete species inventory for ice and pelagic biota of the Central Arctic.

Ecosystem functioning: The flow of matter and energy in ice and seawater substantially changes with time, driven by the strong seasonality of environmental variables (e.g., light and ice freeze-melt cycles) and organism life cycles. Therefore, it was essential to systematically determine organism abundances, biomass, and activity rates throughout the MOSAiC drift. The program aimed to quantify the seasonal fluctuations in algal and bacterial productivity, organismal physiologies (including metatranscriptomes) and life cycles, as well as grazing by micro- and mesozooplankton, diets of key species, and vertical particle fluxes.

Linkages with environment: The combined analysis of ecosystem characteristics with all available MOSAiC environmental data allows us to assess the importance of bottom-up (e.g., light, nutrients, sea ice characteristics) versus top-down (e.g., grazing, predation) controls on biological standing stocks and activities over a complete seasonal cycle. The program aimed to assess the contributions of ecosystem processes to the Arctic climate system, e.g., by driving gas fluxes across ice-ocean-atmosphere interfaces, or by affecting the heat budget of sea ice directly or through interactions with clouds.

These three major focal science areas were approached by considering both their interconnection as well as their relation to the overall MOSAiC science objectives. Therefore, a consistent, coordinated, and methodological framework linking individual measurements within the ECO team was developed. This included strong interdisciplinary partnership with the other MOSAiC teams, like co-located measurements of sea ice and water column properties to identify biologically-relevant linkages between the two habitats. The unique year-round access to the high Arctic environment was used to investigate poorly understood and undersampled habitats and seasons. For example, high heterotrophic biological activities and unique biodiversity patterns in winter were expected to precondition the biological response to the return of the light in spring. We furthermore expected that meta-genomic and -transcriptomic data can be used to identify unique physiological mechanisms that sustain survival of organisms and ecosystem services under polar seasonality. The program aimed to provide information relevant for understanding a wider Arctic system by determining the fluxes of climate-relevant compounds like CO_2.

2. APPROACH AND METHODS

The MOSAiC expedition (PS122) onboard the German research icebreaker RV *Polarstern* (Alfred-Wegener-Institut Helmholtz-Zentrum für Polar- und Meeresforschung, 2017) was organized into 5 cruise legs (Figure 1). The field campaign began in late September 2019, and north of the Laptev Sea (Krumpen et al., 2020; Nicolaus et al., 2022b) the first Central Observatory ice camp was established, which was used on cruise legs 1-3 until May 11, 2020 (Figure 3). Team ECO observations began on 15 October 2019, and the full regular weekly sampling by Team ECO started 31 October 2019, which involved measurements and sampling from the ship and ice floe. Leg 1 ended in mid-December and Leg 2 continued on until the end of February 2020. Leg 3 extended beyond its originally planned date due to logistical constraints caused by the global COVID-19 pandemic, and ended in mid-May 2020, when RV *Polarstern* had to leave the first Central Observatory.

Following a logistically necessary break, leg 4 re-established and occupied a new Central Observatory (Figure 4) at a different location on the same ice floe from 20 June 2020 until the floe disintegrated in the Fram Strait on 31 July 2020. Continued observations were made during leg 5, which involved establishing a new ice camp (Figure 5) located on a new ice floe near the North Pole in the second half of August. The MOSAiC ice drift study ended 20 September 2020, with ECO science operations continuing in the marginal ice zone during the transit back to shore. More details on the MOSAiC campaign, can be found in Nicolaus et al. (2022b), Rabe et al. (2022) and Shupe et al. (2022).

2.1 Water column work program

Sampling and measurements in the water column occurred at frequencies from daily, to weekly, with opportunistic, intensive observation sampling occurring a few times over the duration of the expedition, which involved sampling at hourly time scales for 20-30 hr periods. Sampling frequency was partially based on feasibility and cost-benefit evaluation. For most ECO properties, the primary sampling mode was weekly sampling, matching the anticipated rates of change in ecological properties relative to anticipated achievability of the sampling program by a small onboard team. The daily sampling for chlorophyll *a* (Chl-a) and microbial community structure resolved day-to-day changes in fundamental microbial properties, which would be missed with only once-weekly sampling. Herein, major operations executed by Team ECO organized by sampling frequency are briefly described, while detailed method descriptions will be provided in later, targeted publications.

2.1.1. Continuous measurements and daily sampling approaches

A Membrane-Inlet Mass Spectrometer (MIMS) connected to the ship's flow-through seawater system allowed the continuous measurement of dissolved O_2 and Ar concentrations to calculate O_2/Ar ratios and infer net community production (NCP) (Tortell, 2005; Ulfsbo et al., 2014), Rokitta et al. unpublished results). The depth of the seawater intake port was 11 m below sea level at the keel of the ship. Continuous measurements of these properties were only interrupted during 1) routine maintenance procedures by instrument operators, 2) ship maintenance of flow-through systems, and 3) when discrete bottle sample measurements were performed. Therefore, gaps in continuous data mostly collected during March to October 2020 are approximately 1) once daily for 1-2 hrs, 2) 1-2 times monthly for 3-6 hrs, 3) 3-4 hrs weekly. Onboard, routine calibration with reference gasses allowed for tracking of instrument drift over the course of the expedition.

The AUTOmated FIltration for marine Microbes (AUTOFIM) instrument (iSiTEC GmbH, Bremerhaven, Germany) automatically collected, filtered, and preserved water samples for molecular genetic analyses (Metfies et al., 2016) from December 2019 to October 2020. It is permanently installed on RV *Polarstern* a few meters from the flow-through seawater intake system at 11 m at the bow of the ship. AUTOFIM collected samples on a daily basis, and in some instances at even higher temporal resolution to resolve spatial changes along the drift path. Samples were analyzed for microbial community structure using 16S and 18S rRNA amplicon sequence-based approaches.

The fishcam, an *in situ* video system (FishCam, MacArtney Germany GmbH, Kiel, Germany), was deployed on average at 375 m water depth (range 369 - 376 m) from 23 October to 7 November 2019 and at 213 m depth (range 194 - 215 m) from 12 December 2019 to 11 March 2020 through a hole in the ice, approximately 500 m away from the ship (see Snoeijs-Leijonmalm et al. (2022) for details). The system included two HD Internet Protocol cameras, one looking sideward and one looking downward, two Luxus High-Power LED light sources of 6000 lm each, and a mini-CTD. The system was connected to a personal computer onboard, running PortVis (Serial Port and Video Stream Visualizer) software, version 2.1. Camera images were recorded in LED on:off cycles of 5:55, 15:15, or 55:5 min. Fish were also caught via long lines and fishing rods deployed through the moon pool or holes in the ice (Snoeijs-Leijonmalm et al., 2022).

Further, a number of discrete water samples were manually collected at a daily or near-daily frequency over the duration of the expedition from a single tap of the ship's flow-through seawater system, which was also used for the MIMS measurements. This included separate samples for 1) Chl-a (except from mid-December to end of February), 2) 16S and 18S rRNA amplicon-based microbial community analyses (except from mid-December to end of February), and 3) ice nucleating particles (INPs, full timeseries).

To investigate downward flux, a long-term ice-tethered time-series sediment trap (McLane PARFLUX Mark 78H-21) with 21 sampling cups was deployed at 200 m water depth, and tethered to SYI, located ~1000 m away from the ship (Figure 3). Sinking particles were automatically collected for two week intervals (15 or 16 days) from March to November and every month (29-31 days) from December to February. The sampling cups were filled with salt-saturated artificial seawater and $HgCl_2$ prior to deployment. The sediment trap was operational from 26 October 2019 to 31 July 2020.

2.1.2. Discrete sampling

The primary sampling approach for the weekly ECO time-series of water column biological and chemical properties relied on the ship CTD rosette, a suite of plankton nets, and a number of small animal- and particle-imaging instruments with deployments over three consecutive days per calendar week. The CTD sensor packages, calibration methods, and post-processing are described in Rabe et al. (2022) and Tippenhauer et al. (2023a, 2023b). In brief, discrete biological samples were collected from 12-liter OTD bottles attached to the shipboard 24-bottle CTD rosette (PS-CTD). From November 2019 to May 2020, additional water column sampling was conducted via a 5-liter 12-Niskin bottle CTD rosette from Ocean City (OC-CTD; via a sheltered in-ice hole located 300 meters from RV *Polarstern*; see Figure 3). In the period between mid-March and mid-May, the PS-CTD was not operational due to the loss of the ice hole alongside the ship (see Rabe et al., 2022), so all water column ECO samples were collected at Ocean City. During this period, use of the OC-CTD led to a lower vertical depth resolution as the total water volume collectable in one cast was substantially less with the OC-CTD (60 L) versus the PS-CTD (288 L). All sampling events are listed in Table S4. Sampling order from the individual rosette bottles primarily followed WOCE procedures (Woods 1985), which prioritizes sampling of tracers, gases, and nutrients in time before the sampling of other properties. The sequence prioritized sampling of time-sensitive properties and limited contamination between parameters. Co-location of many properties across a smaller number of depth horizons was prioritized over higher vertical resolution of a few properties (Figure 6). Additionally, upper 200 m water column sampling was prioritized over full water column profiling to better resolve upper ocean interactions with sea ice and the atmosphere. Sample types requiring large volumes (e.g. POC/N, DNA and RNA) made it necessary to collect samples in additional casts following a primary full water column cast used to collect small volume ECO samples. Standard water depth horizons for biological properties were 2 m, 10 m, Chl-a fluorescence maximum (if present based on CTD fluorescence sensor profile) or 20 m, 50 m, 100 m, and the Atlantic Water core depth. The depth of the Atlantic Water core, detected as the local temperature maximum in each profile, varied significantly along the drift path, from approximately 100 m close to Fram Strait up to 400 m in the Amundsen Basin (Rabe et al., 2022; Schulz et al., 2023b). The depth-resolved sampling for Chl-a, nutrients, and total DNA collected from the PS-CTD and OC-CTD rosettes over the drift duration relative to a reference depth (400 m) and bottom depth highlight the focus of sample collections in the upper water column (Figure 7).

Samples collected by team ECO during the routine CTD rosette-based water column sampling included a wide range of standard variables such as inorganic nutrients (nitrate+nitrite, nitrite, silicic acid, phosphate and ammonium) as well as total dissolved nitrogen and total dissolved phosphorus, total dissolved inorganic carbon (DIC) and total alkalinity (TA), dissolved organic carbon (DOC), colored dissolved organic matter (CDOM), Chl-a, algal pigments, POC and PON concentrations as well as their isotopic composition, biogenic silica (bSi), total deoxyribonucleic acid (DNA) and ribonucleic acid (RNA) for sequencing, taxonomic cell counts (via light microscopy), as well as cell abundance (via flow cytometry). Samples for primary and bacterial production, dissolved oxygen, DOM characterization after solid-phase extraction, and ^{14}C-DIC were collected at a lower temporal frequency and with larger gaps due to instrumentation failures. Additionally, several complementary samples were collected on a routine basis, such as those for measurements of O_2/Ar ratios in discrete samples, INPs, neutral sugars, and ^{15}N-nitrate isotopes. Processing of preserved water or filters mainly occurred at the shore-based laboratories, with exceptions of onboard measurements of nutrients (Nov 2019 to May 2020), dissolved oxygen (March to Oct 2020), primary and bacterial production (Dec 2019 to May 2020), and a subset of Chl-a samples (March to May 2020). Details on sample processing methods can be found in supplementary Table S2.

We aimed for all analyses for each variable to be done in the same laboratory and/or using the same instrument to decrease uncertainty due to laboratory or instrument calibration (see supplementary Table S2 for details). In cases where this was not possible (DIC/TA, DNA, RNA, POC/N), interlaboratory calibration samples were collected. In the case of nucleic acid samples, aliquots from the same extracted samples of the core time series were used for specific sequencing approaches in specialized labs (e.g. metabarcoding, genomics, sequencing of specific metazoan or functional primers). Details on the ECO multi-omics sampling program are given in Mock et al. (2022).

The seasonal life cycles and vertical distribution of zooplankton abundance and biomass were studied using imaging tools and plankton nets, deployed on the same or on two consecutive days during a calendar week. From November to March, a multinet midi (Hydrobios), three ring nets, the Underwater Vision Profiler (UVP) and the Light-frame On-sight Key Species Investigation system (LOKI) were deployed through a large hole in the ice alongside the RV *Polarstern* yielding an almost weekly resolution for many targeted parameters (Tables S4 and S5). The multinet was equipped with five nets of 150 µm mesh size to sample five discrete depth intervals between 2000 m and the ocean surface. Those samples were processed for zooplankton identification, abundance, and biomass at shore-based laboratories. The LOKI was deployed approximately weekly from 1000 m to the surface. In addition to high resolution images, the instrument obtained hydrographical parameters, e.g. depth, temperature, salinity, oxygen concentration and fluorescence. The UVP was mounted on the PS-CTD rosette and casts were conducted from various depths to the surface. Ring nets of 1 m^2 area (150- and 1000-µm mesh) and 0.28 m^2 area (53-µm mesh) were deployed to varying depths up to 2000 m, to collect zooplankton for analysis of taxonomy, energy content, biomarkers and gut DNA (Table S4). However, the hole next to the vessel could not be maintained in April and May due to strong ice dynamics. During that period, only a 150-µm mesh Nansen net and the 53-µm mesh ring net could be deployed at the ice hole at OC. The Nansen net was equipped with an opening/closing device and was deployed in a series of single casts to the same depth intervals as sampled by the Multinet down to a maximum depth of 800 m. Additional ring net tows were conducted over the same depth intervals as used for the Multinet to collect animals for biochemical and genetic analyses and physiological rate measurements. In addition, during all seasons, a net was attached to the under-ice Remotely Operated Vehicle (ROV) 'Beast' (Katlein et al., 2017) for sampling 2-3 depth horizons: the ice-ocean interface, 10 m, and 50 m under the ice.

To determine zooplankton abundance and biodiversity, usually complete samples from Multi-, Nansen-, and ROV net casts, as well as samples taken with the small ring net, were preserved with hexamethylenetetramine-buffered 4% formaldehyde, stored at room temperature and subsequently processed in laboratories in Germany (AWI) and the US (University of Rhode Island). Live specimens for biochemical analyses and physiological rate measurements were sorted from ring net samples under a stereomicroscope onboard and determined to the lowest possible taxonomic level. Only when abundances were low, large organisms were also sorted from Multi- and ROV net samples allocated for taxonomic analyses to obtain sufficient individuals. Most of the live specimens (>10,000 individuals during the entire expedition) were deep-frozen, either individually or pooled in groups depending on size, for biochemical measurements (e.g., total lipid content, C/N ratio, energy content, lipid class composition, omega-3 fatty acids and level of animal sterols such as cholesterol and desmosterol, $\delta^{13}C$ and $\delta^{15}N$ values), as well as for molecular studies of gut contents (copepods, amphipods) and for biodiversity (gelatinous zooplankton). Key mesozooplankton species (e.g., *Calanus glacialis, C. hyperboreus, Metridia longa, Themisto spp*.) were photographed prior to freezing to digitally measure certain characteristics, e.g., prosome length (copepods) and oil sac volume (*Calanus* spp.). For experimental work, individuals of key species were incubated for at least 24 h to determine egg production, grazing and respiration rates, and thereafter, deep-frozen to measure organic carbon and nitrogen contents to calculate biomass specific rates (eee details in Case Study 1 below).

2.2. Sea ice coring and processing

The coordinated sea ice sampling by the MOSAiC teams ICE, ECO, and BGC was designed to study the seasonal changes of physical, biological, and geochemical properties of FYI and SYI in an interdisciplinary context (see also Angelopoulos et al., 2022; Nicolaus et al., 2022b; Evgenii Salganik et al., 2023a). During fall 2020, ice areas of undeformed FYI and SYI were identified that were safely accessible by snow machine, relatively homogeneous, and large enough to accommodate repeat visits, potentially for the entire drift. Most importantly, sites had to be located away from RV *Polarstern* to avoid and minimize the impacts of 1) artificial light pollution, 2) regular on-ice foot traffic, 3) fumes and particulate material from the ship's exhaust system and snow machines, and 4) 'technically clean water' discharges from the ship.

Tents were set up at each ice coring site to protect newly extracted ice cores from adverse environmental conditions during sectioning, which could quickly alter ice and its physical, biological, and chemical properties. Cores for biological properties were collected using a 9-cm diameter KOVACS Mark II coring system. All coring events are summarized in supplementary Table S6. Most cores were sectioned and parsed into sterile Whirlpak bags directly inside the tent under low and/or red-light conditions to minimize artifacts. In some instances, complete cores were bagged directly in the field and processed on the ship, but in-field sectioning was prioritized when conditions were amenable. Ice core properties were derived from individual core sections or pooled core sections (Figure 8) depending on individual property requirements. Core section pools provided larger melt volumes and sub-sampling for multiple properties from single horizons. Small-scale horizontal variability was reduced by pooling core sections, creating a more homogeneous master sample from which to derive related properties.

Six to eight full-length ice cores designated for ecological and biological properties were sectioned using similar sectioning schemes and parsed into new, sterile Whirlpak bags in the field. Cores were sectioned from the bottom into two 5 cm sections, and then subsequently at 10 cm intervals from top and bottom, leaving a variable length middle section. Middle sections varied by several cms across 3-4 cores. Two pools (termed ECO1 and ECO2) using this procedure were generated and sub-sampled for a majority of biological properties from these two sets (Figure 8). In addition, the bottom 0-3 cm or 0-5 cm of sea ice from 3-4 cores were collected, sectioned, and pooled for individual sets of measurements of net primary productivity (NPP pool) and occasionally bacterial production (from NPP pool), as well as a pool for metatranscriptomes (RNA pool) in the field. Occasionally, full profiles of BP were measured from ECO1 pools.

A single core was collected for bulk salinity, oxygen isotopic composition, and inorganic nutrients. This core was sectioned in the field at 5 cm intervals from the top and bottom, leaving a variable-length middle section (Nicolaus et al., 2022b; Evgenii Salganik et al., 2023a). Individual cores were collected for DIC/TA and gypsum. These cores were bagged completely in the field and either sectioned and processed onboard, or stored frozen for future processing onshore.

Ice cores and sections were transported back to the ship in coolers, protecting cores from fluctuations in light and temperature. All ECO pool samples were melted after the addition of 0.2 μm filtered surface seawater (typically 50 ml per 1 cm of core section) to reduce the impact of osmotic stress and cell loss (Campbell et al., 2019; Chamberlain et al., 2022; Garrison and Buck, 1986). Ice core sections in bags were melted in the dark at room temperature (18-22°C) and checked every 4-6 hours. Upon completed melt, which took 12 to 40 hours, bags were transferred into dark, temperature-controlled laboratory containers, and parsed for sub-sampling of biological properties under red light to minimize artificial light stimulation of biological activities. Samples for Chl-a, algal pigments (HPLC analyses), particulate organic carbon and nitrogen (POC/N), biogenic silica (BSi), taxonomic counts (light microscopy) and cell abundances (flow cytometry), INPs, and neutral sugars were typically collected from ECO1 pool (Figure 8). DNA samples were filtered through 0.2 μm filters from ECO2 pool, and the filtrate was reserved for DOC and CDOM determinations. For each melted core section, melt volume factors were derived from added meltwater volume, which were used to derive to calculate melted ice volumes. Data are reported as per unit volume melted ice core as no correction for differences in density of ice and melt water were available.

Core sections for measurements of inorganic nutrients and nitrate isotopic composition were directly melted in the dark. Samples were pre-filtered through a 0.45 μm filter membrane and either analyzed directly onboard, or frozen for analysis onshore.

DIC/TA cores were sectioned onboard in a freezer laboratory (-15°C) at 10 cm intervals from top and bottom, with a variable length middle section. Sections were placed inside gas-tight bags and air was removed using a vacuum pump to avoid CO_2 exchange. These core sections were directly melted in the dark at 4°C, without addition of buffer or conservational solution. Melted samples were transferred into 250 ml borosilicate bottles, augmented with 60 µL of saturated mercuric chloride ($HgCl_2$) solution, and sealed with a septum cap to prevent CO_2 exchange with the atmosphere, then stored cool until post-cruise analyses in Japan (Nomura et al., 2020).

2.3. *Event- and process-driven sampling*

In addition to the time-series sampling of water column and sea ice, additional samples were collected either on an opportunistic or event- and process-driven basis (see supplementary Table S7 for an overview on all sampling events). For many of these sampling events, a smaller subset of parameters was sampled, with Chl-a and nutrients being the most regularly sampled properties.

Water samples for biological properties were collected from leads from the upper 1.5 m of water directly below newly forming ice or within the sea surface using peristaltic or hand pumps, from October thru early March, and again from early July till the end of the drift in September 2020. Newly-forming ice was collected by sieves, saws, buckets, and/or ice corers throughout the drift period, except during the continuous melt period between June and end of July 2020. Ecological properties of the seasonally occurring melt ponds were sampled only during August and September 2020. Similar to leads, both ice and water from within and under melt ponds were sampled. Ice from leads and melt ponds was processed without filtered seawater addition on most sampling instances, while filtered seawater was added to ice collected between March and May 2020, similar to the handling of time-series samples of sea ice. Sampling of various stages of ice formation and consolidation was conducted in the marginal ice zone (MIZ) during the transit back to shore at the end of the field campaign (September 2020). Here, a small number of biological properties from sea ice, direct under-ice waters, and the water column was collected from 3 stations. Ice types collected from these transit stations were primarily from ice floe edges, and were not consolidated. The distribution of biological properties in pressure ridges (deformed sea ice) was studied using ice coring of keel blocks and collecting water from ridge keel voids (seawater-filled voids between ice blocks in the ridge keel) and below ridges (see case study 1 for details).

Water directly from the ice-water interface below level ice was collected except for August to October 2020 for project-specific experimental work by deploying a hand pump through a borehole in the ice. Similarly, under-ice water from the upper 2 m of the water column was occasionally sampled via hand pumps in connection to the time-series common coring activities.

In addition to these more opportunistic sampling events, intensive observation periods (IOPs) were included to address research questions on timescales shorter than the one-week interval of the time-series. For example, higher frequency temporal sampling (i.e., 4-10 time points in 20 - 30 hr periods) was conducted to observe potential diurnal dynamics as well as biological changes as a result of important events such as high wind periods, or the onset of freeze. In the beginning of December, a 24-hr IOP with zooplankton collections via both ROV nets and LOKI was conducted. In July, two 24 hr IOPs were conducted. The first one in the beginning of July consisted of 3 LOKI casts and six CTD rosette casts from the ship to cover diurnal patterns in the water column. A second IOP was conducted one week later during rapid melt to also investigate diurnal patterns in the direct under-ice habitat. In September 2020, two IOPs were conducted. In the beginning of September, a 36 hr intensive observation period in collaboration with team OCEAN was conducted to investigate the effects of a high wind event. Collections of under-ice waters occurred within a temporary on-ice laboratory, termed 'EcoLodge,' established during the summer period. From June to mid-August 2020, EcoLodge1 was situated approximately 110 m from the ship on level ice, i.e. closer than other major sites but with an under-ice environment that was comparable in terms of ice thickness to the FYI coring site, and with surface waters less affected by disturbance from the ship compared to the PS-CTD rosette system. Here, under-ice water with brackish salinity (10-15) was sampled using a peristaltic pump, and filtered directly for Chl-a, POC/N, and microbial community structure analyses. Samples for inorganic nutrients and cell abundance were also collected. During August and September, the re-established EcoLodge2 was located approximately 300 m from the ship on level ice and approximately 15 m from a small, dynamic lead. Here, ice thickness was 125-130 cm. EcoLodge2 served as a hub for under-ice water sampling via a peristaltic pump at 14 timepoints over 36 hrs. One week later a similar IOP at EcoLodge2 with 12 time points over 24 hrs was conducted to assess the impacts of the onset of freeze up.

2.4. Modifications to ship-based and on-ice routine operations for ecosystem sampling

A number of regular ship operations were considered as potential sources of contamination, for which we took precautions to limit their potential impact. For example, prior to MOSAiC, the ship would regularly release gray water continuously from an outlet located starboard side at 5 m depth. The location and constant release of gray water posed a potential risk to our sampling efforts as this location was within meters of the main PS-CTD sampling. While gray water is technically clean enough to drink, it could carry residual microbial, DOM and nutrient contamination. Also, there was a chance that the gray water, being less saline than ambient seawater, would float towards the surface and interact with the underside of the ice floe, potentially altering important characteristics of the ice and its development. Therefore, during MOSAiC, gray water was retained in the ship's hold for 2-3 days, had salt added back into the solution to increase its salinity, and pumped to 150 m depth from the ship's moon pool. Gray water pumping was conducted on days when no active water column sampling was conducted.

A monthly cleaning routine of the engine's boiler systems was one aspect of normal ship operations, which we had not been aware of in advance, that may have had an impact on our sampling efforts around the ship. Unlike gray water handling, this operation was not possible to adapt. While the dates of the monthly release and of measurements on and around those dates can be reviewed to identify any abnormalities, no direct measurements on possible contamination were done.

The ship also emitted continuous artificial light during the drift. Due to safety regulations, the use of light near the ship during our water column sampling could not be significantly reduced. When sampling of the PS-CTD rosette during times of natural darkness (i.e., the Polar night), we reduced the light contamination during sampling by combination of room shading and shaded containers for sample collections (Marangoni et al., 2022). Since the floe drifted in different directions and speeds compared to the water column below, the effects of light pollution on water column-based time series sampling of biogeochemical and many biological parameters can be expected to be minimal. However, e.g. physiological rates of sampled organisms as well as diel vertical migration pattern may have been impacted (Ludvigsen et al., 2018). Comparing migration patterns from different devices and locations (e.g., Acoustic Zooplankton Fish Profilers (AZFPs) located at different distances from the ship; Berge et al unpubl. results) may help to evaluate potential impacts. For sea ice, potential impacts of artificial light pollution on photosynthetic biomass and physiology are much larger, as small effects may accumulate over time. To account for this, the long-term sea ice time-series sites were established >1 km from the ship, where light pollution was not detectable. In the field, shaded tents were used for ice processing to reduce the effect of strong ambient light and temperature increases on ice samples during summertime. In the ship-board labs, samples were processed in temperature-controlled, red- and/or low-light conditions.

In addition to reducing artificial light pollution, we also aimed to reduce the introduction of nutrients and dissolved carbon to our sea ice samples through our melt process. For most ecological properties collected from sea ice, buffering the melt process with a known volume of saline solution can reduce the impact of osmotic stress and cell loss (Garrison and Buck, 1986). Therefore, we planned to make and add an artificial saline solution, consisting of distilled water and analytical grade sodium chloride, to our sea ice core sections. However, the onboard nutrient analyzer showed that the artificial saline solution contained about 1 µmol kg^{-1} nitrate+nitrite, which, at the start of the drift, was more than 10 times the ambient sea surface water nitrate+nitrite concentration. Therefore, despite our preparations, filtered surface seawater additions were used in the ice core melting process, which impacts some of our parameters such as DOC or INP.

2.5. Integrative approaches across the Team ECO work program

In the following sections, some of the approaches that were employed to gain a holistic understanding of seasonal variations in species composition and food web dynamics are highlighted. Further, pathways are identified towards synthesizing different data sets to address overarching questions in how organisms, and physical properties and processes, control the flow of material and energy. In addition, the integrated multi-omics approaches are detailed in Mock et al. (2022).

2.5.1. Imaging

Imaging has become an essential tool in zooplankton studies in the last two decades (Giering et al., 2022; Lombard et al., 2019). The *in situ* cameras LOKI and UVP resolve plankton distributions at high vertical resolution (Kiko et al., 2017; Schulz et al., 2015). The main strength of the UVP is detecting marine snow, large-sized single-cell organisms (e.g., Rhizaria; Biard et al., 2016), and gelatinous zooplankton (Stemmann et al., 2008). The resolution of the images (1.5 megapixel, picture size depend on organisms size), however, is relatively low and often does not allow for species identification, especially of the dominant zooplankton group Copepoda. The LOKI concentrates the organisms with a net, leading to a flow-through chamber (Schulz et al., 2010). Jellyfish are often destroyed by the net, but LOKI captures Copepoda and other abundant taxa (e.g., Ostracoda, Chaetognatha) in high quality images, allowing the determination of copepod genera, species, and often developmental stages (Schmid et al., 2016). In addition to *in situ* imaging, preserved net samples collected during MOSAiC have been scanned using the laboratory on-desk system ZooScan and single object images have been extracted with the software application ZooProcess (Gorsky et al., 2010). To classify plankton organisms and share images among experts worldwide, all images taken by LOKI, UVP, and ZooScan have been uploaded to EcoTaxa. This is a web-based platform that is an established tool in classifying zooplankton organisms (Picheral et al., 2017) by applying simple machine learning techniques to predict taxonomic categories from image parameters. ZooProcess automatically provides size-related parameters of each object, and in combination with the taxonomic classification allows for estimating the zooplankton biomass from preserved net samples (Cornils et al., 2022) from the ice-ocean interface to the deep ocean (max. 2000 m).

To study the occurrence of squid and fish in the CAO (Snoeijs-Leijonmalm et al., 2022), a continuously recording deep-sea video system (FishCam, MacArtney Germany GmbH, Kiel, Germany) was deployed at 200-400 m water depth. Part of the videos (180 hrs) were studied in real-time mode (Snoeijs-Leijonmalm et al., 2022) while an automated procedure for identifying periods of interest (i.e., appearance of large organisms) in the extensive remainder of the video material is currently being developed. The combination of visual techniques, machine learning, and discrete sampling of animals and particulate matter can work together to address long-standing questions on the distributions and controls on these ecosystem components, where few such data are available.

2.5.2. Biomarkers and carbon transformations

Biomarkers are molecules (e.g., fatty acids, amino acids, sterols) or isotopic compositions of elements (e.g., carbon) that are somewhat source-specific to primary producers and are incorporated mostly unchanged into the tissue of their consumers. Tracing these biomarkers within the zooplankton and fish community is an essential tool in food web studies that address the relative importance of different sources of organic matter, the role of key Arctic primary producers, and the nutritional status of higher trophic levels (Kohlbach et al., 2022; Kunisch EH et al., 2021; Leu et al., 2020). Compared to previous studies, trophic marker analyses of the MOSAiC samples are improvements in two major aspects. First, a very broad range of trophic markers is being explored including fatty acids, sterols, highly-branched isoprenoids, bulk stable isotope compositions, fatty acid-specific stable isotope compositions, and essential amino acid specific stable isotope compositions (eAA-SIA) to balance the strengths and shortcomings of the individual approaches. Second, all the different trophic markers are measured from the same parent samples of homogenized animal tissue to allow a direct comparison of the results and to link the nutritional status of the animals to their food resources. Alongside the trophic marker approaches, animals were also collected for DNA sequencing of gut content. This approach provides a high taxonomic resolution of the ingested species and will further support the interpretation of the trophic marker data (Cleary, 2015).

One key question for studying Arctic marine food webs is to elucidate the role of ice algae as a source of organic matter. Trophic biomarkers determined across the food web including the particulate organic matter in surface waters and ice cores, as well as zooplankton, will help to identify seasonally varying food web interactions from primary producers to individual zooplankton species. These food web interactions will be linked to primary and bacterial production rates as well as vertical flux studies to enable more complete insights into the Arctic biological system.

2.5.3. Ecological modeling

A variety of bioinformatic and statistical modeling techniques aim at elucidating changes in composition and metabolic potential of Arctic marine microbial communities to improve our understanding of their influence on global biogeochemical cycles. The mechanistic understanding of ecological patterns is initially based on information from gene sequences combined with a descriptive approach of community members using co-occurrence networks that illustrate the occurrence of species at the same place and time (Popa et al., 2020). This graph approach, in which nodes are species and edges represent the correlation strength of their seasonality patterns, enables identification of i) central species (node hubs) and ii) species communities (network clusters) that are defined by several populations which are abundant in the same time period (Berry and Widder, 2014). The outcome of such studies allows us to investigate the seasonality of microbial community composition, activities, and functions. Further, it enables the identification and definition of yet unknown ecological processes. These processes include the interaction of present species with each other and the environment. To understand this interaction in detail and especially to identify key parameters with strong impact on the Arctic ecology, it is necessary to combine all measured data into a modeling framework (Faust and Raes, 2012). For example, the co-occurrence information of photoautotrophic species with grazers isolated from the ice and water column combined with environmental parameters like water depth, temperature, daylight, etc., can be modeled using a Lotka-Volterra (LV) framework (Lotka, 1920; Volterra, 1927) with seasonal forcing approach (Sauve et al., 2020; Vandermeer, 1996). As a result, these models can be used to test several species interaction scenarios after varying the environmental parameters (Succurro and Ebenhöh, 2018). Furthermore, extending the LV by the dynamics of the available resources within the ecosystem (MacArthur consumer-resource models; Goldford et al., 2018; MacArthur, 1970) permits the development of a powerful, theoretical tool to explain the formation and occupation of ecological niches in dependence on external parameters with predictive capabilities for several future scenarios.

Microbial community structure and metabolic potential data are also being leveraged for biogeochemical predictions using machine learning. These techniques are well suited to complex, high dimensional, community structure data and can be used to extract patterns of succession and biogeochemical signatures from sequence information (Bowman, 2021). For example, the Random Forest (RF) regression model is effective at predicting biogeochemical signatures from amplicon sequence data, providing the potential for extending the data coverage of less frequently sampled key biogeochemical variables (Dutta et al., 2022). Additionally, potential microbial drivers for these processes can be identified by applying permutation to the RF models to assess the contributions of specific community members to model performance (DiMucci et al., 2018). Self-organizing maps (SOMs) are used to partition the microbial community into functionally distinct modes that can be applied as discrete variables in a variety of statistical (Bowman et al., 2017) and mechanistic (Kim et al., 2022) models. This discrete variable reflects key genetic traits of the microbial community, provides reasonable estimates of physiology, and allows for correlation between variability in taxonomic structure and function. Eco-physiological information can then be used to modify and better parameterize data-assimilative marine biogeochemical models for hypothesis testing and *in silico* experimentation – such as quantifying previously identified questions regarding microbial controls on ecological processes and assessing the sensitivity of carbon flow through the microbial food web to climate change scenarios.

3. RESULTS

The MOSAiC Ecosystem work program generated > 50,000 unique samples and activity measurements characterizing organisms and processes from viruses to fish.

We sampled 195 CTD rosette casts, 44 multi-nets, and 21 FYI and 20 SYI common ice coring events. We also collected samples from > 40 time points and sites during events and IOPs covering a complete Arctic seasonal cycle. A majority of sampling events were co-located in time and space or spanned long periods of continuous measurement and/or sample collection (Figure 6). Vertical distributions of most properties in the upper 400 m of the water column were resolved over the drift, but, when possible, also full water column depth profiles of core properties at once-weekly intervals were collected (Figures 7). The resolution of the year-long observations to map essential ecosystem properties differed depending on complexity of sampling and needed volumes, e.g. nutrient sampling could be executed more frequently and with greater vertical resolution (Figures 7A, B) than Chl-a (Figures 7C, D) and total DNA sampling (Figures 7E, F).

3.1. Environmental controls over the drift period

The MOSAiC expedition provided a wealth of environmental observations from ice, ocean, and atmosphere. These data provide a critical context to interpret the biological observations during the drift period. An evaluation of the meteorological conditions during the MOSAiC drift indicates that unusually cold temperatures relative to decades-long climatology occurred in November 2019 and March 2020 (Rinke et al., 2021). Additionally, Rinke et al. (2021) also identified that the 2019-2020 drift year had more frequent storm events in spring, and that summer had a longer sea ice melt season, from late May to early September, approximately a month longer than the median from 1979 – 2019. Also, relative to climatology, the July and August 2020 period was the all-time warmest.

Throughout winter, RV *Polarstern* drifted in northerly directions, with the northernmost location at 88.6°N reached at the end of February 2020. Throughout spring and summer, the floe drifted in southerly directions, with periods of faster (mid-March to mid-April) and slower (mid-April to mid-July) drift speeds. The annual changes in air and water temperature, surface ocean salinity, incoming PAR (photosynthetically active radiation), and surface ocean nutrient concentrations along the drift track are illustrated in Figure 9. These properties are relevant examples of environmental changes over the annual cycle, which potentially influence ecosystem processes. Air temperatures at 2 m (Figure 9B) varied between values as low as -40°C in March and up to 6°C during the summer months (Cox et al., 2023; Shupe et al., 2022), driving sea ice freeze-up and melt (Nicolaus et al., 2022b; Evgenii Salganik et al., 2023a). Upper water column (10 m depth) temperatures (Figure 9C) were much less variable, with average daily temperatures near the freezing point during most of the year. Except for the transit periods, maximal temperatures of about -1.3°C were reached at the end of July. Surface ocean salinity (Figure 9C) reflected drift location (Rabe et al., 2022; Schulz et al., 2023b), with rather low levels during drift in the TPD in winter 2019/20. In February and March, TPD influence was gradually replaced by an increasing contribution of more saline Atlantic-influenced waters. After crossing the Gakkel Ridge in late March, average daily surface salinity remained high until reaching the ice edge in Fram Strait with stronger influence of lower salinity waters from the polar waters of the East Greenland Current during July 2020 (Schulz et al., 2023b).

Solar incoming irradiance (Figure 9D), shown as PAR, at the surface of the sea ice decreased quickly in fall and was below the detection limit from 8th of October until March 13th, marking the period of the polar night. Surface PAR increased as the solar elevation increased, and reached maximal values of >1300 μmol photons m^{-2} s^{-1} from May to July (note the data gap between mid-July and mid-August). Thereafter, PAR decreased again, with daily maximum values below 200 μmol photons m^{-2} s^{-1} at the end of the drift.

Nutrient concentrations in surface waters (upper 30 m) varied with water masses and through the seasons as the floe drifted (Figure 9E). As the floe drifted northwards, silicic acid and phosphate concentrations increased from November to January, from 1.5 to 4.7 μmol kg^{-1} and 0.19 to 0.52 μmol kg^{-1}, respectively. Nitrate remained mostly constant until February at 1.05±0.37 μmol kg^{-1}. Silicic acid was nearly constant until early February, but phosphate concentrations dropped to 0.35 μmol kg^{-1} after early January. Trends diverged further thereafter as the drifted further southward, with nitrate and phosphate increasing to 4.7 and 0.42 μmol kg^{-1}, respectively, in May, but with silicic acid decreasing to 2.5 μmol kg^{-1}. These opposing trends for the different nutrients likely reflect characteristics of the different water masses as distinguished using the temperature and salinity observations, with increasing influence of Atlantic waters containing relatively more nitrate and phosphate, and less silicic acid. When sampling at the floe resumed in the second half of June, maximum sea water nitrate, silicic acid, and phosphate concentrations of 6.0, 7.5, and 0.66 μmol kg^{-1}, respectively, were measured. Towards the end of August though, as the drift continued southwestward, nitrate levels quickly decreased to <0.5 μmol kg^{-1}, but phosphate (~0.58 μmol kg^{-1}) and silicic acid (7.8 μmol kg^{-1}) remained comparably high. This is consistent with polar waters of the East Greenland Current in Fram Strait, with more influence of silicic acid rich Pacific-derived waters and/or the Transpolar Drift. Thereafter, nutrient concentrations were variable between ~0.5 – 2 μmol kg^{-1} nitrate, 1-9 μmol kg^{-1} silicic acid, and 0.2-0.7 μmol kg^{-1} phosphate over the summer and fall, as RV *Polarstern* repositioned on a new floe close to the North Pole.

3.2. Observed organisms and biodiversity

Despite the extreme seasonal variations in irradiance and other environmental drivers (Figure 9), the same functional and taxonomic groups (flagellates, dinoflagellates, and diatoms) were the major contributors to the sea ice protist assemblages in the different seasons (Figure 10), although there were seasonal changes in their relative and absolute abundances. Ongoing analyses based on taxonomic counts via light microscopy, cell abundances via flow cytometry, 18S-metabarcoding, and metagenomics (e.g., metagenome-assembled genomes of protists) (Table S2) will elucidate seasonal trends in ice and water column protists in unprecedented detail. Interestingly, the same groups and genera (e.g., *Gymnodinium* spp., *Pseudo-nitzschia* spp., unidentified flagellates) contributed significantly to the protist communities in both habitats over the fully annual cycle despite strong variations in environmental conditions (Figure 9). Importantly, significant contributions of both in-ice microalgae (e.g., *Nitzschia frigida*) as well as under-ice-attached microalgae such as *Melosira arctica* to the protist assemblages were observed. The latter species was so abundant in certain under-ice habitats that it formed its own microhabitat, which team ECO sampled in more detail.

A diverse and abundant zooplankton community (Figure 11) was observed over the entire MOSAiC campaign. Ongoing analyses focus on the interplay between seasonal (Figure 9) as well as regional patterns to decipher their seasonally resolved biogeography. The different methods employed to assess fish (Table S2) show that their stocks in the Central Arctic Ocean were very low. Still, Atlantic cod was found unexpectedly as far north as 85.9°N, along with lanternfish, armhook squid, and the Arctic endemic polar cod *Boreogadus saida* (Snoeijs-Leijonmalm et al., 2022).

Consequences of different community structures for food web dynamics and biogeochemistry are being addressed at each trophic level by different methods along the drift track and over the annual cycle. Initial analyses indicate active fecal pellet production and sinking in both winter and summer season (Figure 12). Analyses of carbon, nitrogen, algal pigments, and material types from sinking particulate organic matter collected in short-term and long-term sediment traps will enable estimates of time-integrated fluxes of material over specific periods of the winter and summer seasons below level- and ridged sea ice, and from along the drift track at 200 m depth. Additionally, ongoing analyses of particle size spectra from the LISST and UVP will allow higher resolution estimates of POM fluxes. Profiles from the UVP also generated images of particles > 100 micron in size and based on machine learning techniques, these images can be cataloged into particle-specific types, further informing changes in particle size abundances and distributions along the drift.

3.3. Potential impacts of diverse and ephemeral habitats on ecosystem processes

Consistent with previous research, our initial observations suggest that the presence of meltwater layers represents a drastic change in the environmental and chemical nature of the upper ocean, and elicit changes in biological properties and activities (Smith et al., 2022). Stratification in the upper 1-2 m of the ocean creates a strong gradient and boundaries which most organisms are unable to cross, thus creating small microhabitats within each of these layers. These adjacent layers may support potentially disparate activity rates, standing stocks, and biogeochemical fluxes despite their close spatial relation. As such, meltwater layers may introduce habitat structuring which greatly impacts ecosystem functioning. Furthermore, meltwater layer formation affects the gas exchange process with the atmosphere, such that a meltwater layer at the surface may lead to the equilibrium of gases with the atmosphere, thereby reducing the gradient of concentration with the atmosphere and the flux (Smith et al., 2023; von Appen et al., 2021). The mixing of meltwater and the underlying seawater during summertime potentially produces water with low CO_2 concentration.

Based on opportunistic sampling, we could observe ecosystem processes in various other sea ice types, resulting from different formation processes (Figure 13). Summer season sampling in leads (Figure 13 A, B) and water close to the bottom of the ice provided further insight into how ice dynamics and ephemeral phenomena may alter biological responses over time-scales missed by our regular weekly sampling. It indicated the formation of extremely high biomass layers on the boundary between meltwater and seawater, with distinct composition and biogeochemical characteristics (Smith et al., 2023).New ice formations, typically ranging from 1 to 10 cm in thickness, and from loosely-formed crystals to consolidated nilas ice, were sampled periodically throughout the drift, primarily from leads near or across the central floe (Figure 13 C, D), with preliminary data indicating higher organismal abundances and Chl-a concentrations than the surrounding seawater (data not shown). Our series of samples of newly formed ice at different time periods over the annual cycle will provide us with complementary data on how environmental conditions (Figure 9) influence biological and ecological processes during initial thermodynamic ice formation. Sea-ice ridges (Figure 13 G, H) were also sampled periodically for biological properties and vertical export of material during MOSAiC. This habitat featured seawater-filled voids with an accumulation and high activity of microbial biota (see 3.5.1. for details).

3.4. Gaps in time-series measurements

Overall, the MOSAiC ecological field program captured a large number of co-located properties at a regular frequency. However, with differing competencies across each field team, and despite efforts to cross-train and build redundancy in skill sets, there are some gaps in the ecosystem time-series measurements. While risk assessments and prioritization schemes were devised, execution in the field was determined by what could be achieved by the field team, and different factors at different times contributed to variations in the continuity of specific data sets. Here, we outline the key gaps in measurements, so that future users of MOSAiC ECO data sets can easily identify when in the annual cycle certain measurements are not available. Activity rate measurements, such as primary and bacterial production, only began in January and late December 2019, respectively. Samples for water column DOM characterization after solid-phase extraction are only available from April, May, August and September 2020. ^{15}N-nitrate isotopes from sea ice were collected from December 2019 onwards. RNA samples from bottom portions of sea ice are only available from April 2020 onwards. There were no daily discrete sample collections for Chl-a and microbial community structure from December 2019 to end of February 2020. Likewise, MIMS data from December 2019 to the beginning of March 2020 is of substantially lower reliability compared to the rest of the drift.

3.5. Case Studies

In the following, two selected case studies are presented to illustrate the kinds of results the ECO team is working on to address specific scientific questions. These examples have been chosen because they demonstrate the interdisciplinary connections within MOSAiC, specifically regarding the role the geophysical restructuring of ice had on habitat and with respect to how biological processes contributed to elemental transformations and influenced central Arctic biogeochemistry.

3.5.1. Pressure ridges, unique habitats for ice-associated biota?

Level, undeformed sea ice provides a wide range of niches for ice-related organisms, ranging from biota living in the brine channel systems within the ice to under-ice flora and fauna living at the ice-water interface (Lund-Hansen et al., 2020). These level sea-ice systems are studied in detail using the ICE and ECO time-series (see also Nicolaus et al., 2022b). However, deformed sea ice in pressure ridges adds substantial three-dimensional diversity in the available habitat space through macroporosity (voids filled with seawater between ice blocks, often referred to as rubble) in the ridge keels (Fig. 14). Ridge keels in the Arctic can reach substantial ice drafts exceeding 20 m keel depth (Wadhams and Toberg, 2012), making ridge coring or observations of voids within ridges exceptionally challenging. Sporadic observations from previous Arctic studies suggested unique biological hotspots associated with the water filled voids in unconsolidated keel rubble and ice block surfaces within the pressure ridges (Fernández-Méndez et al., 2018; Gradinger et al., 2010; Syvertsen, 1991). Truly understanding the ecological processes associated to pressure ridges was the core of one dedicated research project (*Safe HAVens for ice-associated flora and fauna in a seasonally ice-covered Arctic Ocean (HAVOC))*, that across several MOSAiC teams performed detailed and interdisciplinary observations of ridges (Figure 14) in the MOSAiC Central Observatories (CO1 and CO2), with the aim to study the year-round physical and biological characteristics of sea ice ridges.

Relocations of *Polarstern* and sea-ice deformation events in the CO caused disruptions in the time-series, resulting in four different pressure ridge sites being studied during December 2019 and August 2020, with most HAVOC data being collected between January and July 2020. Sampling included ice drilling, coring, and ridge ice and void water sampling to study the temporal evolution of physical characteristics of pressure ridges such as consolidation and melting (Lange et al., 2023; E. Salganik et al., 2023; Evgenii Salganik et al., 2023b). Further, the ridges were studied as habitats by examining the relationship between ridge structure and biological properties (e.g., algal and microbial diversity in ice and void water), under-ice hyperspectral imaging of algal biomass distribution along the pressure ridge keels (Figure 15), and vertical particle flux in the proximity of the ridges using sediment traps. The essential comparative measurements of level first-year and second-year sea ice properties were provided by the ICE and ECO time-series data.

Ongoing interdisciplinary discussions within the HAVOC team already showcased significant science gains.

- Ridge consolidation: Freeze and melt cycles within ridge rubble are more complex than for level sea ice and significantly impact biological habitat diversity and availability. For example, refreezing of snow-slush transported to ridge keel during dynamic event in early spring and surface meltwater in summer led to rapid ridge consolidation with implications on the structure and functioning of the microbial community and habitat loss for larger fauna in ridge keels (Salganik et al., 2023ab, Lange et al., 2023).

- Hyperspectral imaging of the bottom of level and ridged sea ice indicates higher fractions of ice surfaces inhabited by algae in the ridged ice (Figure 16). For this purpose, a new Relative ice algal Biomass Index (RBI) was developed (Lange et al., submitted).
- Ice surfaces and water-filled voids within ridges contained distinct microalgal and bacterial communities in contrast to level sea ice and seawater.
- Changes in ice structure due to ridge formation, consolidation, and melting have consequences on biological processes reaching beyond the physical location of ridges, as frozen organic material can be released during ridge formation in winter, and melt water can accumulate under level ice next to ridges during summer, both affecting food availability and habitat for under-ice fauna and flora, respectively.
- A new sediment trap deployment methodology under the ridge revealed unique ice-associated particle dynamics and vertical flux measurements,

Upcoming analyses will focus on comprehensive characterizations of ridge properties (e.g., using time-series data) and will be compared to those from level ice and under-ice seawater samples. This will help to assess how ridge biodiversity and ecosystem functioning are driven by this specific physical habitat (i.e. find answers to the who, how and why?). In addition to the knowledge gain, the field experience with sampling ridges provides an additional legacy product by HAVOC and MOSAiC through methodological recommendations for future ridge studies.

3.3.2. Effects of seasonally changing mesozooplankton grazing on carbon and nitrogen cycling in the central Arctic

Mesozooplankton are important transformers of organic carbon (C) and nitrogen (N), converting phytoplankton and microzooplankton into larger-sized biomass (Figure 17). Mesozooplankton feeding activity and fecal pellet production regulates the retention of organic C and N in the upper ocean mixed layer versus their transfer to deeper waters. The Arctic mesozooplankton community is often dominated by copepods of the genus *Calanus*, including two high-Arctic species (*C. hyperboreus* and *C. glacialis*) as well as the advected North Atlantic indicator species *C. finmarchicus* (Ershova et al., 2021). These species' life cycles differ in their adaptations to Arctic seasonality. Until MOSAiC, there had been no year-round direct measurements of *Calanus*-related food web dynamics in the Central Arctic. This is a complex and challenging task, as evaluating the importance of mesozooplankton-mediated transformations and fluxes requires quantification both of standing stocks and of rate processes as well as understanding of zooplankton diet in relation to food abundance. It was achievable within the MOSAiC framework only through the tight collaboration of several science teams providing time series data of ocean and sea ice physical properties, food availability (microalgae and microzooplankton abundances and standing stocks), as well as quantification of mesozooplankton standing stocks and distributions. These time series data provide the necessary context for a research project (Collaborative Research: The role of planktonic lower trophic levels in carbon and nitrogen transformations in the Central Arctic, a MOSAiC proposal) focused on direct measurements of the transformations of C and N by the zooplankton using rate process measurements. The key overarching questions are:

- How closely aligned are the life histories and productivity cycles of the dominant secondary producers to the ice algal and/or phytoplankton blooms?
- What are the transformations that occur (e.g., respiration, feeding, growth/reproduction, fecal pellet export) and how do these vary throughout the year?
- How do food webs change seasonally? What is the importance of ice vs. water column production to spring zooplankton productivity and how important is the microbial food web during summer to growth and overwintering survival of mesozooplankton?

To answer these questions, project members participated in the MOSAiC cruise from December 2019 to October 2020, with supportive measurements provided by Team ECO before that period. The experimental studies included measurements of respiration, egg production timing and rates, egg hatching success of two dominant copepods (*C. glacialis* and *C. hyperboreus*), and grazing rates on both phytoplankton and microzooplankton of dominant copepods (*C. glacialis, C. hyperboreus, Metridia longa*). These experiments were augmented by DNA gut content analyses. In spring and early summer, when the ice floe had drifted across the Gakkel Ridge into the more Atlantic-influenced Nansen Basin, the Atlantic indicator species *C. finmarchicus* also was included. Individual copepods were photographed for identification and used for determination of carbon and nitrogen content, and trophic marker characteristics.

The final detailed analyses of the data sets will relate the experimental rate measurements to their distribution as estimated from nets and the LOKI, prey type and food concentrations will be augmented by gut DNA contents. The outcomes of will provide critical data to all three ECO science questions (‘who’, ‘how’, and ‘why’), help determine the C and N flow through the planktonic ecosystem (Figure 17) during different seasons over the course of the drift (Figure 9), and provide critical information for integrative ecosystem modeling during the ECO synthesis phase.

4. STATUS, LINKAGES, PERSPECTIVES, AND SCIENTIFIC IMPACTS

4.1. Current status and major achievements

MOSAiC ECO sample and data analyses are still ongoing, and new and exciting data and scientific findings will continue to emerge over the next decade. Nevertheless, some major achievements can already be identified, some of which will lead to a step-change in understanding of the ‘whos, hows, and whys’ of the high Arctic ecosystem:

- The largest number of samples to assess biodiversity ever collected at such a high spatiotemporal resolution in the central Arctic Ocean will allow for a comprehensive ecosystem description from viruses to fish and squid for all seasons along the drift.
- Unprecedentedly high winter standing stocks and activity levels of organisms in the largely unstudied high Arctic polar night were observed.
- The biological property measurements in a diverse range of seasonally-occurring habitats were conducted, including in-depth characterizations of biological hotspots (e.g., pressure ridges, meltwater layers).
- Rate measurements for key biological processes (e.g., primary and bacterial production, zooplankton grazing and respiration rates) throughout all seasons provide a crucial foundation for the parameterization of biogeochemical models over complete annual cycles.
- The largest sequencing effort for polar ecosystems will provide a benchmark for biodiversity change (Mock et al., 2022).
- Cross-cutting analysis have revealed that Central Arctic biological processes can affect the atmospheric composition during the melt season (Yue et al., 2023) and have the potential to impact cloud processes (Creamean et al., 2022).
- MOSAiC ECO supported a large and diverse suite of projects covering either a particular season or environment, or a full year, which will enable us to obtain a wealth of knowledge on specific aspects of species biology and ecology, and a better understanding of seasonal changes in these aspects.

The co-located, in-depth characterization of environmental conditions driven by the interdisciplinary character of MOSAiC allows to link biological observations to abiotic driving factors (e.g., for fast transition periods that are hard to predict in terms of timing), and in turn to determine when biological interactions are likely the main driving force of ecosystem dynamics (Behrenfeld, 2010). As one example, nutrients, representing one major controlling factor of Arctic productivity (Randelhoff et al., 2020; Tremblay et al., 2015), indicate strong spatial differences across water masses along the drift (Schulz et al., 2023b) that dominate variability due to potential signals of seasonal uptake and limitation dynamics. The presence of surface ocean nitrate concentrations around 2 µM at the end of summer and into fall at >84 °N warrant close inspection concerning the dynamics supplying nutrients to the sunlit layers, potentially indicating iron limitation of primary production in Nansen Basin (Rijkenberg et al., 2018). This could lead to a paradigm shift in our understanding of Arctic primary production (Ardyna and Arrigo, 2020; Tremblay et al., 2015; Wassmann and Reigstad, 2011). The large imprint that water masses had on important environmental drivers such as nutrient concentrations illustrate that many statements about the Arctic cannot be generalized but need to be region-specific.

The interdisciplinary approach of MOSAiC will also allow us to better parameterize and map cross-disciplinary linkages that may not be obvious a-priori. For example, sea ice algae might change the energy absorption of ice and ocean (Manizza et al., 2013), thereby affecting Arctic heat budgets along the atmosphere-ice-ocean continuum (Shupe et al., 2022). New tools such as hyperspectral imagers deployed on remotely operated vehicles (see case study 1) may enable comprehensive mapping of ice algae potentially facilitating improved quantitative evaluation of biological effects on ice transmission and heat budgets.

Comprehensive studies of a number of periodically-occurring habitats found them to be biological hotspots, including meltwater-influenced systems and pressure ridges. Unique habitat-specific processes may provide major additions to fluxes of energy and matter; thus, their quantification is needed for a complete view on high Arctic biogeochemistry and ecology. Our data will allow us to evaluate the relative role of these short-lived hotspot habitats compared to the perennial habitats, such as level sea ice. Several of these habitats develop during the summer season (e.g., melt ponds, meltwater layers, unconsolidated water-filled voids in pressure ridges), but later in the year may have residual structuring of habitats, which affect organismal life strategies during different periods of the annual cycle. While these features primarily form during the summertime, their altered states can persist into later seasons and even the following year. For example, remnants or “fingerprints” of these hotspots may be identifiable, such as refrozen melt ponds or refrozen (consolidated) voids in ridges, and characterized during the winter season as overwintering habitats for a range of Arctic organisms.

4.2. Challenges and Lessons Learned

MOSAiC observations and samples were conducted year-round, often in challenging conditions. This required frequently adapting standard ship and on-ice operations and team operations as well as adjusting the science objectives. Given the major focus of MOSAiC on interactions between atmosphere, sea ice, and ocean, we intentionally limited our work program to focus on the ecological and biogeochemical components that are relevant for the sea ice and upper ocean, excluding the deepest water layers and the benthos. Additionally, in an effort to focus on measurements that would elucidate biological feedbacks in the Arctic climate system, we did not include observations of megafauna, such as sea birds and mammals, although they provide important ecosystem services and are highly impacted by climate change (Hamilton et al., 2022).

Some unique challenges we addressed in the preparation phase were related to potential impacts of the anticipated long-term drift on the scientific data collection. Key adaptations were made in conjunction with other science teams and the ship´s crew (see section 2.4 for details). Additionally, during the preparation phase, we took steps to train and prepare field personnel to execute a variety of tasks and protocols encompassing a broader range of activities than they would have been responsible for within an expedition of narrower scope than MOSAiC. Building competencies and redundancies in the skill sets of field personnel was important to realizing the diverse work program. However, it was not always possible, and in some instances gaps in our time-series measurements exist because it was not feasible for the field team to accomplish all the tasks (see Section 3.4). Additional modifications were necessary onboard based on expected irregular disturbances (e.g., storms, ice break-up) as well as unexpected events (e.g., the COVID-19 outbreak). In the future, improved prioritization of sample collections, development of more semi-automated sampling and processing devices, and increased training on unfamiliar data logging routines will strengthen execution of complex work programs. Our experience with MOSAiC ECO work will also provide us with the opportunity to better determine which suites of properties are most needed for addressing future questions and objectives related to high Arctic ecosystem changes.

Our data analyses will need to disentangle temporal versus spatial aspects to observed changes in biological properties and ecological processes over the course of the drift. This can be nicely illustrated by the development of nitrate concentrations over the course of the expedition (Figure 9E). Even though nitrate is considered one of the two major limiting factors for Arctic primary production (Tremblay et al., 2015), its concentrations increased over the main microalgal growing season, i.e., from March to July. While this seems counterintuitive at first, it can be explained by the drift of the ice floe into areas with increasingly larger influence by nitrate-rich Atlantic water masses (Rabe et al., 2022; Schulz et al., 2023b). Such water mass effects also influence other measured parameters such as DOM characteristics (Gonçalves-Araujo et al., 2016, Kong et al., under review), and potentially the presence or absence of certain organismal groups and species (Kaiser et al., 2022). Also, the faster-than-expected drift speed of the main MOSAiC floe resulted in earlier arrival into Atlantic inflow-influenced waters and proximity to the ice edge, resulting in significant deformation and instability of the first Central Observatory. Therefore, after the logistical departure in May 2020, the ice camp had to be relocated to a different part of the original ice floe and a second Central Observatory was established. While these aspects are part of the nature of a drift campaign, their influence on how one can interpret our observations is central to our understanding of ecosystem processes during the MOSAiC field year.

4.3. Ecosystem research in the context of Arctic System Science

MOSAiC was designed to improve our understanding of the governing principles of the Arctic climate system and thus can be used in an earth system science approach. This is particularly urgent as the Arctic is warming four times faster than the global average (Rantanen et al., 2022). Developing baseline knowledge on the ‘who’, ‘how’, and ‘why’ of the high Arctic was the foundational principle of the ecosystem science program, and the data already demonstrate multiple connections within the ecosystem compartments and to the whole Arctic system including the presence of INPs of marine biological origin (Creamean et al., 2022). The Arctic Ocean can be both a source and sink for greenhouse gases, like CO_2 and methane. Annual cycles of fluxes of such substances are currently being investigated in relation to bacterial biodiversity, algal activity, and respiration. For instance, it is expected that a combination of the broad scope of information from several MOSAiC science teams will help resolve the “ocean methane paradox” explaining periodically enhanced CH_4 concentrations in ocean surface waters (Rees et al., 2022). Great uncertainty exists regarding the future role of the Arctic Ocean as a source or sink for CO_2, where melting of sea ice combined with increased productivity could regionally lead to an intensified sink (Rees et al., 2022), while other Arctic areas might experience a reduction of carbon fixation and export due to increased sea ice melt-induced stratification (von Appen et al., 2021). Other processes which can potentially lead to CO_2 outgassing by the Arctic Ocean include decreased solubility driven by warmer temperatures, equilibration with the atmosphere (Cai et al., 2010; Else et al., 2013), or wind-driven mixing of surface waters with more carbon-rich subsurface layers (Lannuzel et al., 2020). MOSAiC ECO data will fill important regional and pan-Arctic knowledge gaps in our understanding and may help to determine those mechanisms that will drive the effects of climate change on the Arctic carbon cycle.

A set of different ecosystem and fully coupled Arctic Ocean models will be essential tools for integrating information across the ecosystem and the entire Arctic system using MOSAiC data, targeting not only specific questions like carbon cycling in the Arctic or production of climate relevant greenhouse gases, but also transferring these process-focused knowledge gains into products to understand climate change on larger regional and temporal scales. The unprecedented increase in knowledge on biodiversity and gene expressions in relation to environmental variables (Mock et al., 2022) will allow for the application of models to elucidate metabolic and energetic fluxes within the Arctic microbial consortia (Succurro and Ebenhöh, 2018). This combined application of different model types (e.g. see will be an important tool to differentiate the intertwined role of spatial and temporal variability in MOSAiC data sets.

5. OUTLOOK

The knowledge created by the ecological research during MOSAiC will provide a lasting legacy for future studies focusing on the Arctic System. For the first time, biodiversity and ecosystem functioning were studied on multiple trophic levels over a full seasonal cycle using traditional and novel approaches.

The legacy of MOSAiC goes beyond publications, developing novel sampling approaches and the openly accessible data archives. Indeed, the open and growing network of researchers across many nations and disciplines can be expected to have a lasting effect on Arctic marine research, particularly considering the high number of early career scientists that are already involved. New spin-off projects initiated through MOSAiC include projects on microbial processing and biogeochemical modeling, remote sensing of under-ice blooms, sea ice-ecosystem modeling, and a yearround ecosystem study in an Arctic fjord. The gained knowledge will help to evaluate the importance of the Arctic for climate regulation. Although incomplete, several publications have demonstrated the broad range of currently known ecosystem services provided by the Arctic marine system to humans including regulation of greenhouse gases and biodiversity (Malinauskaite et al., 2019). MOSAiC-based knowledge will also support political decision-making processes through, e.g., Arctic Council initiatives on the management of Arctic marine ecosystems (e.g. PAME). Although MOSAiC ECO covers a very broad range of ecological topics and will fill many knowledge gaps, many research questions remain unanswered or are now newly defined. The free, findable, accessible, interoperable, and reusable MOSAiC data will be a major milestone of success, providing together with the gained knowledge, the backbone for interdisciplinary marine Arctic research for decades to come.

The broad range of realized measurements and samples from MOSAiC ECO will make it possible to move from the observed answers of the 'who' and 'how' to developing process-based mechanistic understanding of the 'why', also by means of modeling approaches (see below). Mechanistic understanding in turn will allow moving beyond the specific locations and conditions during our observational period. The observation of high levels of biomass presence and organismal activity during the months-long cold and dark polar night, for example, provides the foundations for new investigations regarding overwintering mechanisms, strategies, and physiological adaptations. The combination of rate measurements, observations on different life stages, physiological and food web experimental work, as well as information originating from metagenomics and metatranscriptomics will allow an improved understanding the current overwintering mechanisms. Also, it will provide improve scenarios regarding the potential impacts of a future warmer Arctic with a reduced and changed ice cover, for example on effects on winter survival, annual productivity, and biogeochemical cycles. Here, synergies between the ECO team and the BGC science with its focus on trace and greenhouse gases as well as cycling of sulfur, nitrogen and carbon will be essential. Entrainment of the detected processes and rates into ecosystem and biogeochemical models will also greatly improve the validity of such future scenario estimations. While a one-year field-period cannot observe climate change trends directly, MOSAiC science is a step-change in Arctic ecosystem understanding that will provide a baseline upon which future changes can be identified, while also providing the potential for improved projections of future changes based on the advanced process-based interdisciplinary understanding.

Data accessibility statement

Drift track data for each MOSAiC leg is available via Pangaea (Haas, 2020; Kanzow, 2020; Rex, 2021a, 2021b, 2020).

Combined surface ocean temperature and salinity from different sensors as described in (Schulz et al., 2023b) is available via the Arctic Data Center (Schulz et al., 2023a),

Air temperatures at 2 m over the MOSAiC floe are available at the Arctic Data Center (Cox, 2023).

Incoming PAR data was derived from radiation station measurements published at PANGAEA (Nicolaus et al., 2023b, 2023a, 2022a).

Data publication of nutrient data is under way. Data is available upon request from Sinhué Torres-Valdes (sinhue.torres-valdes@awi.de). Other metadata shown is either available in the supplementary information or will be published together with the data once quality controlled, and are available from the authors upon request.

Author contributions

Developed the concept and design: AAF and RRG with input from co-authors
Conducted the field sampling: AAF, CJMH, CJA, YB, JPB, JB, DB, RGC, GC, EJC, JMC, ESD, SLE, AAF, JG, CEG, NH, AI, BAL, KM, OM, DN, LMO, SR, SS, ES, KS, KMS, PSL, JS, AS, STV, AT, AU, ALW
Drafted and revised the article: AAF, CJMH and RRG with contributions from co-authors
Approved the submitted version for publication: all co-authors

Acknowledgements

This manuscript is part of the international Multidisciplinary drifting Observatory for the Study of the Arctic Climate (MOSAiC) with the tag MOSAiC20192020 and the Project ID AWI_PS122_00. We thank the cruise participants, ship's crew and logistics support as well as everyone else who contributed to the realization of MOSAiC (Nixdorf et al. 2021). This work was supported by the Swedish Polar Research Secretariat as part of the MOSAiC 2019-2020 expedition. Water column nutrient analyses on land were carried out at the AWI Nutrient Facility.
L. Heitmann, S. Spahic, T. Brenneis, A. Terbrüggen, G. Guillou, K.-U. Ludwichowski, K.U. Richter, D. Scholz, T. Klüver, J. Roa, and R. Flerus are acknowledged for technical support. S. Tippenhauer, M. Hoppmann, J. Schaffer, and K. Schulz are acknowledged for their help with CTD sampling and data provision. We thank J. Grosse for sampling and measurements on leg 2. V. Moulton and R. M. Leggett are acknowledged for the help with genomic and transcriptomic analyses. We thank Prune Leroy for essential contributions to the sequencing-based characterization of biodiversity. M. Künsting and Y. Nowak are acknowledged for their help with the schematic overview figure. We thank the science journalist Marlene Göring for her help during Leg 5 field sampling.

Funding information

This work was funded by The German Federal Ministry for Education and Research (BMBF) through financing the Alfred-Wegener-Institut Helmholtz Zentrum für Polar- und Meeresforschung (AWI) and the Polarstern expedition PS122 under grant N-2014-H-060_Dethloff and by AWI through its projects: AWI_ECO, AWI_BGC, AWI_ATMO, AWI_ICE, and AWI_SNOW.
The funding for AE and MC was provided by the Helmholtz Association and by the MicroARC project (03F0802A) within the Changing Arctic Ocean program, jointly funded by the UKRI Natural Environment Research Council (NERC) and the German Federal Ministry of Education and Research (BMBF).

ALW and HS were funded through the UK Natural Environment Research Council’s (NERC) contribution to MOSAiC, grant NE/S002596/1 for the SIMbRICS project.
AU received funding from the Swedish Research Council Formas (grant no. 2018-01398) and the Carl Trygger Foundation (grant no. CTS 15:505).
BLwas supported by a Fellowship from the Hanse-Wissenschaftskolleg Institute for Advanced Study, Delmenhorst, Germany.
CJMH received funding from the German Ministry for Education and Research (BMBF) through the project NiceLABpro (grant no. 03F0867A).
DKP received funding from the United States National Science Foundation, NSF-OPP 2138785.
DN was supported by the Japan Society for the Promotion of Science (grant numbers: JP18H03745; JP18KK0292; JP17KK0083; JP17H04715; JP20H04345), a grant from the Joint Research Program of the Japan Arctic Research Network Center, and the Arctic Challenge for Sustainability II (ArCS II) project.
KS was funded through the UK Natural Environment Research Council’s (NERC) contribution to MOSAiC, the SYM-PEL project (NE/S002502/1).
JB, BL and EJC were supported by the National Science Foundation under the grant no. NSF-OPP 1821911.
JMC, TH, KB and CM were supported by the Department of Energy's Atmospheric Radiation Measurement (DOE ARM) User Facility (grant #: DE-AC05-76RL01830) and DOE's Atmospheric Systems Research (DOE ASR) Program (grant #s: DE-SC0019745 and DE-SC0022046).
JS, MAVL, and DB were supported by the Dutch Research Council (NWO), through the Netherlands Polar Programme (NPP), Project no 866.18.002.
MAG, RGR, AL, EL, GB, NA, PA, BAL, ES, JG, LMO, and OM were supported by the Research Council of Norway (RCN) through the project HAVOC (grant no. 280292). MAG and BAL were also supported by the RCN through the project CAATEX (grant no. 280531) and ES by RCN project INTERAAC (grant no. 328957).
MAG was also supported through the European Union’s Horizon 2020 research and innovation program project ARICE (EU grant no. 730965).
MDS was funded by the National Science Foundation (OPP-1724551) and the NOAA Physical Sciences Laboratory (NA22OAR4320151).
MO was funded by the US National Science Foundation under award number OPP-1735862.
OE and EO were supported by the Deutsche Forschungsgemeinschaft (DFG) under grant number EB 418/6-1 (From Dusk till Dawn) as well as Germany's Excellence Strategy - EXC-2048/1 - project ID 390686111.
PSL, SB, MB, SLE, JPB and AT were supported by the Swedish Research Council VR (2018-04685), the Swedish Research Council Formas (2018-00509) and the Swedish Polar Research Secretariat (2019-153).
PSL, SB, HF, BN, NH, CG, SS, FLS, MB, AS and MV were supported by the European Commission (EASME/EMFF/2018/003) and the Swedish Polar Research Secretariat (2019-153).
STV received funds from the NERC-BMBF PEANUTS Project (Grant No. 03F0804A).

TM received funding from the USA Department of Energy (DOE) Joint Genome Institute (10.46936/10.25585/60001271, DE-AC02-05CH11231), the Natural Environment Research Council UK (NE/S002596/1, NE/S007334/1, NE/K004530/1, NE/R000883/1, NE/R012644/1) and the Leverhulme Trust (RPG-2017-364).

References

Alfred-Wegener-Institut Helmholtz-Zentrum für Polar- und Meeresforschung, 2017. Polar Research and Supply Vessel POLARSTERN Operated by the Alfred-Wegener-Institute. J. Large-Scale Res. Facil. 3, A119. https://doi.org/10.17815/jlsrf-3-163

Angelopoulos, M., Damm, E., Simões Pereira, P., Abrahamsson, K., Bauch, D., Bowman, J., Castellani, G., Creamean, J., Divine, D.V., Dumitrascu, A., 2022. Deciphering the properties of different arctic ice types during the growth phase of MOSAiC: Implications for future studies on gas pathways. Front. Earth Sci. 10, 864523.

Ardyna, M., Arrigo, K.R., 2020. Phytoplankton dynamics in a changing Arctic Ocean. Nat. Clim. Change. https://doi.org/10.1038/s41558-020-0905-y

Ardyna, M., Mundy, C.J., Mills, M.M., Oziel, L., Grondin, P.-L., Lacour, L., Verin, G., van Dijken, G., Ras, J., Alou-Font, E., Babin, M., Gosselin, M., Tremblay, J.-É., Raimbault, P., Assmy, P., Nicolaus, M., Claustre, H., Arrigo, K.R., 2020. Environmental drivers of under-ice phytoplankton bloom dynamics in the Arctic Ocean. Elem. Sci. Anthr. 8. https://doi.org/10.1525/elementa.430

Ashjian, C.J., Campbell, R.G., Welch, H.E., Butler, M., Van Keuren, D., 2003. Annual cycle in abundance, distribution, and size in relation to hydrography of important copepod species in the western Arctic Ocean. Deep Sea Res. Part Oceanogr. Res. Pap. 50, 1235–1261. https://doi.org/10.1016/S0967-0637(03)00129-8

Assmy, P., Fernández-Méndez, M., Duarte, P., Meyer, A., Randelhoff, A., Mundy, C.J., Olsen, L.M., Kauko, H.M., Bailey, A., Chierici, M., Cohen, L., Doulgeris, A.P., Ehn, J.K., Fransson, A., Gerland, S., Hop, H., Hudson, S.R., Hughes, N., Itkin, P., Johnsen, G., King, J.A., Koch, B.P., Koenig, Z., Kwasniewski, S., Laney, S.R., Nicolaus, M., Pavlov, A.K., Polashenski, C.M., Provost, C., Rösel, A., Sandbu, M., Spreen, G., Smedsrud, L.H., Sundfjord, A., Taskjelle, T., Tatarek, A., Wiktor, J., Wagner, P.M., Wold, A., Steen, H., Granskog, M.A., 2017. Leads in Arctic pack ice enable early phytoplankton blooms below snow-covered sea ice. Sci. Rep. 7, 40850. https://doi.org/10.1038/srep40850

Babin, M., Arrigo, K., Bélanger, S., Forget, M.-H., 2015. Ocean Colour Remote Sensing in Polar Seas.

Balmonte, J.P., Teske, A., Arnosti, C., 2018. Structure and function of high Arctic pelagic, particle-associated and benthic bacterial communities. Environ. Microbiol. 20, 2941–2954. https://doi.org/10.1111/1462-2920.14304

Barber, D.G., Hop, H., Mundy, C.J., Else, B., Dmitrenko, I.A., Tremblay, J.-E., Ehn, J.K., Assmy, P., Daase, M., Candlish, L.M., Rysgaard, S., 2015. Selected physical, biological and biogeochemical implications of a rapidly changing Arctic Marginal Ice Zone. Overarching Perspect. Contemp. Future Ecosyst. Arct. Ocean 139, 122–150. https://doi.org/10.1016/j.pocean.2015.09.003

Behrenfeld, M.J., 2010. Abandoning Sverdrup's Critical Depth Hypothesis on phytoplankton blooms. Ecology 91, 977–989.

Berge, J., Daase, M., Renaud, P.E., Ambrose, W.G., Darnis, G., Last, K.S., Leu, E., Cohen, J.H., Johnsen, G., Moline, M.A., Cottier, F., Varpe, Ø., Shunatova, N., Bałazy, P., Morata, N., Massabuau, J.-C., Falk-Petersen, S., Kosobokova, K., Hoppe, C.J.M., Węsławski, J.M., Kukliński, P., Legeżyńska, J., Nikishina, D., Cusa, M., Kędra, M., Włodarska-Kowalczuk, M., Vogedes, D., Camus, L., Tran, D., Michaud, E., Gabrielsen, T.M., Granovitch, A., Gonchar, A., Krapp, R., Callesen, T.A., 2015. Unexpected Levels of Biological Activity during the Polar Night Offer New Perspectives on a Warming Arctic. Curr. Biol. 25, 2555–2561. https://doi.org/10.1016/j.cub.2015.08.024

Berry, D., Widder, S., 2014. Deciphering microbial interactions and detecting keystone species with co-occurrence networks. Front. Microbiol. 5, 219.

Biard, T., Stemmann, L., Picheral, M., Mayot, N., Vandromme, P., Hauss, H., Gorsky, G., Guidi, L., Kiko, R., Not, F., 2016. In situ imaging reveals the biomass of giant protists in the global ocean. Nature 532, 504–507.

Bluhm, B.A., Gebruk, A.V., Gradinger, R., Hopcroft, R.R., Huettmann, F., Kosobokova, K.N., Sirenko, B.I., Weslawski, J.M., 2011. Arctic Marine Biodiversity. Oceanography 24, 232–248.

Bluhm, B.A., Hop, H., Vihtakari, M., Gradinger, R., Iken, K., Melnikov, I.A., Søreide, J.E., 2018. Sea ice meiofauna distribution on local to pan-Arctic scales. Ecol. Evol. 8, 2350–2364. https://doi.org/10.1002/ece3.3797

Bluhm, B.A., Kosobokova, K.N., Carmack, E.C., 2015. A tale of two basins: An integrated physical and biological perspective of the deep Arctic Ocean. Overarching Perspect. Contemp. Future Ecosyst. Arct. Ocean 139, 89–121. https://doi.org/10.1016/j.pocean.2015.07.011

Boetius, A., Anesio, A.M., Deming, J.W., Mikucki, J.A., Rapp, J.Z., 2015. Microbial ecology of the cryosphere: sea ice and glacial habitats. Nat. Rev. Microbiol. 13, 677–690. https://doi.org/10.1038/nrmicro3522

Bowman, J.S., 2021. Making sense of a scent-sensing metaphor for microbes and environmental predictions. Msystems 6, 10–1128.

Bowman, J.S., Amaral-Zettler, L.A., J Rich, J., M Luria, C., Ducklow, H.W., 2017. Bacterial community segmentation facilitates the prediction of ecosystem function along the coast of the western Antarctic Peninsula. ISME J. 11, 1460–1471. https://doi.org/10.1038/ismej.2016.204

Cai, W.-J., Chen, L., Chen, B., Gao, Z., Lee, S.H., Chen, J., Pierrot, D., Sullivan, K., Wang, Y., Hu, X., Huang, W.-J., Zhang, Y., Xu, S., Murata, A., Grebmeier, J.M., Jones, E.P., Zhang, H., 2010. Decrease in the CO_2 Uptake Capacity in an Ice-Free Arctic Ocean Basin. Science 329, 556–559. https://doi.org/10.1126/science.1189338

Campbell, K., Lange, B.A., Landy, J.C., Katlein, C., Nicolaus, M., Anhaus, P., Matero, I., Gradinger, R., Charette, J., Duerksen, S., Tremblay, P., Rysgaard, S., Tranter, M., Haas, C., Michel, C., 2022. Net heterotrophy in High Arctic first-year and multi-year spring sea ice. Elem. Sci. Anthr. 10, 00040. https://doi.org/10.1525/elementa.2021.00040

Campbell, K., Mundy, C.J., Juhl, A.R., Dalman, L.A., Michel, C., Galley, R.J., Else, B.E., Geilfus, N.X., Rysgaard, S., 2019. Melt Procedure Affects the Photosynthetic Response of Sea Ice Algae. Front. Earth Sci. 7.

Carlyle, C.G., Roth, J.D., Yurkowski, D.J., Kohlbach, D., Young, B.G., Brown, T.A., Riget, F.F., Dietz, R., Ferguson, S.H., 2022. Spatial variation in carbon source use and trophic position of ringed seals across a latitudinal gradient of sea ice. Ecol. Indic. 145, 109746. https://doi.org/10.1016/j.ecolind.2022.109746

Chamberlain, E.J., Balmonte, J.P., Torstensson, A., Fong, A.A., Snoeijs-Leijonmalm, P., Bowman, J.S., 2022. Impacts of sea ice melting procedures on measurements of microbial community structure. Elem. Sci. Anthr. 10, 00017. https://doi.org/10.1525/elementa.2022.00017

Cleary, A.C., 2015. Distributions and interactions in three groups of polar marine plankton. University of Rhode Island.

Clement Kinney, J., W. Maslowski, R. Osinski, M. Jin, M. Frants, N. Jeffery, Y. J. Lee (2020) Hidden production: On the importance of pelagic phytoplankton blooms beneath Arctic sea ice, J. Geophys. Res. Oceans, 125(9), e2020JC016211, https://doi.org/10.1029/2020JC016211

Clement Kinney, J., M. Frants, W. Maslowski, R. Osinski, N. Jeffery, M. Jin, Y. J. Lee (2023) Evaluation of Under Sea-ice Phytoplankton Blooms in the Fully-Coupled, High-Resolution Regional Arctic System Model, J. Geophys. Res. Oceans, 128, e2022JC019000, https://doi.org/10.1029/2022JC019000

Cornils, A., Thomisch, K., Hase, J., Hildebrandt, N., Auel, H., Niehoff, B., 2022. Testing the usefulness of optical data for zooplankton long-term monitoring: Taxonomic composition, abundance, biomass, and size spectra from ZooScan image analysis. Limnol. Oceanogr. Methods 20, 428–450. https://doi.org/10.1002/lom3.10495

Cox, C., 2023. Atmospheric Surface Flux Station #40 measurements (Level 3 Final), Multidisciplinary Drifting Observatory for the Study of Arctic Climate (MOSAiC), central Arctic, October 2019 - September 2020. NSF Arctic Data Center.

Cox, C.J., Gallagher, M.R., Shupe, M.D., Persson, P.O.G., Solomon, A., Fairall, C.W., Ayers, T., Blomquist, B., Brooks, I.M., Costa, D., 2023. Continuous observations of the surface energy budget and meteorology over the Arctic sea ice during MOSAiC. Sci. Data 10, 519.

Creamean, J.M., Barry, K., Hill, T.C., Hume, C., DeMott, P.J., Shupe, M.D., Dahlke, S., Willmes, S., Schmale, J., Beck, I., 2022. Annual cycle observations of aerosols capable of ice formation in central Arctic clouds. Nat. Commun. 13, 3537.

DiMucci, D., Kon, M., Segrè, D., 2018. Machine learning reveals missing edges and putative interaction mechanisms in microbial ecosystem networks. Msystems 3, 10–1128.

Dutta, A., Goldman, T., Keating, J., Burke, E., Williamson, N., Dirmeier, R., Bowman, J.S., 2022. Machine learning predicts biogeochemistry from microbial community structure in a complex model system. Microbiol. Spectr. 10, e01909-21.

Ehrlich, J., Schaafsma, F.L., Bluhm, B.A., Peeken, I., Castellani, G., Brandt, A., Flores, H., 2020. Sympagic Fauna in and Under Arctic Pack Ice in the Annual Sea-Ice System of the New Arctic. Front. Mar. Sci. 7.

Else, B., Papakyriakou, T., Asplin, M., Barber, D., Galley, R., Miller, L., Mucci, A., 2013. Annual cycle of air-sea CO_2 exchange in an Arctic polynya region. Glob. Biogeochem. Cycles 27, 388–398.

Ershova, E.A., Kosobokova, K.N., Banas, N.S., Ellingsen, I., Niehoff, B., Hildebrandt, N., Hirche, H.-J., 2021. Sea ice decline drives biogeographical shifts of key Calanus species in the central Arctic Ocean. Glob. Change Biol. 27, 2128–2143. https://doi.org/10.1111/gcb.15562

Falkowski, P.G., Barber, R.T., Smetacek, V., 1998. Biogeochemical Controls and Feedbacks on Ocean Primary Production. Science 281, 200–206.

https://doi.org/10.1126/science.281.5374.200

Faust, K., Raes, J., 2012. Microbial interactions: from networks to models. Nat. Rev. Microbiol. 10, 538–550.

Fernández-Méndez, M., Olsen, L.M., Kauko, H.M., Meyer, A., Rösel, A., Merkouriadi, I., Mundy, C.J., Ehn, J.K., Johansson, A.M., Wagner, P.M., Ervik, Å., Sorrell, B.K., Duarte, P., Wold, A., Hop, H., Assmy, P., 2018. Algal Hot Spots in a Changing Arctic Ocean: Sea-Ice Ridges and the Snow-Ice Interface. Front. Mar. Sci. 5.

Fouilland, E., Gosselin, M., Rivkin, R.B., Vasseur, C., Mostajir, B., 2007. Nitrogen uptake by heterotrophic bacteria and phytoplankton in Arctic surface waters. J. Plankton Res. 29, 369–376. https://doi.org/10.1093/plankt/fbm022

Fransson, A., Chierici, M., Miller, L.A., Carnat, G., Shadwick, E., Thomas, H., Pineault, S., Papakyriakou, T.N., 2013. Impact of sea-ice processes on the carbonate system and ocean acidification at the ice-water interface of the Amundsen Gulf, Arctic Ocean. J. Geophys. Res. Oceans 118, 7001–7023. https://doi.org/10.1002/2013JC009164

Fransson, A., Chierici, M., Skjelvan, I., Olsen, A., Assmy, P., Peterson, A.K., Spreen, G., Ward, B., 2017. Effects of sea-ice and biogeochemical processes and storms on under-ice water fCO_2 during the winter-spring transition in the high A rctic O cean: Implications for sea-air CO_2 fluxes. J. Geophys. Res. Oceans 122, 5566–5587.

Fransson, A., Chierici, M., Yager, P.L., Smith Jr., W.O., 2011. Antarctic sea ice carbon dioxide system and controls. J. Geophys. Res. Oceans 116. https://doi.org/10.1029/2010JC006844

Garrison, D.L., Buck, K.R., 1986. Organism losses during ice melting: A serious bias in sea ice community studies. Polar Biol. 6, 237–239. https://doi.org/10.1007/BF00443401

Giering, S.L., Culverhouse, P.F., Johns, D.G., McQuatters-Gollop, A., Pitois, S.G., 2022. Are plankton nets a thing of the past? An assessment of in situ imaging of zooplankton for large-scale ecosystem assessment and policy decision-making. Front. Mar. Sci. 9, 986206.

Goldford, J.E., Lu, N., Bajić, D., Estrela, S., Tikhonov, M., Sanchez-Gorostiaga, A., Segrè, D., Mehta, P., Sanchez, A., 2018. Emergent simplicity in microbial community assembly. Science 361, 469–474.

Gonçalves-Araujo, R., Granskog, M.A., Bracher, A., Azetsu-Scott, K., Dodd, P.A., Stedmon, C.A., 2016. Using fluorescent dissolved organic matter to trace and distinguish the origin of Arctic surface waters. Sci. Rep. 6, 33978.

Gorsky, G., Ohman, M.D., Picheral, M., Gasparini, S., Stemmann, L., Romagnan, J.-B., Cawood, A., Pesant, S., García-Comas, C., Prejger, F., 2010. Digital zooplankton image analysis using the ZooScan integrated system. J. Plankton Res. 32, 285–303. https://doi.org/10.1093/plankt/fbp124

Gosselin, M., Levasseur, M., Wheeler, P.A., Horner, R.A., Booth, B.C., 1997. New measurements of phytoplankton and ice algal production in the Arctic Ocean. Deep Sea Res. Part II Top. Stud. Oceanogr. 44, 1623–1644. https://doi.org/10.1016/S0967-0645(97)00054-4

Gradinger, R., Bluhm, B., Iken, K., 2010. Arctic sea-ice ridges—Safe heavens for sea-ice fauna during periods of extreme ice melt? Obs. Explor. Arct. Can. Basin Chukchi Sea Hidden Ocean RUSALCA Exped. 57, 86–95. https://doi.org/10.1016/j.dsr2.2009.08.008

Granskog, M.A., Fer, I., Rinke, A., Steen, H., 2018. Atmosphere-Ice-Ocean-Ecosystem Processes in a Thinner Arctic Sea Ice Regime: The Norwegian Young Sea ICE (N-ICE2015) Expedition. J. Geophys. Res. Oceans 123, 1586–1594. https://doi.org/10.1002/2017JC013328

Haas, C., 2020. Links to master tracks in different resolutions of POLARSTERN cruise PS122/2, Arctic Ocean - Arctic Ocean, 2019-12-13 - 2020-02-24 (Version 2). Alfred Wegener Inst. Helmholtz Cent. Polar Mar. Res. Bremerhaven https://doi.org/10.1594/PANGAEA.924674

Hamilton, B.M., Jantunen, L., Bergmann, M., Vorkamp, K., Aherne, J., Magnusson, K., Herzke, D., Granberg, M., Hallanger, I.G., Gomiero, A., 2022. Microplastics in the atmosphere and cryosphere in the circumpolar North: a case for multicompartment monitoring. Arct. Sci. 8, 1116–1126.

Hobbs, L., Banas, N.S., Cottier, F.R., Berge, J., Daase, M., 2020. Eat or Sleep: Availability of Winter Prey Explains Mid-Winter and Spring Activity in an Arctic *Calanus* Population. Front. Mar. Sci. 7.

Hop, H., Vihtakari, M., Bluhm, B.A., Assmy, P., Poulin, M., Gradinger, R., Peeken, I., von Quillfeldt, C., Olsen, L.M., Zhitina, L., Melnikov, I.A., 2020. Changes in Sea-Ice Protist Diversity With Declining Sea Ice in the Arctic Ocean From the 1980s to 2010s. Front. Mar. Sci. 7, 243. https://doi.org/10.3389/fmars.2020.00243

Hop, H., Wold, A., Meyer, A., Bailey, A., Hatlebakk, M., Kwasniewski, S., Leopold, P., Kuklinski, P., Søreide, J.E., 2021. Winter-Spring Development of the Zooplankton Community Below Sea Ice in the Arctic Ocean. Front. Mar. Sci. 8.

Hoppe, C.J.M., 2022. Always ready? Primary production of Arctic phytoplankton at the end of the polar night. Limnol. Oceanogr. Lett. 7, 167–174. https://doi.org/10.1002/lol2.10222

Ibarbalz, F.M., Henry, N., Mahé, F., Ardyna, M., Zingone, A., Scalco, E., Lovejoy, C., Lombard, F., Jaillon, O., Iudicone, D., Malviya, S., Tara Oceans Coordinators, Sullivan, M.B., Chaffron, S., Karsenti, E., Babin, M., Boss, E., Wincker, P., Zinger, L., de Vargas, C., Bowler, C., Karp-Boss, L., 2023. Pan-Arctic plankton community structure and its global connectivity. Elem. Sci. Anthr. 11, 00060. https://doi.org/10.1525/elementa.2022.00060

Ingvaldsen, R.B., Assmann, K.M., Primicerio, R., Fossheim, M., Polyakov, I.V., Dolgov, A.V., 2021. Physical manifestations and ecological implications of Arctic Atlantification. Nat. Rev. Earth Environ. 2, 874–889.

Intergovernmental Panel on Climate Change (IPCC) (Ed.), 2023. Frontmatter, in: Climate Change 2021 – The Physical Science Basis: Working Group I Contribution to the Sixth Assessment Report of the Intergovernmental Panel on Climate Change. Cambridge University Press, Cambridge, pp. i–ii.

Johnsen, G., Leu, E., Gradinger, R., 2020. Marine Micro- and Macroalgae in the Polar Night, in: Berge, J., Johnsen, G., Cohen, J.H. (Eds.), POLAR NIGHT Marine Ecology: Life and Light in the Dead of Night. Springer International Publishing, Cham, pp. 67–112. https://doi.org/10.1007/978-3-030-33208-2_4

Kaiser, P., Hagen, W., Bode-Dalby, M., Auel, H., 2022. Tolerant but facing increased competition: Arctic zooplankton versus Atlantic invaders in a warming ocean. Front. Mar. Sci. 9, 908638.

Kanzow, T., 2020. Links to master tracks in different resolutions of POLARSTERN cruise PS122/3, Arctic Ocean - Longyearbyen, 2020-02-24 - 2020-06-04 (Version 2).

Alfred Wegener Inst. Helmholtz Cent. Polar Mar. Res. Bremerhaven https://doi.org/10.1594/PANGAEA.924681

Katlein, C., Schiller, M., Belter, H.J., Coppolaro, V., Wenslandt, D., Nicolaus, M., 2017. A New Remotely Operated Sensor Platform for Interdisciplinary Observations under Sea Ice. Front. Mar. Sci. 4.

Kauko, H.M., Taskjelle, T., Assmy, P., Pavlov, A.K., Mundy, C.J., Duarte, P., Fernández-Méndez, M., Olsen, L.M., Hudson, S.R., Johnsen, G., Elliott, A., Wang, F., Granskog, M.A., 2017. Windows in Arctic sea ice: Light transmission and ice algae in a refrozen lead. J. Geophys. Res. Biogeosciences 122, 1486–1505. https://doi.org/10.1002/2016JG003626

Kiko, R., Biastoch, A., Brandt, P., Cravatte, S., Hauss, H., Hummels, R., Kriest, I., Marin, F., McDonnell, A.M., Oschlies, A., 2017. Biological and physical influences on marine snowfall at the equator. Nat. Geosci. 10, 852–858.

Kim, H.H., Bowman, J.S., Luo, Y.-W., Ducklow, H.W., Schofield, O.M., Steinberg, D.K., Doney, S.C., 2022. Modeling polar marine ecosystem functions guided by bacterial physiological and taxonomic traits. Biogeosciences 19, 117–136. https://doi.org/10.5194/bg-19-117-2022

Kohlbach, D., Graeve, M., A. Lange, B., David, C., Peeken, I., Flores, H., 2016. The importance of ice algae-produced carbon in the central Arctic Ocean ecosystem: Food web relationships revealed by lipid and stable isotope analyses. Limnol. Oceanogr. 61, 2027–2044. https://doi.org/10.1002/lno.10351

Kohlbach, D., Smik, L., Belt, S.T., Hop, H., Wold, A., Graeve, M., Assmy, P., 2022. A multi-trophic marker approach reveals high feeding plasticity in Barents Sea under-ice fauna. Prog. Oceanogr. 208, 102895.

Kosobokova, K., Hirche, H.-J., 2000. Zooplankton distribution across the Lomonosov Ridge, Arctic Ocean: species inventory, biomass and vertical structure. Deep Sea Res. Part Oceanogr. Res. Pap. 47, 2029–2060.

Krembs, C., Eicken, H., Deming, J.W., 2011. Exopolymer alteration of physical properties of sea ice and implications for ice habitability and biogeochemistry in a warmer Arctic. Proc. Natl. Acad. Sci. 108, 3653–3658.

Krumpen, T., Birrien, F., Kauker, F., Rackow, T., von Albedyll, L., Angelopoulos, M., Belter, H.J., Bessonov, V., Damm, E., Dethloff, K., Haapala, J., Haas, C., Harris, C., Hendricks, S., Hoelemann, J., Hoppmann, M., Kaleschke, L., Karcher, M., Kolabutin, N., Lei, R., Lenz, J., Morgenstern, A., Nicolaus, M., Nixdorf, U., Petrovsky, T., Rabe, B., Rabenstein, L., Rex, M., Ricker, R., Rohde, J., Shimanchuk, E., Singha, S., Smolyanitsky, V., Sokolov, V., Stanton, T., Timofeeva, A., Tsamados, M., Watkins, D., 2020. The MOSAiC ice floe: sediment-laden survivor from the Siberian shelf. The Cryosphere 14, 2173–2187. https://doi.org/10.5194/tc-14-2173-2020

Kunisch EH, Graeve M, Gradinger R, Haug T, Kovacs KM, Lydersen C, Varpe Ø, Bluhm BA, 2021. Ice-algal carbon supports harp and ringed seal diets in the European Arctic: evidence from fatty acid and stable isotope markers. Mar. Ecol. Prog. Ser. 675, 181–197.

Kvernvik, A.C., Hoppe, C.J.M., Lawrenz, E., Prášil, O., Greenacre, M., Wiktor, J.M., Leu, E., 2018. Fast reactivation of photosynthesis in arctic phytoplankton during the polar night. J. Phycol. 54, 461–470. https://doi.org/doi:10.1111/jpy.12750

Lange, B.A., Salganik, E., Macfarlane, A., Schneebeli, M., Høyland, K., Gardner, J., Müller, O., Divine, D.V., Kohlbach, D., Katlein, C., Granskog, M.A., 2023. Snowmelt contribution to Arctic first-year ice ridge mass balance and rapid consolidation during summer melt. Elem. Sci. Anthr. 11, 00037. https://doi.org/10.1525/elementa.2022.00037

Lannuzel, D., Tedesco, L., van Leeuwe, M., Campbell, K., Flores, H., Delille, B., Miller, L., Stefels, J., Assmy, P., Bowman, J., Brown, K., Castellani, G., Chierici, M., Crabeck, O., Damm, E., Else, B., Fransson, A., Fripiat, F., Geilfus, N.-X., Jacques, C., Jones, E., Kaartokallio, H., Kotovitch, M., Meiners, K., Moreau, S., Nomura, D., Peeken, I., Rintala, J.-M., Steiner, N., Tison, J.-L., Vancoppenolle, M., Van der Linden, F., Vichi, M., Wongpan, P., 2020. The future of Arctic sea-ice biogeochemistry and ice-associated ecosystems. Nat. Clim. Change 10, 983–992. https://doi.org/10.1038/s41558-020-00940-4

Laurion, I., Demers, S., Vézina, A. F., 1995. The microbial food web associated with the ice algal assemblage: biomass and bacterivory of nanoflagellate protozoans in Resolute Passage (High Canadian Arctic). Mar. Ecol. Prog. Ser. 120, 77–87.

Leu, E., Brown, T.A., Graeve, M., Wiktor, J., Hoppe, C.J.M., Chierici, M., Fransson, A., Verbiest, S., Kvernvik, A.C., Greenacre, M.J., 2020. Spatial and Temporal Variability of Ice Algal Trophic Markers—With Recommendations about Their Application. J. Mar. Sci. Eng. 8. https://doi.org/10.3390/jmse8090676

Leu, E., Mundy, C.J., Assmy, P., Campbell, K., Gabrielsen, T.M., Gosselin, M., Juul-Pedersen, T., Gradinger, R., 2015. Arctic spring awakening – Steering principles behind the phenology of vernal ice algal blooms. Prog. Oceanogr. 139, 151–170. https://doi.org/10.1016/j.pocean.2015.07.012

Lombard, F., Boss, E., Waite, A.M., Vogt, M., Uitz, J., Stemmann, L., Sosik, H.M., Schulz, J., Romagnan, J.-B., Picheral, M., 2019. Globally consistent quantitative observations of planktonic ecosystems. Front. Mar. Sci. 6, 196.

Lotka, A.J., 1920. Analytical note on certain rhythmic relations in organic systems. Proc. Natl. Acad. Sci. 6, 410–415.

Ludvigsen, M., Berge, J., Geoffroy, M., Cohen, J.H., De La Torre, P.R., Nornes, S.M., Singh, H., Sørensen, A.J., Daase, M., Johnsen, G., 2018. Use of an autonomous surface vehicle reveals small-scale diel vertical migrations of zooplankton and susceptibility to light pollution under low solar irradiance. Sci. Adv. 4, eaap9887.

Lund-Hansen, L.C., Hawes, I., Hancke, K., Salmansen, N., Nielsen, J.R., Balslev, L., Sorrell, B.K., 2020. Effects of increased irradiance on biomass, photobiology, nutritional quality, and pigment composition of Arctic sea ice algae. Mar. Ecol. Prog. Ser. 648, 95–110.

MacArthur, R., 1970. Species packing and competitive equilibrium for many species. Theor. Popul. Biol. 1, 1–11.

Malinauskaite, L., Cook, D., Davíðsdóttir, B., Ögmundardóttir, H., Roman, J., 2019. Ecosystem services in the Arctic: a thematic review. Ecosyst. Serv. 36, 100898.

Manizza, M., Follows, M.J., Dutkiewicz, S., Menemenlis, D., Hill, C.N., Key, R.M., 2013. Changes in the Arctic Ocean CO_2 sink (1996–2007): A regional model analysis. Glob. Biogeochem. Cycles 2012GB004491. https://doi.org/10.1002/2012gb004491

Marangoni, L.F., Davies, T., Smyth, T., Rodríguez, A., Hamann, M., Duarte, C., Pendoley, K., Berge, J., Maggi, E., Levy, O., 2022. Impacts of artificial light at night in marine ecosystems—A review. Glob. Change Biol. 28, 5346–5367.

Melnikov, I., 1980. Ecosystem of the Arctic drift ice. Biol. Cent. Arct. Basin Mosc. Nauka 61–97.

Metfies, K., Schroeder, F., Hessel, J., Wollschläger, J., Micheller, S., Wolf, C., Kilias, E., Sprong, P., Neuhaus, S., Frickenhaus, S., Petersen, W., 2016. High-resolution monitoring of marine protists based on an observation strategy integrating automated on-board filtration and molecular analyses. Ocean Sci 12, 1237–1247. https://doi.org/10.5194/os-12-1237-2016

Miller, L.A., Carnat, G., Else, B.G., Sutherland, N., Papakyriakou, T.N., 2011. Carbonate system evolution at the Arctic Ocean surface during autumn freeze-up. J. Geophys. Res. Oceans 116.

Mo, A., Kim, D., Yang, E.J., Jung, J., Ko, Y.H., Kang, S.-H., Cho, K.-H., Park, K., Kim, T.-W., 2022. Factors affecting the subsurface aragonite undersaturation layer in the Pacific Arctic region. Mar. Pollut. Bull. 183, 114060.

Mock, T., Boulton, W., Balmonte, J.-P., Barry, Kevin, Bertilsson, S., Bowman, J., Buck, M., Bratbak, G., Chamberlain, E.J., Cunliffe, M., Creamean, J., Ebenhöh, O., Eggers, S.L., Fong, A.A., Gardner, J., Gradinger, R., Granskog, M.A., Havermans, C., Hill, T., Hoppe, C.J.M., Korte, K., Larsen, A., Müller, O., Nicolaus, A., Oldenburg, E., Popa, O., Rogge, S., Schäfer, H., Shoemaker, K., Snoeijs-Leijonmalm, P., Torstensson, A., Valentin, K., Vader, A., Barry, Kerrie, Chen, I.-M.A., Clum, A., Copeland, A., Daum, C., Eloe-Fadrosh, E., Foster, Brian, Foster, Bryce, Grigoriev, I.V., Huntemann, M., Ivanova, N., Kuo, A., Kyrpides, N.C., Mukherjee, S., Palaniappan, K., Reddy, T.B.K., Salamov, A., Roux, S., Varghese, N., Woyke, T., Wu, D., Leggett, R.M., Moulton, V., Metfies, K., 2022. Multiomics in the central Arctic Ocean for benchmarking biodiversity change. PLOS Biol. 20, e3001835. https://doi.org/10.1371/journal.pbio.3001835

Nicolaus, M., Anhaus, P., Hoppmann, M., Tao, R., Katlein, C., 2023a. Spectral radiation fluxes, albedo and transmittance from autonomous measurement from Radiation Station 2020R12, deployed during MOSAiC 2019/20. https://doi.org/10.1594/PANGAEA.948712

Nicolaus, M., Belter, H.J., Rohde, J., Hoppmann, M., Tao, R., Katlein, C., 2023b. Spectral radiation fluxes, albedo and transmittance from autonomous measurement from Radiation Station 2019R8, deployed during MOSAiC 2019/20. https://doi.org/10.1594/PANGAEA.948876

Nicolaus, M., Hoppmann, M., Tao, R., Katlein, C., 2022a. Spectral radiation fluxes, albedo and transmittance from autonomous measurement from Radiation Station 2020R22, deployed during MOSAiC 2019/20, Alfred Wegener Institute, Helmholtz Centre for Polar and Marine Research, Bremerhaven. PANGAEA. https://doi.org/10.1594/PANGAEA.942602

Nicolaus, M., Perovich, D.K., Spreen, G., Granskog, M.A., von Albedyll, L., Angelopoulos, M., Anhaus, P., Arndt, S., Belter, H.J., Bessonov, V., Birnbaum, G., Brauchle, J., Calmer, R., Cardellach, E., Cheng, B., Clemens-Sewall, D., Dadic, R., Damm, E., de Boer, G., Demir, O., Dethloff, K., Divine, D.V., Fong, A.A., Fons, S., Frey, M.M., Fuchs, N., Gabarró, C., Gerland, S., Goessling, H.F., Gradinger, R., Haapala, J., Haas, C., Hamilton, J., Hannula, H.-R., Hendricks, S., Herber, A., Heuzé, C., Hoppmann, M., Høyland, K.V., Huntemann, M., Hutchings, J.K., Hwang, B., Itkin, P., Jacobi, H.-W., Jaggi, M., Jutila, A., Kaleschke, L., Katlein, C., Kolabutin, N., Krampe, D., Kristensen, S.S., Krumpen, T., Kurtz, N., Lampert, A., Lange, B.A., Lei, R., Light, B., Linhardt, F., Liston, G.E., Loose, B., Macfarlane, A.R., Mahmud, M., Matero, I.O., Maus, S., Morgenstern, A., Naderpour, R., Nandan, V., Niubom, A., Oggier, M., Oppelt, N., Pätzold, F., Perron, C., Petrovsky, T., Pirazzini, R., Polashenski, C., Rabe, B., Raphael, I.A., Regnery, J., Rex, M., Ricker, R., Riemann-Campe, K., Rinke, A., Rohde, J., Salganik, E., Scharien, R.K., Schiller, M., Schneebeli, M., Semmling, M., Shimanchuk, E., Shupe, M.D., Smith, M.M., Smolyanitsky, V., Sokolov, V., Stanton, T., Stroeve, J., Thielke, L., Timofeeva, A., Tonboe, R.T., Tavri, A., Tsamados, M., Wagner, D.N., Watkins, D., Webster, M., Wendisch, M., 2022b. Overview of the MOSAiC expedition: Snow and sea ice. Elem. Sci. Anthr. 10, 000046. https://doi.org/10.1525/elementa.2021.000046

Nomura, D., Granskog, M.A., Fransson, A., Chierici, M., Silyakova, A., Ohshima, K.I., Cohen, L., Delille, B., Hudson, S.R., Dieckmann, G.S., 2018. CO_2 flux over young and snow-covered Arctic pack ice in winter and spring. Biogeosciences 15, 3331–3343.

Nomura, D., Wongpan, P., Toyota, T., Tanikawa, T., Kawaguchi, Y., Ono, T., Ishino, T., Tozawa, M., Tamura, T.P., Yabe, I.S., 2020. Saroma-ko Lagoon Observations for sea ice Physico-chemistry and Ecosystems 2019 (SLOPE2019). Bull. Glaciol. Res. 38, 1–12.

Olsen, L.M., Laney, S.R., Duarte, P., Kauko, H.M., Fernández-Méndez, M., Mundy, C.J., Rösel, A., Meyer, A., Itkin, P., Cohen, L., Peeken, I., Tatarek, A., Różańska-Pluta, M., Wiktor, J., Taskjelle, T., Pavlov, A.K., Hudson, S.R., Granskog, M.A., Hop, H., Assmy, P., 2017. The seeding of ice algal blooms in Arctic pack ice: The multiyear ice seed repository hypothesis. J. Geophys. Res. Biogeosciences 122, 1529–1548. https://doi.org/10.1002/2016JG003668

Patrohay, E., Gradinger, R., Marquardt, M., Bluhm, B.A., 2022. First trait-based characterization of Arctic ice meiofauna taxa. Polar Biol. 45, 1673–1688. https://doi.org/10.1007/s00300-022-03099-0

Picheral, M., Colin, S., Irisson, J.-O., 2017. EcoTaxa, a tool for the taxonomic classification of images.

Polyakov, I.V., Alkire, M.B., Bluhm, B.A., Brown, K.A., Carmack, E.C., Chierici, M., Danielson, S.L., Ellingsen, I., Ershova, E.A., Gårdfeldt, K., Ingvaldsen, R.B., Pnyushkov, A.V., Slagstad, D., Wassmann, P., 2020. Borealization of the Arctic Ocean in Response to Anomalous Advection From Sub-Arctic Seas. Front. Mar. Sci. 7.

Popa, O., Oldenburg, E., Ebenhöh, O., 2020. From sequence to information. Philos. Trans. R. Soc. B 375, 20190448.

Poulin, M., Daugbjerg, N., Gradinger, R., Ilyash, L., Ratkova, T., von Quillfeldt, C., 2011. The pan-Arctic biodiversity of marine pelagic and sea-ice unicellular eukaryotes: a first-attempt assessment. Mar. Biodivers. 41, 13–28. https://doi.org/10.1007/s12526-010-0058-8

Qi, D., Ouyang, Z., Chen, L., Wu, Y., Lei, R., Chen, B., Feely, R.A., Anderson, L.G., Zhong, W., Lin, H., Polukhin, A., Zhang, Yixing, Zhang, Yongli, Bi, H., Lin, X., Luo, Y., Zhuang, Y., He, J., Chen, J., Cai, W.-J., 2022. Climate change drives rapid decadal acidification in the Arctic Ocean from 1994 to 2020. Science 377, 1544–1550. https://doi.org/10.1126/science.abo0383

Rabe, B., Heuzé, C., Regnery, J., Aksenov, Y., Allerholt, J., Athanase, M., Bai, Y., Basque, C., Bauch, D., Baumann, T.M., Chen, D., Cole, S.T., Craw, L., Davies, A., Damm, E., Dethloff, K., Divine, D.V., Doglioni, F., Ebert, F., Fang, Y.-C., Fer, I., Fong, A.A., Gradinger, R., Granskog, M.A., Graupner, R., Haas, C., He, H., He, Y., Hoppmann, M., Janout, M., Kadko, D., Kanzow, T., Karam, S., Kawaguchi, Y., Koenig, Z., Kong, B., Krishfield, R.A., Krumpen, T., Kuhlmey, D., Kuznetsov, I., Lan, M., Laukert, G., Lei, R., Li, T., Torres-Valdés, S., Lin, Lina, Lin, Long, Liu, H., Liu, N., Loose, B., Ma, X., McKay, R., Mallet, M., Mallett, R.D.C., Maslowski, W., Mertens, C., Mohrholz, V., Muilwijk, M., Nicolaus, M., O'Brien, J.K., Perovich, D., Ren, J., Rex, M., Ribeiro, N., Rinke, A., Schaffer, J., Schuffenhauer, I., Schulz, K., Shupe, M.D., Shaw, W., Sokolov, V., Sommerfeld, A., Spreen, G., Stanton, T., Stephens, M., Su, J., Sukhikh, N., Sundfjord, A., Thomisch, K., Tippenhauer, S., Toole, J.M., Vredenborg, M., Walter, M., Wang, H., Wang, L., Wang, Y., Wendisch, M., Zhao, J., Zhou, M., Zhu, J., 2022. Overview of the MOSAiC expedition: Physical oceanography. Elem. Sci. Anthr. 10, 00062. https://doi.org/10.1525/elementa.2021.00062

Randelhoff, A., Holding, J., Janout, M., Sejr, M.K., Babin, M., Tremblay, J.-É., Alkire, M.B., 2020. Pan-Arctic Ocean Primary Production Constrained by Turbulent Nitrate Fluxes. Front. Mar. Sci. 7.

Rantanen, M., Karpechko, A.Yu., Lipponen, A., Nordling, K., Hyvärinen, O., Ruosteenoja, K., Vihma, T., Laaksonen, A., 2022. The Arctic has warmed nearly four times faster than the globe since 1979. Commun. Earth Environ. 3, 168. https://doi.org/10.1038/s43247-022-00498-3

Rees, A.P., Bange, H.W., Arévalo-Martínez, D.L., Artioli, Y., Ashby, D.M., Brown, I., Campen, H.I., Clark, D.R., Kitidis, V., Lessin, G., 2022. Nitrous oxide and methane in a changing Arctic Ocean. Ambio 51, 398–410.

Rex, M., 2021a. Master tracks in different resolutions of POLARSTERN cruise PS122/4, Longyearbyen - Arctic Ocean, 2020-06-04 - 2020-08-12. Alfred Wegener Inst. Helmholtz Cent. Polar Mar. Res. Bremerhaven. https://doi.org/10.1594/PANGAEA.926829

Rex, M., 2021b. Master tracks in different resolutions of POLARSTERN cruise PS122/5, Arctic Ocean - Bremerhaven, 2020-08-12 - 2020-10-12. Alfred Wegener Inst. Helmholtz Cent. Polar Mar. Res. Bremerhaven. https://doi.org/10.1594/PANGAEA.926910

Rex, M., 2020. Links to master tracks in different resolutions of POLARSTERN cruise PS122/1, Tromsø - Arctic Ocean, 2019-09-20 - 2019-12-13 (Version 2). Alfred Wegener Inst. Helmholtz Cent. Polar Mar. Res. Bremerhaven. https://doi.org/10.1594/PANGAEA.924668

Rijkenberg, M.J.A., Slagter, H.A., Rutgers van der Loeff, M., van Ooijen, J., Gerringa, L.J.A., 2018. Dissolved Fe in the Deep and Upper Arctic Ocean With a Focus on Fe Limitation in the Nansen Basin. Front. Mar. Sci. 5.

Rinke, A., Cassano, J.J., Cassano, E.N., Jaiser, R., Handorf, D., 2021. Meteorological conditions during the MOSAiC expedition: Normal or anomalous? Elem. Sci. Anthr. 9, 00023. https://doi.org/10.1525/elementa.2021.00023

Royo-Llonch, M., Sánchez, P., Ruiz-González, C., Salazar, G., Pedrós-Alió, C., Sebastián, M., Labadie, K., Paoli, L., M. Ibarbalz, F., Zinger, L., Churcheward, B., Babin, M., Bork, P., Boss, E., Cochrane, G., de Vargas, C., Gorsky, G., Grimsley, N., Guidi, L., Hingamp, P., Iudicone, D., Jaillon, O., Kandels, S., Not, F., Ogata, H., Pesant, S., Poulton, N., Raes, J., Sardet, C., Speich, S., Setmmann, L., Sullivan, M.B., Chaffron, S., Eveillard, D., Karsenti, E., Sunagawa, S., Wincker, P., Karp-Boss, L., Bowler, C., Acinas, S.G., Tara Oceans Coordinators, 2021. Compendium of 530 metagenome-assembled bacterial and archaeal genomes from the polar Arctic

Ocean. Nat. Microbiol. 6, 1561–1574. https://doi.org/10.1038/s41564-021-00979-9

Rudels, B., Carmack, E., 2022. Arctic Ocean water mass structure and circulation. Oceanography 35, 52–65.

Rybakova, E., Kremenetskaia, A., Vedenin, A., Boetius, A., Gebruk, A., 2019. Deep-sea megabenthos communities of the Eurasian Central Arctic are influenced by ice-cover and sea-ice algal falls. PLoS One 14, e0211009.

Rysgaard, S., Glud, R., Sejr, M., Bendtsen, J., Christensen, P., 2007. Inorganic carbon transport during sea ice growth and decay: A carbon pump in polar seas. J. Geophys. Res. Oceans 112.

Rysgaard, S., Glud, R.N., Lennert, K., Cooper, M., Halden, N., Leakey, R., Hawthorne, F., Barber, D., 2012. Ikaite crystals in melting sea ice–implications for pCO_2 and pH levels in Arctic surface waters. The Cryosphere 6, 901–908.

Salganik, Evgenii, Katlein, C., Lange, B.A., Matero, I., Lei, R., Fong, A.A., Fons, S.W., Divine, D., Oggier, M., Castellani, G., Bozzato, D., Chamberlain, E.J., Hoppe, C.J.M., Müller, O., Gardner, J., Rinke, A., Pereira, P.S., Ulfsbo, A., Marsay, C., Webster, M.A., Maus, S., Høyland, K.V., Granskog, M.A., 2023a. Temporal evolution of under-ice meltwater layers and false bottoms and their impact on summer Arctic sea ice mass balance. Elem. Sci. Anthr. 11, 00035. https://doi.org/10.1525/elementa.2022.00035

Salganik, Evgenii, Lange, B.A., Itkin, P., Divine, D., Katlein, C., Nicolaus, M., Hoppmann, M., Neckel, N., Ricker, R., Høyland, K.V., 2023b. Different mechanisms of Arctic first-year sea-ice ridge consolidation observed during the MOSAiC expedition. Elem. Sci. Anthr. 11.

Salganik, E., Lange, B.A., Katlein, C., Matero, I., Anhaus, P., Muilwijk, M., Høyland, K.V., Granskog, M.A., 2023. Observations of preferential summer melt of Arctic sea-ice ridge keels from repeated multibeam sonar surveys. The Cryosphere 17, 4873–4887. https://doi.org/10.5194/tc-17-4873-2023

Sauve, A.M., Taylor, R.A., Barraquand, F., 2020. The effect of seasonal strength and abruptness on predator–prey dynamics. J. Theor. Biol. 491, 110175.

Schmid, M.S., Aubry, C., Grigor, J., Fortier, L., 2016. The LOKI underwater imaging system and an automatic identification model for the detection of zooplankton taxa in the Arctic Ocean. Methods Oceanogr. 15, 129–160.

Schulz, J., Barz, K., Ayon, P., Luedtke, A., Zielinski, O., Mengedoht, D., Hirche, H.-J., 2010. Imaging of plankton specimens with the lightframe on-sight keyspecies investigation (LOKI) system. J. Eur. Opt. Soc.-Rapid Publ. 5.

Schulz, J., Möller, K.O., Bracher, A., Hieronymi, M., Cisewski, B., Zielinski, O., Voss, D., Gutzeit, E., Dolereit, T., Niedzwiedz, G., 2015. Aquatische optische Technologien in Deutschland. Mar. Sci. Rep.-Meereswissenschaftliche Berichte 97, 1–83.

Schulz, K., Koenig, Z., Muilwijk, M., 2023a. The Eurasian Arctic Ocean along the MOSAiC drift (2019-2020): Core hydrographic parameters. https://doi.org/10.18739/A21J9790B

Schulz, K., Koenig, Z., Muilwijk, M., Bauch, D., Hoppe, C.J., Droste, E., Hoppmann, M., Chamberlain, E.J., Laukert, G., Stanton, T., 2023b. The Eurasian Arctic Ocean along the MOSAiC drift (2019-2020): An interdisciplinary perspective on properties and processes. https://doi.org/10.31223/X5TT2W

Sherr, E.B., Sherr, B.F., Wheeler, P.A., Thompson, K., 2003. Temporal and spatial variation in stocks of autotrophic and heterotrophic microbes in the upper water column of the central Arctic Ocean. Deep Sea Res. Part Oceanogr. Res. Pap. 50, 557–571. https://doi.org/10.1016/S0967-0637(03)00031-1

Shupe, M.D., Rex, M., Blomquist, B., Persson, P.O.G., Schmale, J., Uttal, T., Althausen, D., Angot, H., Archer, S., Bariteau, L., Beck, I., Bilberry, J., Bucci, S., Buck, C., Boyer, M., Brasseur, Z., Brooks, I.M., Calmer, R., Cassano, J., Castro, V., Chu, D., Costa, D., Cox, C.J., Creamean, J., Crewell, S., Dahlke, S., Damm, E., de Boer, G., Deckelmann, H., Dethloff, K., Dütsch, M., Ebell, K., Ehrlich, A., Ellis, J., Engelmann, R., Fong, A.A., Frey, M.M., Gallagher, M.R., Ganzeveld, L., Gradinger, R., Graeser, J., Greenamyer, V., Griesche, H., Griffiths, S., Hamilton, J., Heinemann, G., Helmig, D., Herber, A., Heuzé, C., Hofer, J., Houchens, T., Howard, D., Inoue, J., Jacobi, H.-W., Jaiser, R., Jokinen, T., Jourdan, O., Jozef, G., King, W., Kirchgaessner, A., Klingebiel, M., Krassovski, M., Krumpen, T., Lampert, A., Landing, W., Laurila, T., Lawrence, D., Lonardi, M., Loose, B., Lüpkes, C., Maahn, M., Macke, A., Maslowski, W., Marsay, C., Maturilli, M., Mech, M., Morris, S., Moser, M., Nicolaus, M., Ortega, P., Osborn, J., Pätzold, F., Perovich, D.K., Petäjä, T., Pilz, C., Pirazzini, R., Posman, K., Powers, H., Pratt, K.A., Preußer, A., Quéléver, L., Radenz, M., Rabe, B., Rinke, A., Sachs, T., Schulz, A., Siebert, H., Silva, T., Solomon, A., Sommerfeld, A., Spreen, G., Stephens, M., Stohl, A., Svensson, G., Uin, J., Viegas, J., Voigt, C., von der Gathen, P., Wehner, B., Welker, J.M., Wendisch, M., Werner, M., Xie, Z., Yue, F., 2022. Overview of the MOSAiC expedition: Atmosphere. Elem. Sci. Anthr. 10, 00060. https://doi.org/10.1525/elementa.2021.00060

Shupe, M.D., Rex, M., Dethloff, K., Damm, E., Fong, A.A., Gradinger, R., Heuzé, C., Loose, B., Makarov, A., Maslowski, W., Nicolaus, M., Perovich, D., Rabe, B., Rinke, A., Sokolov, V., Sommerfeld, A., 2020. Arctic Report Card 2020: The MOSAiC Expedition: A Year Drifting with the Arctic Sea Ice. Arctic Report Card. https://doi.org/10.25923/9g3v-xh92

Smith, M.M., Angot, H., Chamberlain, E.J., Droste, E.S., Karam, S., Muilwijk, M., Webb, A.L., Archer, S.D., Beck, I., Blomquist, B.W., Bowman, J., Boyer, M., Bozzato, D., Chierici, M., Creamean, J., D'Angelo, A., Delille, B., Fer, I., Fong, A.A., Fransson, A., Fuchs, N., Gardner, J., Granskog, M.A., Hoppe, C.J.M., Hoppema, M., Hoppmann, M., Mock, T., Muller, S., Müller, O., Nicolaus, M., Nomura, D., Petäjä, T., Salganik, E., Schmale, J., Schmidt, K., Schulz, K.M., Shupe, M.D., Stefels, J., Thielke, L., Tippenhauer, S., Ulfsbo, A., van Leeuwe, M., Webster, M., Yoshimura, M., Zhan, L., 2023. Thin and transient meltwater layers and false bottoms in the Arctic sea ice pack—Recent insights on these historically overlooked features. Elem. Sci. Anthr. 11, 00025. https://doi.org/10.1525/elementa.2023.00025

Smith, M.M., von Albedyll, L., Raphael, I.A., Lange, B.A., Matero, I., Salganik, E., Webster, M.A., Granskog, M.A., Fong, A., Lei, R., 2022. Quantifying false bottoms and under-ice meltwater layers beneath Arctic summer sea ice with fine-scale observations. Elem Sci Anth 10, 000116.

Snoeijs-Leijonmalm Pauline, Flores Hauke, Sakinan Serdar, Hildebrandt Nicole, Svenson Anders, Castellani Giulia, Vane Kim, Mark Felix C., Heuzé Céline, Tippenhauer Sandra, Niehoff Barbara, Hjelm Joakim, Hentati Sundberg Jonas, Schaafsma Fokje L., Engelmann Ronny, 2022. Unexpected fish and squid in the central Arctic deep scattering layer. Sci. Adv. 8, eabj7536. https://doi.org/10.1126/sciadv.abj7536

Søreide, J.E., Leu, E., Berge, J., Graeve, M., Falk-Petersen, S., 2010. Timing of blooms, algal food quality and *Calanus glacialis* reproduction and growth in a changing Arctic. Glob. Change Biol. 16, 3154–3163. https://doi.org/10.1111/j.1365-2486.2010.02175.x

Stemmann, L., Youngbluth, M., Robert, K., Hosia, A., Picheral, M., Paterson, H., Ibanez, F., Guidi, L., Lombard, F., Gorsky, G., 2008. Global zoogeography of fragile macrozooplankton in the upper 100–1000 m inferred from the underwater video profiler. ICES J. Mar. Sci. 65, 433–442.

Succurro, A., Ebenhöh, O., 2018. Review and perspective on mathematical modeling of microbial ecosystems. Biochem. Soc. Trans. 46, 403–412.

Syvertsen, E.E., 1991. Ice algae in the Barents Sea: types of assemblages, origin, fate and role in the ice-edge phytoplankton bloom. Polar Res. 10, 277–288.

Taskjelle, T., Granskog, M.A., Pavlov, A.K., Hudson, S.R., Hamre, B., 2017. Effects of an Arctic under-ice bloom on solar radiant heating of the water column. J. Geophys. Res. Oceans 122, 126–138. https://doi.org/10.1002/2016JC012187

Tedesco, L., Vichi, M., Scoccimarro, E., 2019. Sea-ice algal phenology in a warmer Arctic. Sci. Adv. 5, eaav4830. https://doi.org/10.1126/sciadv.aav4830

Tippenhauer, S., Vredenborg, M., Heuzé, C., Ulfsbo, A., Rabe, B., Granskog, M.A., Allerholt, J., Balmonte, J.P., Campbell, R.G., Castellani, G., Chamberlain, E., Creamean, J., D'Angelo, A., Dietrich, U., Droste, E.S., Eggers, L., Fang, Y.-C., Fong, A.A., Gardner, J., Graupner, R., Grosse, J., He, H., Hildebrandt, N., Hoppe, C.J.M., Hoppmann, M., Kanzow, T., Karam, S., Koenig, Z., Kong, B., Kuhlmey, D., Kuznetsov, I., Lan, M., Liu, H., Mallet, M., Mohrholz, V., Muilwijk, M., Müller, O., Olsen, L.M., Rember, R., Ren, J., Sakinan, S., Schaffer, J., Schmidt, K., Schuffenhauer, I., Schulz, K., Shoemaker, K., Spahic, S., Sukhikh, N., Svenson, A., Torres-Valdés, S., Torstensson, A., Wischnewski, L., Zhuang, Y., 2023a. Physical oceanography water bottle samples based on ship CTD during POLARSTERN cruise PS122. https://doi.org/10.1594/PANGAEA.959965

Tippenhauer, S., Vredenborg, M., Heuzé, C., Ulfsbo, A., Rabe, B., Granskog, M.A., Allerholt, J., Balmonte, J.P., Campbell, R.G., Castellani, G., Chamberlain, E., Creamean, J., D'Angelo, A., Dietrich, U., Droste, E.S., Eggers, L., Fang, Y.-C., Fong, A.A., Gardner, J., Graupner, R., Grosse, J., He, H., Hildebrandt, N., Hoppe, C.J.M., Hoppmann, M., Kanzow, T., Karam, S., Koenig, Z., Kong, B., Kuhlmey, D., Kuznetsov, I., Lan, M., Liu, H., Mallet, M., Mohrholz, V., Muilwijk, M., Müller, O., Olsen, L.M., Rember, R., Ren, J., Sakinan, S., Schaffer, J., Schmidt, K., Schuffenhauer, I., Schulz, K., Shoemaker, K., Spahic, S., Sukhikh, N., Svenson, A., Torres-Valdés, S., Torstensson, A., Wischnewski, L., Zhuang, Y., 2023b. Physical oceanography water bottle samples based on Ocean City CTD during POLARSTERN cruise PS122. https://doi.org/10.1594/PANGAEA.959966

Tortell, P.D., 2005. Dissolved gas measurements in oceanic waters made by membrane inlet mass spectrometry. Limnol. Oceanogr. Methods 3, 24–37.

Tremblay, J.-É., Anderson, L.G., Matrai, P., Coupel, P., Bélanger, S., Michel, C., Reigstad, M., 2015. Global and regional drivers of nutrient supply, primary production and CO_2 drawdown in the changing Arctic Ocean. Prog. Oceanogr. 139, 171–196. https://doi.org/10.1016/j.pocean.2015.08.009

Ulfsbo, A., Cassar, N., Korhonen, M., van Heuven, S., Hoppema, M., Kattner, G., Anderson, L.G., 2014. Late summer net community production in the central Arctic Ocean using multiple approaches. Glob. Biogeochem. Cycles 2014GB004833. https://doi.org/10.1002/2014gb004833

Vandermeer, J., 1996. Seasonal isochronic forcing of Lotka Volterra equations. Prog.

Theor. Phys. 96, 13–28.

Volterra, V., 1927. Variazioni e fluttuazioni del numero d’individui in specie animali conviventi. Societá anonima tipografica" Leonardo da Vinci".

von Appen, W.-J., Waite, A.M., Bergmann, M., Bienhold, C., Boebel, O., Bracher, A., Cisewski, B., Hagemann, J., Hoppema, M., Iversen, M.H., 2021. Sea-ice derived meltwater stratification slows the biological carbon pump: results from continuous observations. Nat. Commun. 12, 7309.

Wadhams, P., Toberg, N., 2012. Changing characteristics of arctic pressure ridges. Polar Sci. 6, 71–77.

Wang, S.W., Budge, S.M., Iken, K., Gradinger, R.R., Springer, A.M., Wooller, M.J., 2015. Importance of sympagic production to Bering Sea zooplankton as revealed from fatty acid-carbon stable isotope analyses. Mar. Ecol. Prog. Ser. 518, 31–50.

Wassmann, P., Reigstad, M., 2011. Future Arctic Ocean seasonal ice zones and implications for pelagic-benthic coupling. Oceanography 24, 220–231. https://doi.org/10.5670/ oceanog.2011.74.

Wiedmann, I., Ershova, E., Bluhm, B.A., Nöthig, E.-M., Gradinger, R.R., Kosobokova, K., Boetius, A., 2020. What Feeds the Benthos in the Arctic Basins? Assembling a Carbon Budget for the Deep Arctic Ocean. Front. Mar. Sci. 7.

Wietz, M., Bienhold, C., Metfies, K., Torres-Valdés, S., von Appen, W.-J., Salter, I., Boetius, A., 2021. The polar night shift: seasonal dynamics and drivers of Arctic Ocean microbiomes revealed by autonomous sampling. ISME Commun. 1, 76. https://doi.org/10.1038/s43705-021-00074-4

Yue, F., Angot, H., Blomquist, B., Schmale, J., Hoppe, C.J., Lei, R., Shupe, M.D., Zhan, L., Ren, J., Liu, H., 2023. The Marginal Ice Zone as a dominant source region of atmospheric mercury during central Arctic summertime. Nat. Commun. 14, 4887.

Zeebe, R.E., Eicken, H., Robinson, D.H., Wolf-Gladrow, D., Dieckmann, G.S., 1996. Modeling the heating and melting of sea ice through light absorption by microalgae. J. Geophys. Res. Oceans 101, 1163–1181.

Tables

Table 1. MOSAiC ecosystem core measurements. Catalog of biological and biogeochemical properties and processes measured during the MOSAiC expedition. Additional geochemical properties (i.e. gases) were measured by the MOSAiC Biogeochemistry Team. Details can be found in the supplementary Table S2.

ECO variable	Sampled environments	Method
Nutrients (nitrate+nitrite, ammonium, phosphate, silicic acid, dissolved organic nitrogen, dissolved organic phosphorus)	Water column, ice, special habitats	Colourimetric continuous flow; AA3 (SEAL)
Dissolved oxygen (DO)	water column	Winkler titration
Carbonate chemistry: total alkalinity (TA) and dissolved inorganic carbon DIC)	water column, special habitats	VINDTA
Carbonate chemistry: TA, DIC	ice, special habitats	Coulometry/ VINDTA
Dissolved organic carbon (DOC) and nitrogen (DON), concentrations	water column, ice, special habitats	TOC-VCPN, high temperature catalytic combustion
Dissolved organic matter characterization and chemometrics	water column, special habitats	Ultrahigh resolution mass spectrometry
Particulate organic carbon and nitrogen (POC and PON); stable isotopic composition and concentrations	water column, ice, special habitats, short- and longterm sediment traps	%C, %N, $\delta^{13}C$, $\delta^{15}N$; EA-IRMS (Flash 2000-Delta V Plus, Thermo Scientific)
POC and PON, concentrations	water column, ice, special habitats, short- and longterm sediment traps	Euro EA 3000, HEKAtech
Biogenic silica (bSi)	water column, ice,	Photometrically after NaOH digestion
Oceanic particle size spectra and distributions	Water column	Optical - Underwater Vision Profiler (UVP)
Chlorophyll *a* (Chl-a)	water column, ice, special habitats	Fluorometric analyses of extractd samples
Pigment biomarkers	water column, ice, special habitats	High Performance Liquid Chromatography (HPLC)
Enumeration and diversity of prokaryotes, eukaryotic microbes and viruses	water column, ice, special habitats	Attune NxT (ThermoFisher) and Facs Calibur (Becton Dickson) flow cytometers (FCM)
Diversity and abundance of protists	water column, ice, special habitats, sediment traps	Inverse light microscopy
Diversity of prokaryotes and eukaryotic microbes	water column, ice, special habitats, underway	16S/18S rRNA amplicon sequencing (Illumina)

Metagenomes	water column, ice, special habitats	Illumina
Metatranscriptomes	water column, ice, special habitats	Illumina
Primary productivity (NPP)	water column, ice, special habitats, underway	^{14}C-based incubations
Net community production (NCP)	surface water	MIMS O_2/Ar
Bacterial productivity (BP)	water column, ice, special habitats, underway	3H-leucine incubations
PSII fluorescence-based photophysiology	water column, special habitats	FRRF; FastOcean with FastAct /Fastact2 (Chelsea Tech)
Mesozooplankton: abundance/distribution	water column	Microscopy, Zooscan
Small mesozooplanton: abundance/distribution	water column	Microscopy, Zooscan
Macrozooplankton: abundance/distribution	water column	Microscopy, Zooscan
Macrozooplankton: biomarkers	water column	diverse
Macrozooplankton: carbon & nitrogen	water column	Elemental analyser
Surface mesozooplankton: biomarkers	water column	diverse
Surface mesozooplankton: carbon & nitrogen	water column	Elemental analyser
Surface mesozooplankton: individual respiration	water column	optodes
Deep mesozooplankton: biomarkers	water column	diverse
Deep mesozooplankton: carbon & nitrogen	water column	Elemental analyser
Deep mesozooplankton: individual respiration	water column	optodes
Mesozooplankton: high vertical resolution distribution	water column	Microscopy, Zooscan
Under-ice fauna: abundance/distribution	ice	Microscopy
Grazing rates (microzooplankton & copepods)	water column	experiments
Egg production (copepods)	water column	experiments
Gut contents & DNA (fish, copepods, amphipods)	water column	Microscopy, scales, DNA
Energy content macrofauna	water column	oxygen calorimeter

Figures

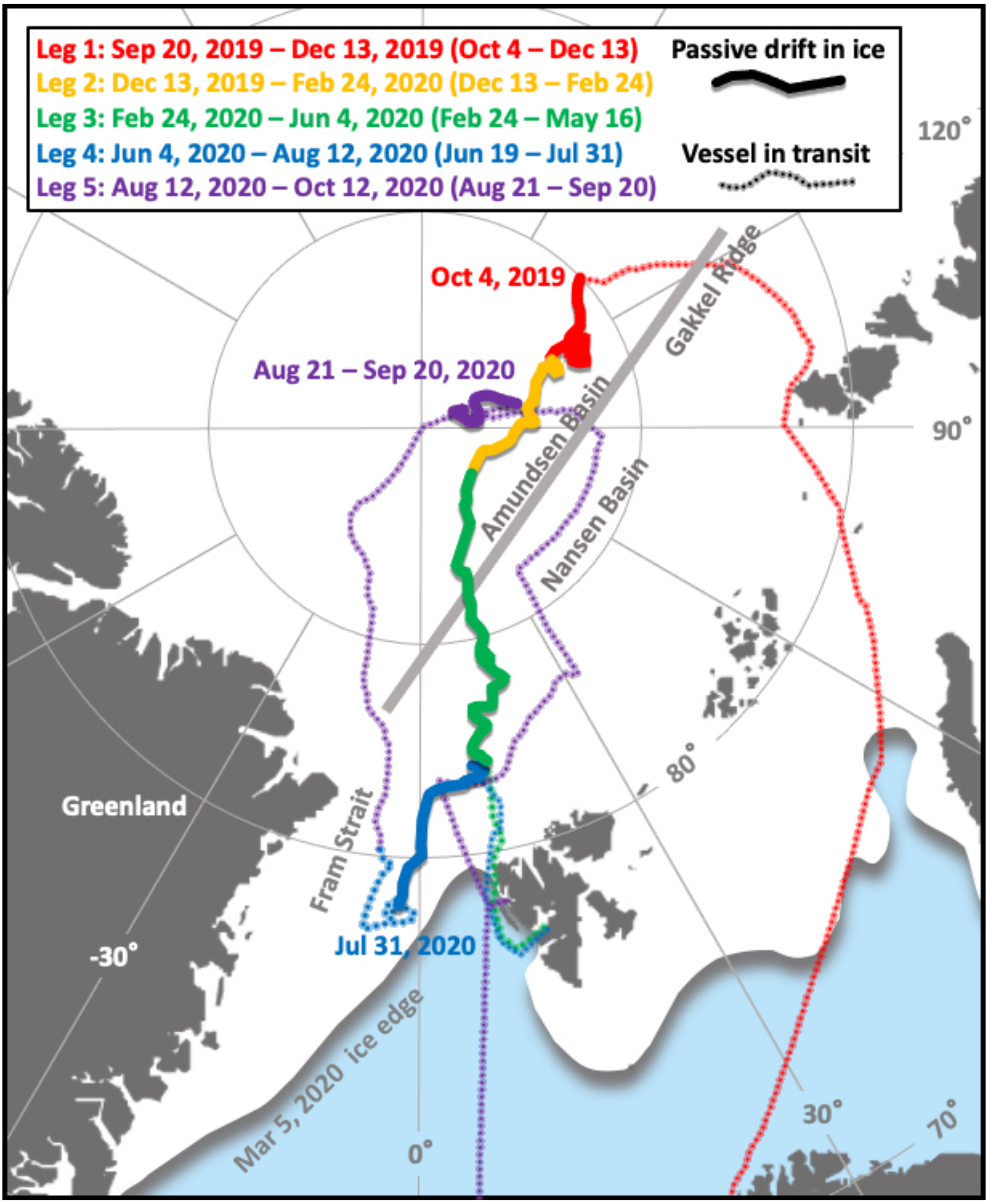

Figure 1. MOSAiC expedition track. Passive periods of drift are shown in solid-colored lines, with each color-coded line delineating one of the MOSAiC legs. Dates are periods of each leg and dates shown in parentheses identify passive drift periods per leg. Dotted lines depict transit tracks of the ship initially and for repositioning after legs 3 and 4. The solid grey line approximates the location of the Gakkel Ridge between the Amundsen and Nansen Basins. The approximate sea ice edge at the

annual maximum (Mar 5, 2020) and minimum (Sept 15, 2020) is also shown. Modified after (Shupe et al., 2020).

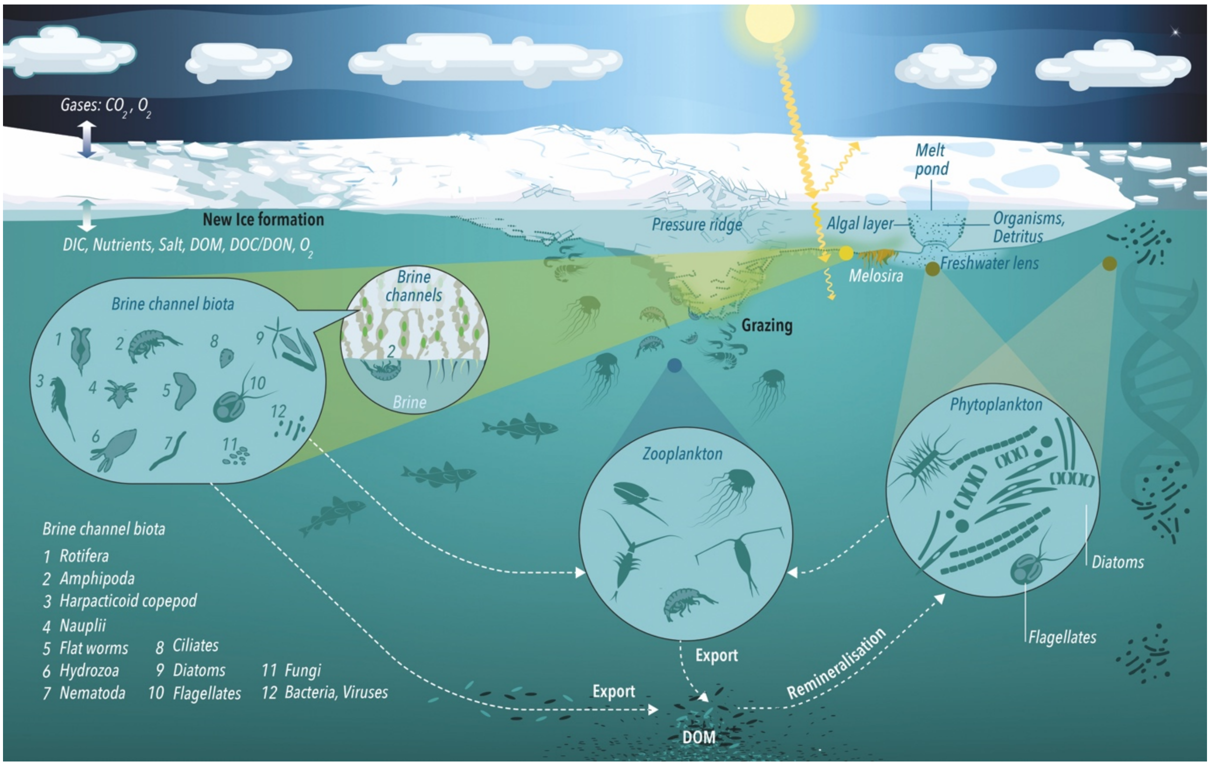

Figure 2. Ecosystem compartments and processes of the Central Arctic. Illustrated are the primary components and processes investigated by the ECO team during the MOSAiC (Multidisciplinary drifting Observatory for the Study of Arctic Climate) expedition.

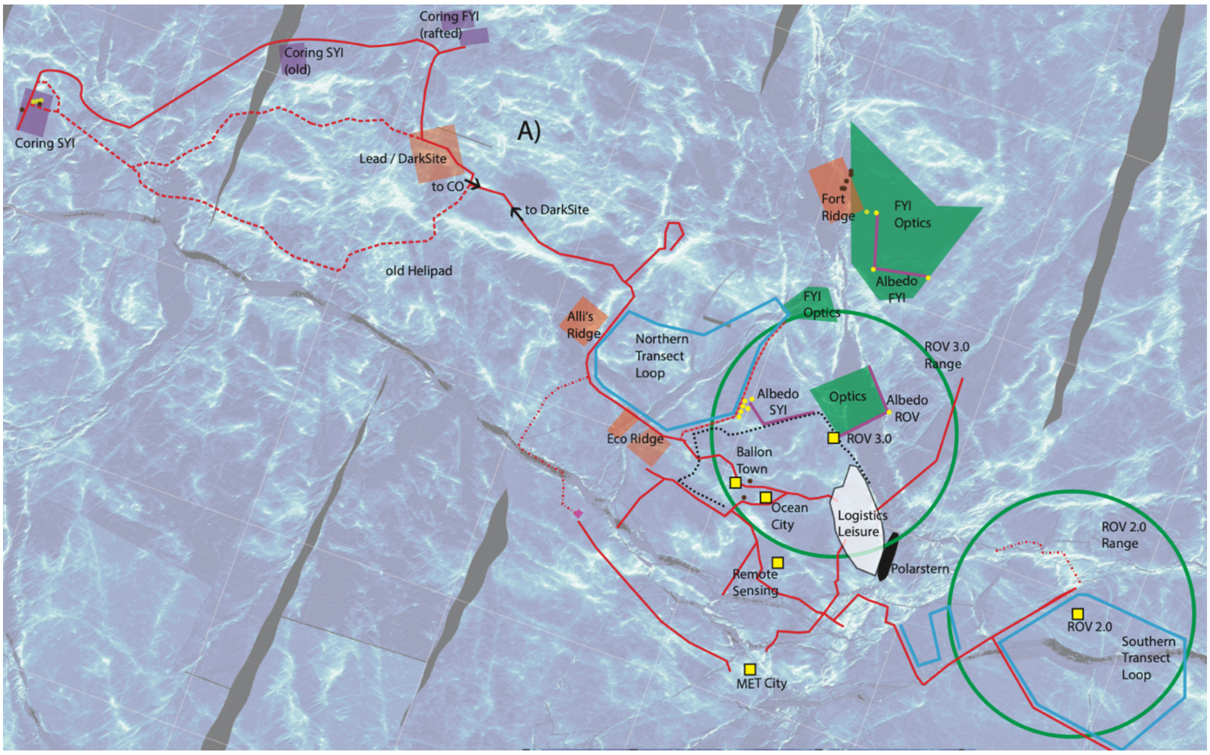

Figure 3. Main sampling locations and measurement sites of the first MOSAiC Central Observatory in April 2020. Map background shows the airborne laser scanner (ALS) image from April 23, 2020 with grey areas indicating no data. White, brighter areas depict sea ice of greater elevation (i.e. ridge sails). Some site locations were approximate due to active ice dynamics. Sites labeled "old" were previously active sampling locations, but were no longer accessible and maintained after the winter. The primary water column sampling locations during October 2019 and May 2020 were conducted at RV *Polarstern* (black) and Ocean City (yellow square). Common ice coring sites are shown in purple and approximately 1 km from RV *Polarstern*. The map had been simplified to show main sampling and measurement positions for the ecosystem work program. Additional MOSAiC measurement sites from teams ATMO, ICE, and OCEAN can be viewed in the respective MOSAiC Overviews by Nicolaus et al. (2022b), Rabe et al. (2022) and Shupe et al. (2022).

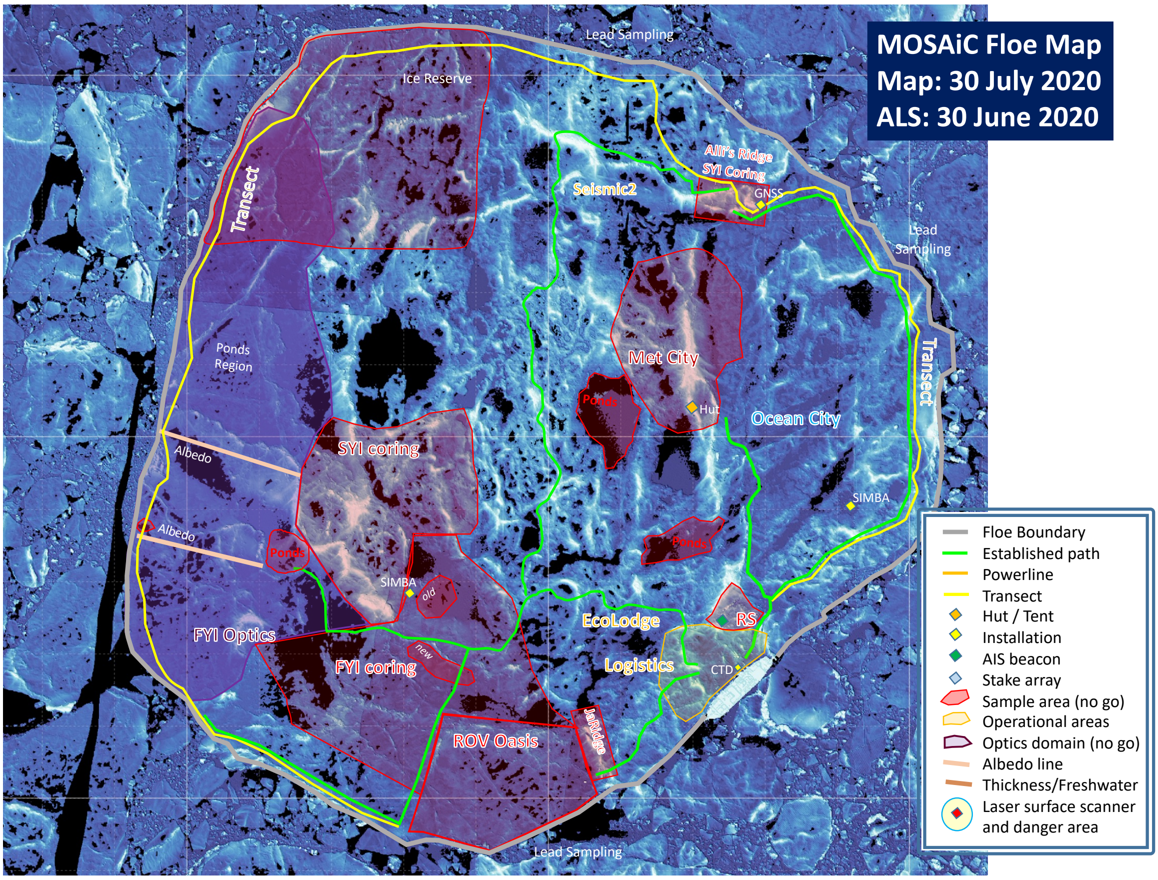

Figure 4. Main sampling locations and measurement sites of the second MOSAiC Central Observatory during summer 2020. Primary water column sampling was from RV *Polarstern* (light blue, lower righthand side). Ocean City did not have a CTD-rosette system. FYI coring site was an original portion of the FYI site established in Oct 2019. SYI coring site adjacent to FYI shown here was a reserve SYI site identified earlier, but was not actively sampled. Original SYI coring site is not depicted in this map as that part of the ice floe detached from the main floe. SYI coring in June and July 2020 occurred near Alli's ridge. ECO Lodge was established beyond the perimeter of the logistics area. The map had been simplified to show main sampling and measurement positions for the ecosystem work program. Additional MOSAiC measurement sites from teams ATMO, ICE, and OCEAN can be viewed in the respective MOSAiC Overviews by Nicolaus et al. (2022b), Rabe et al. (2022) and Shupe et al. (2022).

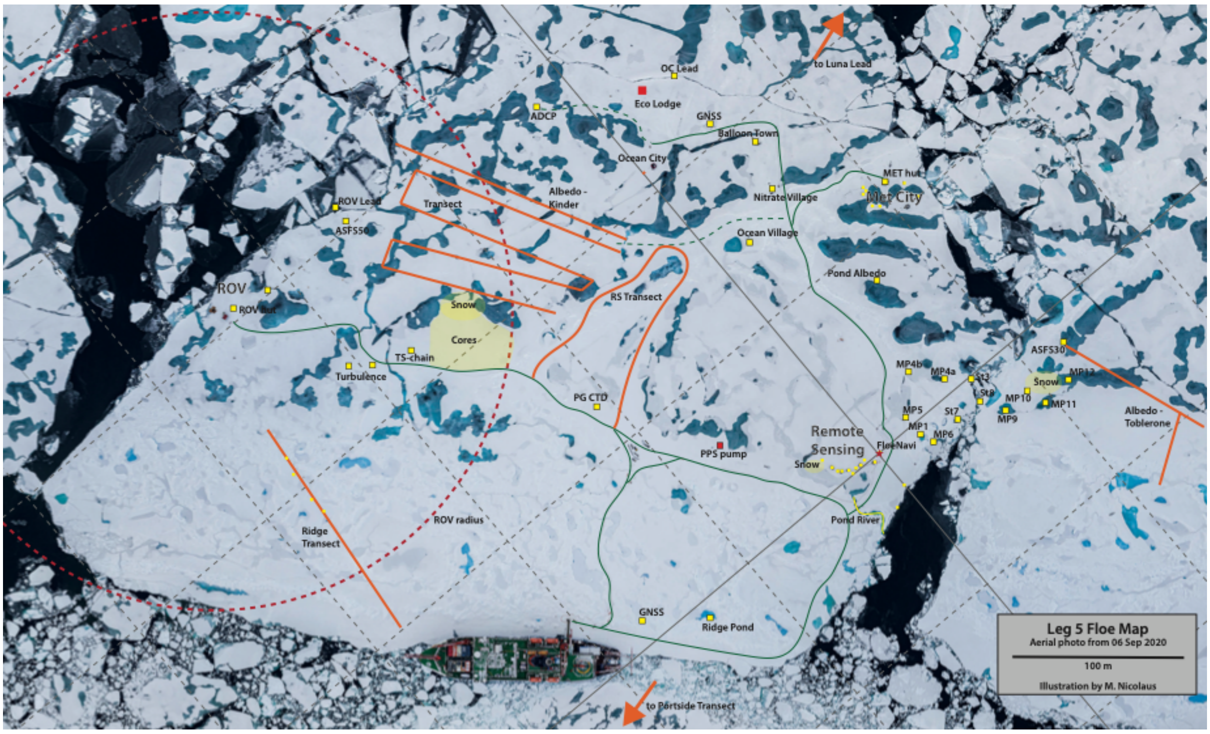

Figure 5. Main sampling locations and measurement sites of the third MOSAiC Central Observatory during late summer 2020. The background of the map is an aerial photo of the ice floe (photo credit S. Graupner). Primary water column sampling was from RV *Polarstern* (light blue, lower righthand side). Ocean City did not have a CTD-rosette system. Ice cores (not new ice formations) in August and September 2020 were sampled from a single site (yellow area). New ice formation and waters from the upper ocean (1-2m) were sampled at RS, OC, ROV, and Luna leads. ECO Lodge (red square) was established adjacent to Ocean City lead, approximately 300 m from the ship. The map had been simplified to show main sampling and measurement positions for the ecosystem work program. Additional MOSAiC measurement sites from teams ATMO, ICE, and OCEAN can be viewed in the respective MOSAiC Overviews by Nicolaus et al. (2022b), Rabe et al. (2022) and Shupe et al. (2022).

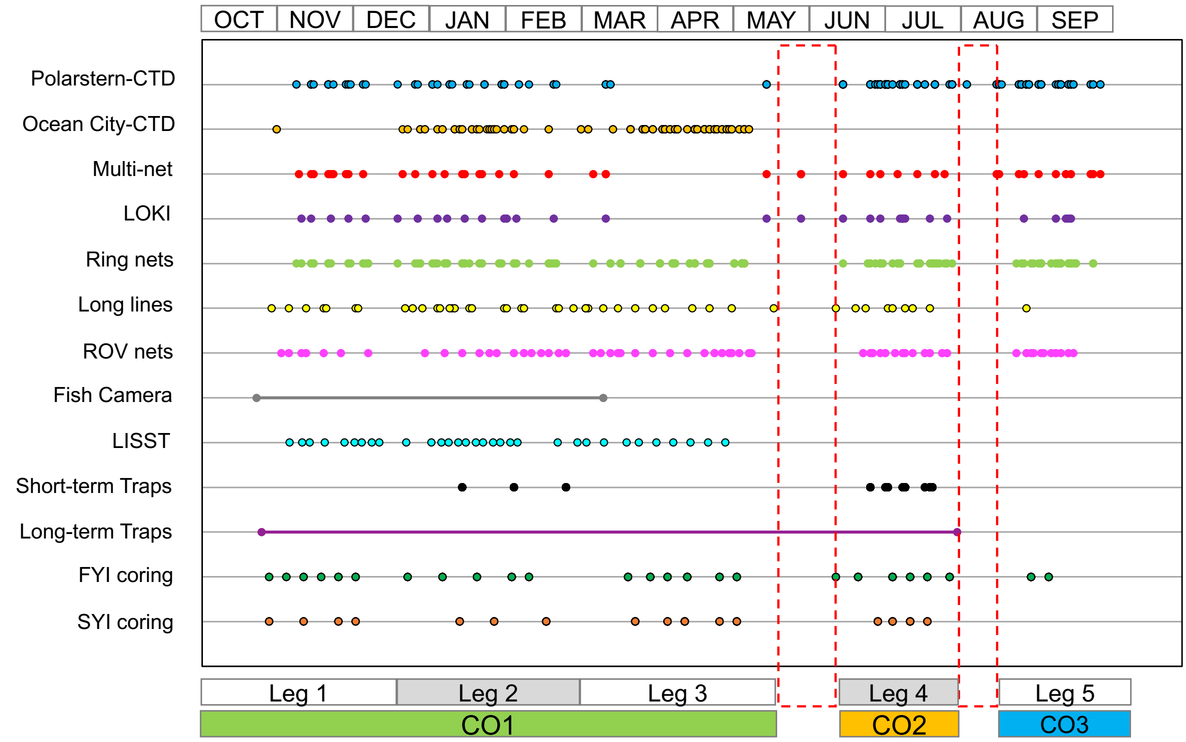

Figure 6. Ecosystem observations and measurements during the field phase of MOSAiC. Each row shows the dates of a sampling event for a specific type of gear (e.g. Polarstern-CTD) or sampling activity (e.g. FYI coring). Solid lines indicate instrumentation deployed through the ice for a continuous period. A number of parameters are collected from an individual sampling event, such as deployment of the Polarstern-CTD rosette system. Alternating white and grey horizontal bars at the bottom of the chart indicate the MOSAiC leg. Colored horizontal bars indicate from which Central Observatory (CO) samples were collected. Dashed red line boxes identify the periods when RV Polarstern was transiting to/from an ice floe. LOKI = Light-frame On-sight Key species Investigation system (zooplankton camera system). ROV nets = Plankton nets towed by a Remotely Operated Vehicle. LISST = Laser In-Situ Scattering and Transmissometer (particle counter). FYI = First Year Ice. SYI = Second Year Ice.

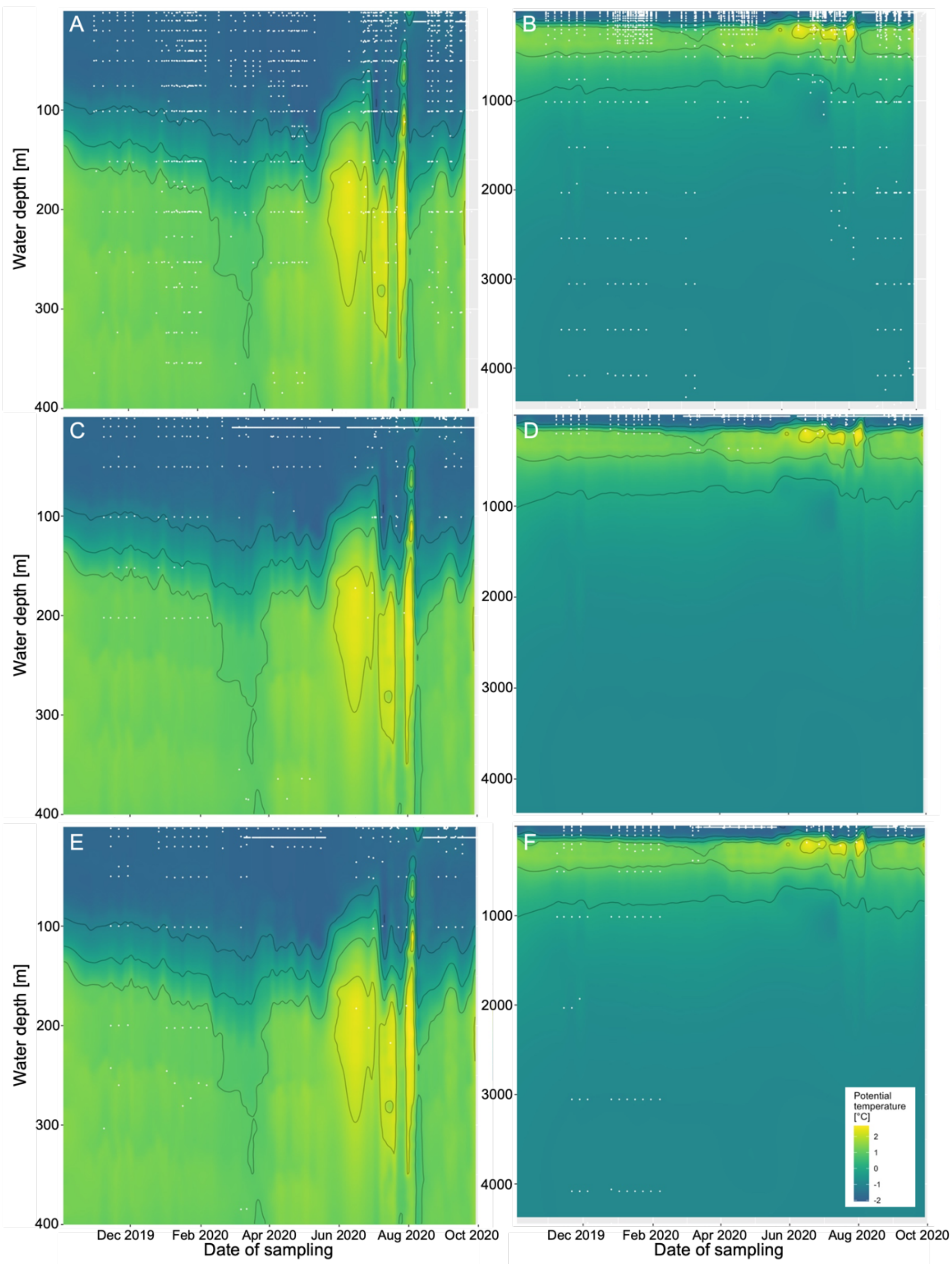

Figure 7. Distribution of CTD-rosette-based water column samples for nutrients, Chl-a, and total DNA in depth and time. Discrete samples (while circles) for the upper 400 m (A, C, and E) and for full depth (0-4000 m; B, D, and F) are overlain on temperature contours with isotherms shown by thin, solid lines. Temperature data shown here are from temperature sensors mounted to the CTD-rosette system. During mid-March to May 2020, the Polarstern-CTD was not operational due to the closure of the ice hole alongside the ship; water column sampling was limited to the upper 1000 m using the OC-CTD-rosette system. A) Nutrient samples collected in the upper 400 m; B) Nutrient samples collected over the full water column depth; C) Chl-a samples collected in the upper 400 m; D) Chl-a samples collected over the full water column depth; E) Total DNA samples collected

in the upper 400 m; F) Total DNA samples collected over the full water column depth.

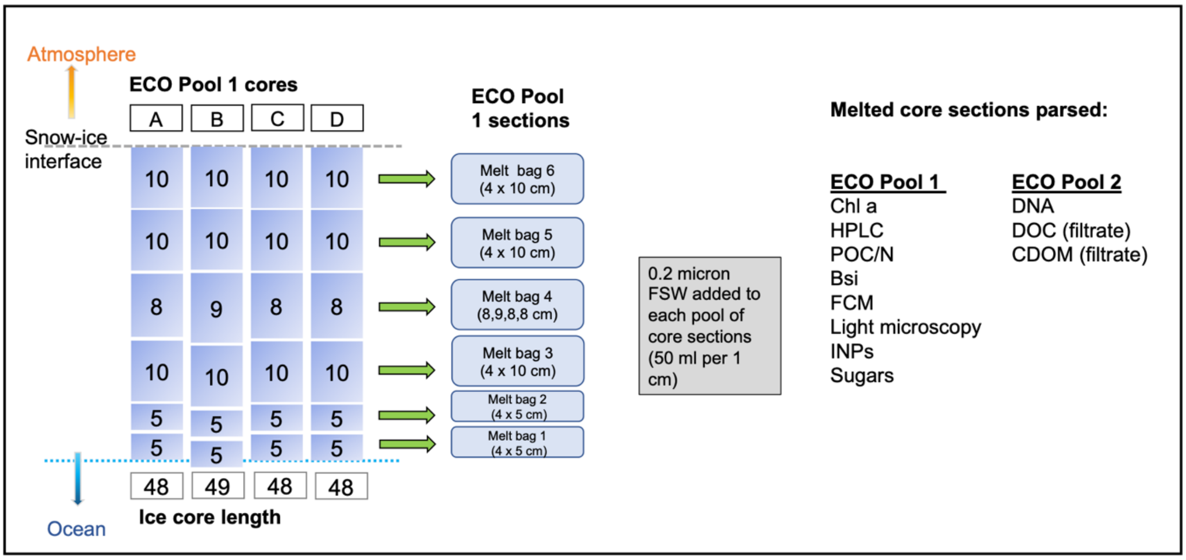

Figure 8. Ecological sea ice core pooling and processing. Full length cores were sectioned in the field and placed in prelabeled melt bags. Filtered seawater (FSW) was added onboard to each melt bag, and after complete melt, pooled sample were parsed for different properties. When possible, 2 ECO pools were generated. Properties collected from each pool are shown, see Table 1 for abbreviation explanations. Additional samples were collected from SALO18 and DIC/TA cores as well as additional bottom sections.

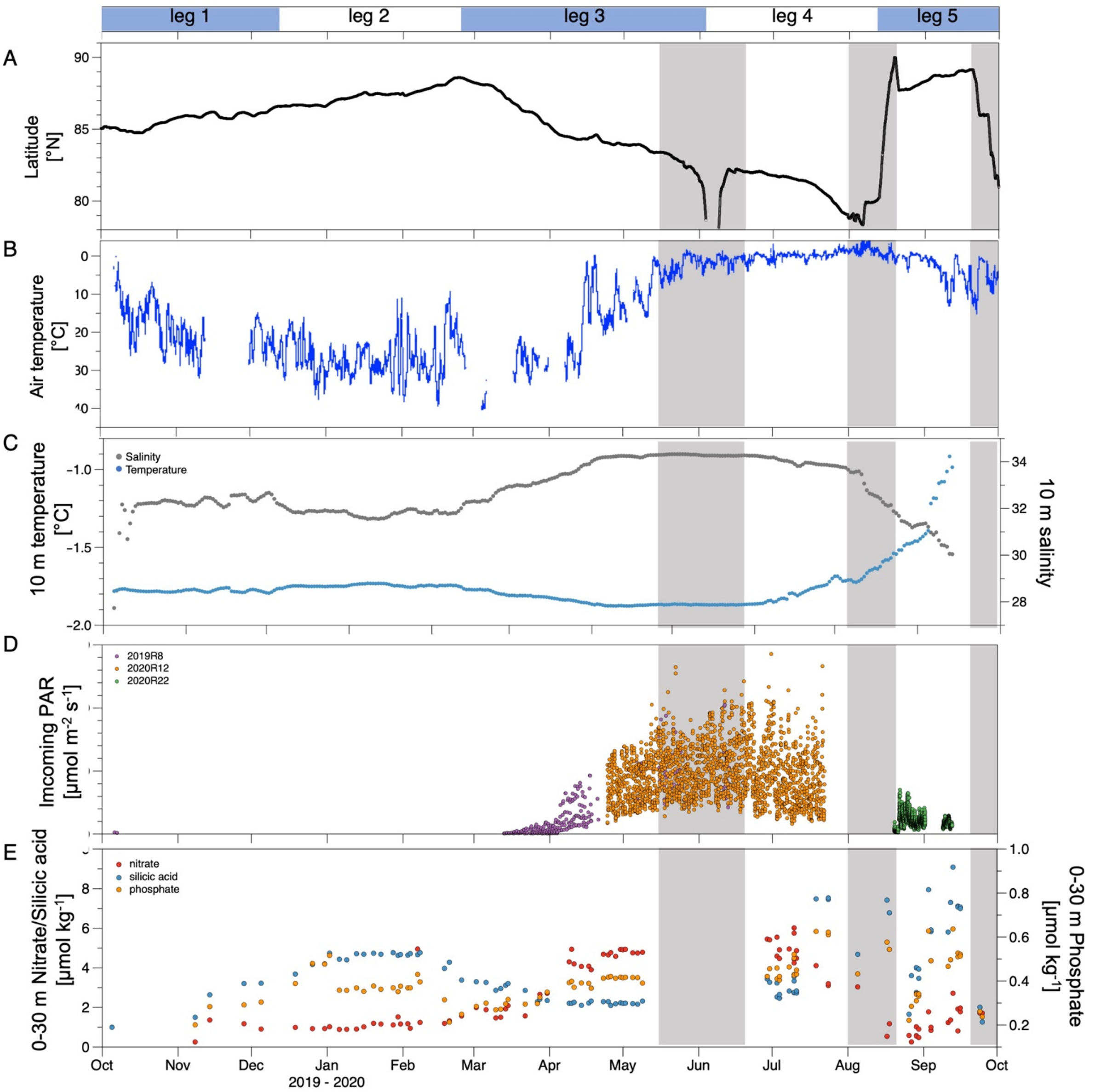

Figure 9. Environmental conditions over the annual cycle. A) latitude (°N), B) air and C) surface ocean temperature (blue) and salinity (grey) at 10 ±3 m depth, D) incoming PAR (photosynthetically active radiation, 400-700 nm, measured as photon flux density), and E) surface ocean nutrients (nitrate+nitrite, silicic acid, and phosphate) from the upper 30 m water depths. Grey shaded areas indicate transit periods. Here, latitude and nutrients are from the location of RV *Polarstern*, while PAR, water temperature, and surface air temperature are representative of CO conditions.

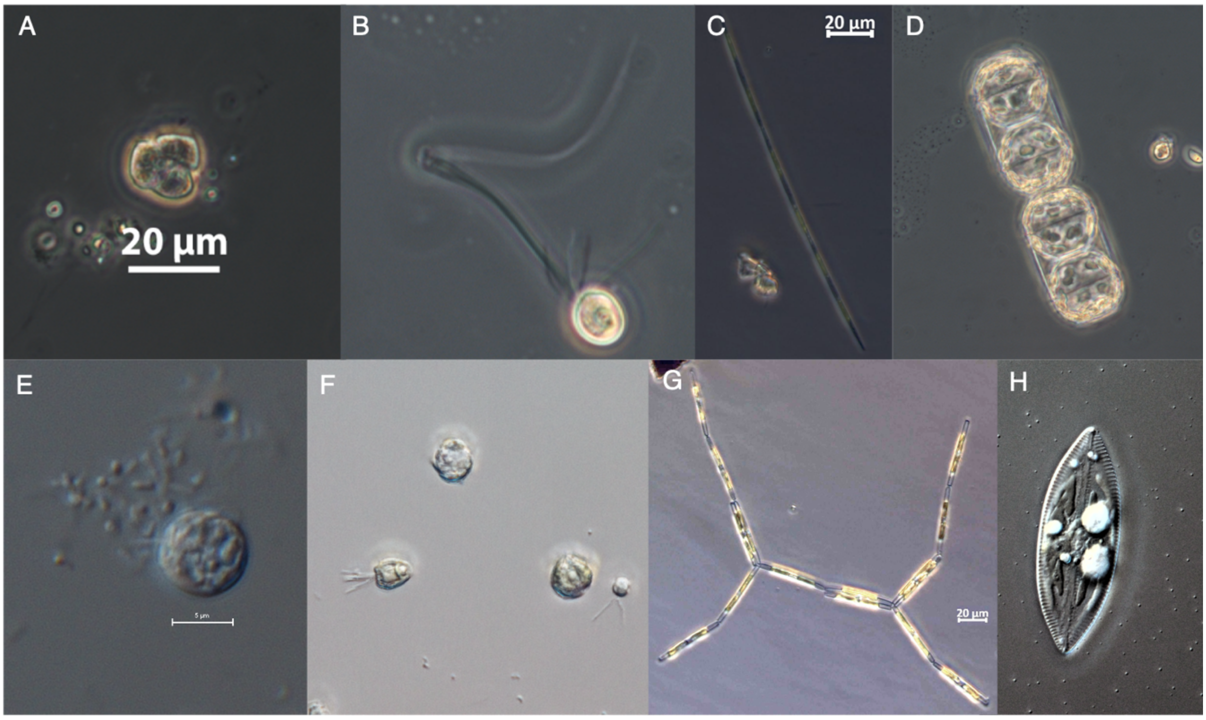

Figure 10. Dominant pelagic (water column) and sympagic (ice-associated) protists during the MOSAiC cruise. A) dinoflagellate belonging to Gymnodiniaceae, B) unidentified flagellate, C) *Pseudo-nitzschia* sp. and D) *Melosira arctica* from water column samples; E) and F) unidentified flagellates, G) *Nitzschia frigida* and H) *Navicula* sp. from bottom sea ice samples.

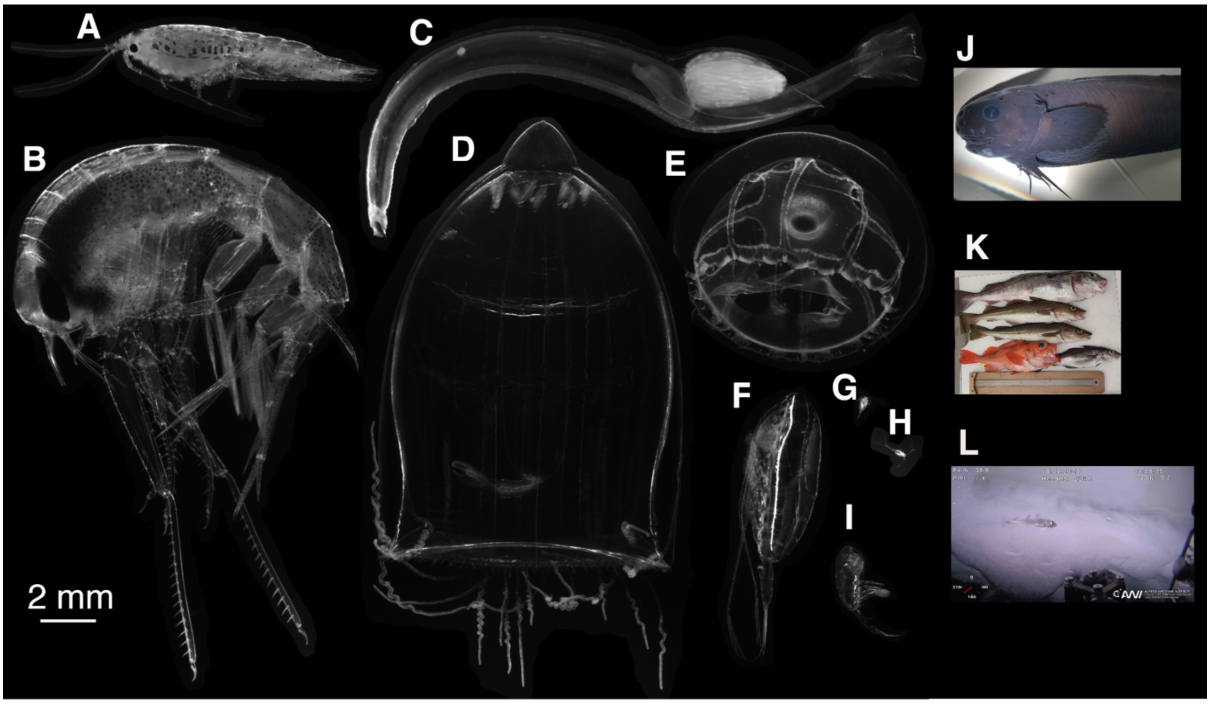

Figure 11. Zooplankton and fish species caught during the MOSAiC cruise. A) *Apherusa glacialis*, B) *Themisto libellula*, C) *Eukrohnia hamata*, D) *Aglantha digitale*, E) *Botrynema ellinorae*, F) *Calanus hyperboreus*, G) *Microcalanus sp.,* H) *Oithona similis*, I) *Metridia longa*, J) *Paraliparis bathybius*, K) from top to bottom: Haddock (*Melanogrammus aeglefinus)*, 2 x Atlantic cod (*Gadus morhua*), Beaked redfish (*Sebastes mentella*), Haddock (*Melanogrammus aeglefinus)*; L) *Boreogadus saida*. The specimens A - I were obtained with the LOKI (Lightframe on-sight key species investigation), further sampling methods were J) zooplankton ring net, K) longlines, and L) ROVnet camera.

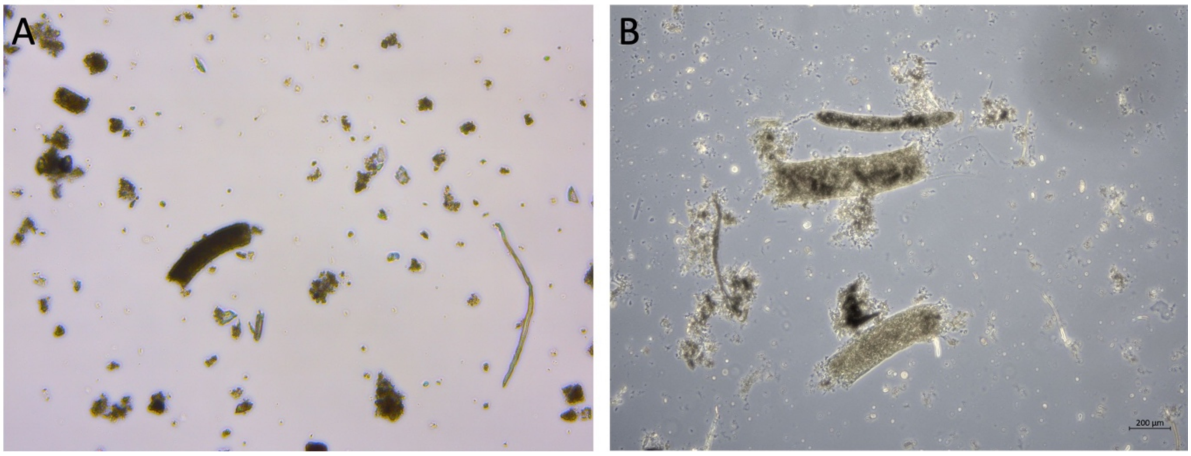

Figure 12. Sediment trap material from winter vs summer. Overview images of sediment trap material from A) January 14, and B) July 21, 2020.

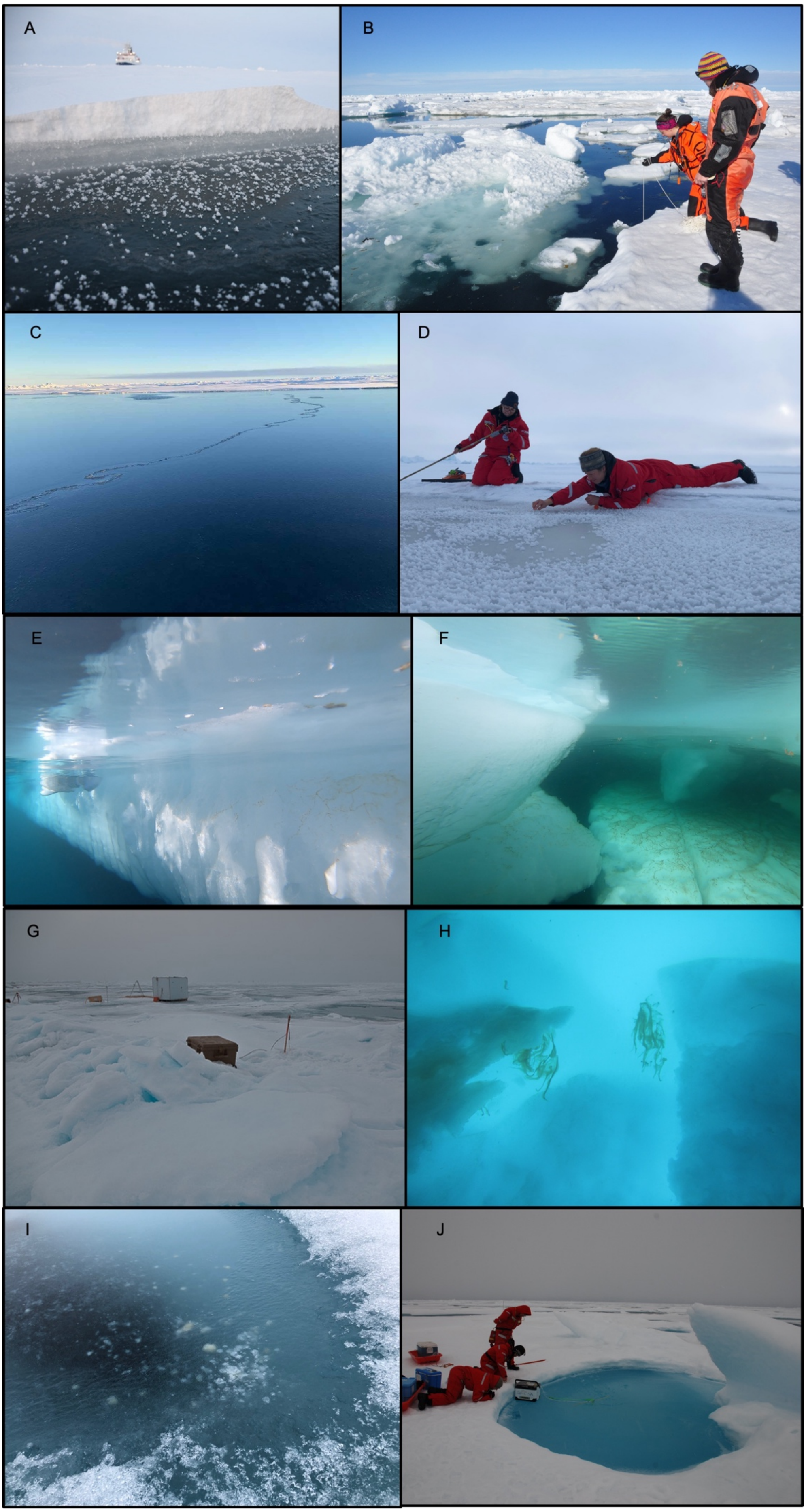
A
B
C
D
E
F
G
H
I
J

Figure 13. A variety of different seawater and sea ice habitats sampled over the drift year. A) Frost flowers developing on a refrozen lead on March 11, 2020; B) Sampling an open lead on 22, 2020; C) New ice formation on a lead located near ECO Lodge 2 on September 07, 2020; D) Sampling new ice and direct under-ice waters from a lead located near ECO Lodge 2 on September 12, 2020; E) Underwater photos of ice blocks within an open lead from July 01, 2020 and F) from the same location on 29, 2020, showing the development of thin, stratified fresh and brackish layers within leads. G) Jaridge Observatory from the surface with piled up ice blocks on June 26, 2020; H) Underwater photo of ice blocks in Jaridge Observatory with strands of Melosira; I) Refrozen surface of a melt pond showing large aggregate material through the ice surface from Aug 21, 2020; and J) Melt pond sampling from August 31, 2020.

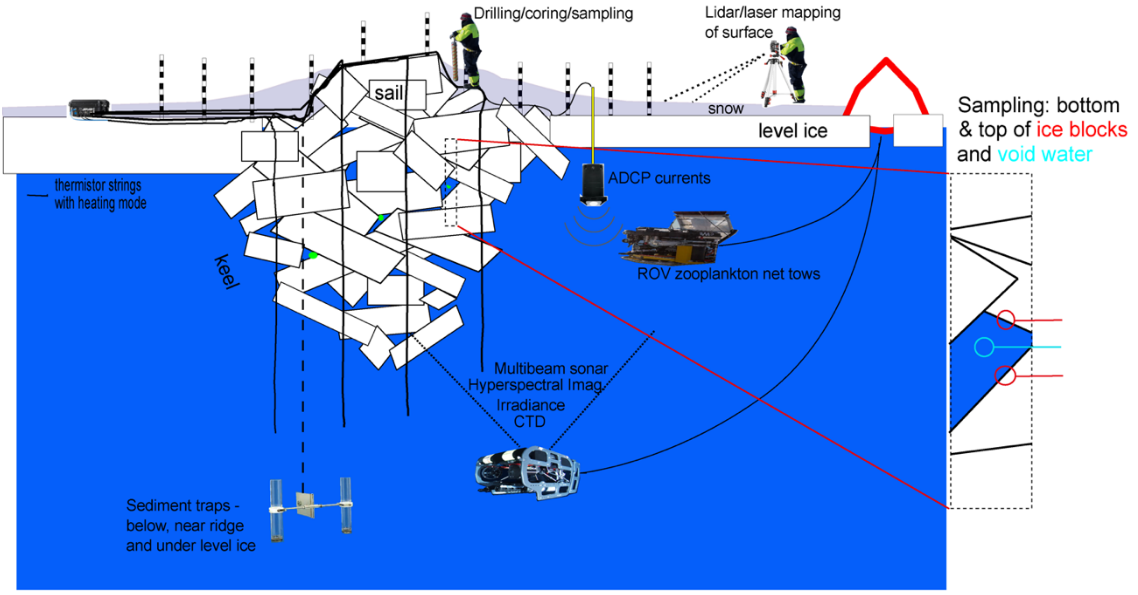

Figure 14. Components of the multidisciplinary ridge sampling strategy during MOSAiC. Schematic representation of the sampling strategy of sea ice ridges developed by the HAVOC project~~.~~, including autonomous systems (e.g. thermistor strings), coring and drilling, sampling of ice and void water in the ridge keel, as well as ROV- and sediment trap-based measurements, with the former including zooplankton net tows and various sensor-based measurements (including hyperspectral imager mapping of the ice underside, see Figure 16).

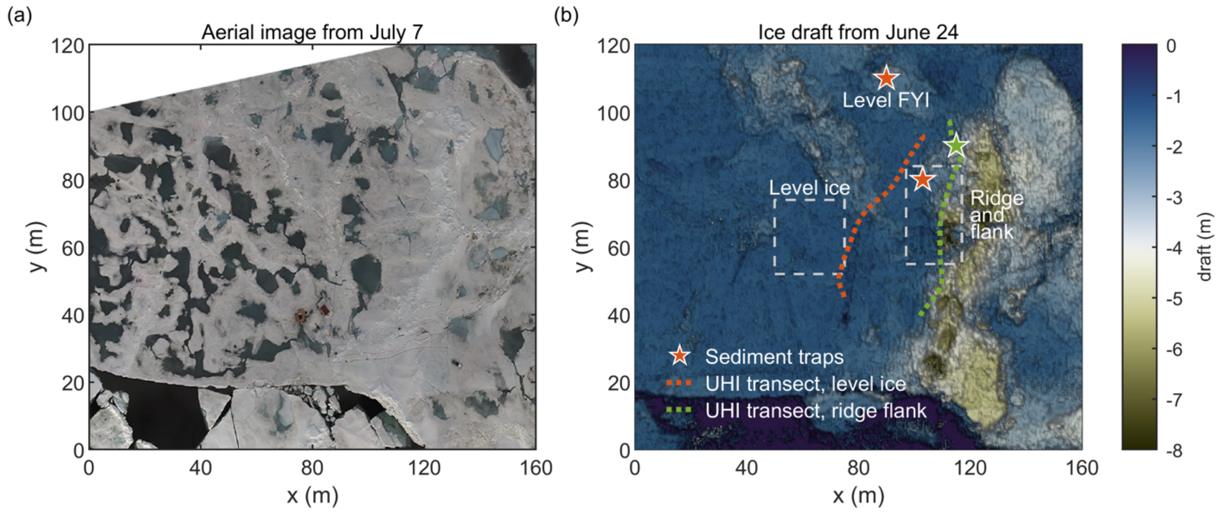

Figure 15. The Jaridge ridge sampling areas during summer 2020. A) Shows an aerial image of the study area with ponded level ice and the Jaridge ridge sampling site. Shading in B) indicates ice draft from the ROV multibeam sonar with keel depths of the pressure ridge exceeding 7 m, and red stars indicate locations of deployed sediment traps, and the blue star the location of underwater hyperspectral imager (UHI) data collection shown in Figure 16.

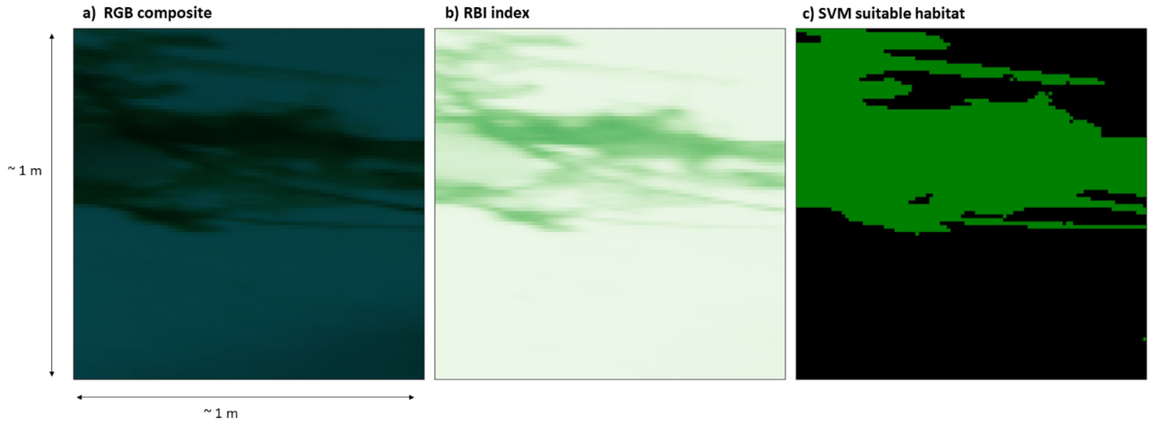

Figure 16. Determination of ice algal habitable space in pressure ridges and level sea ice using underwater hyperspectral image (UHI) information. A) An example of composite RGB (red, green, and blue) image of one area along the ridge flank transect (blue star in Figure 15b) compared to model results to estimate B) relative algal quantity estimated via the Relative ice algal Biomass Index (RBI), and C) inhabited area based on support vector machine (SVM) machine learning approaches of sea ice using the signature of the spectral light transmitted through the ridge (Lange et al., submitted).

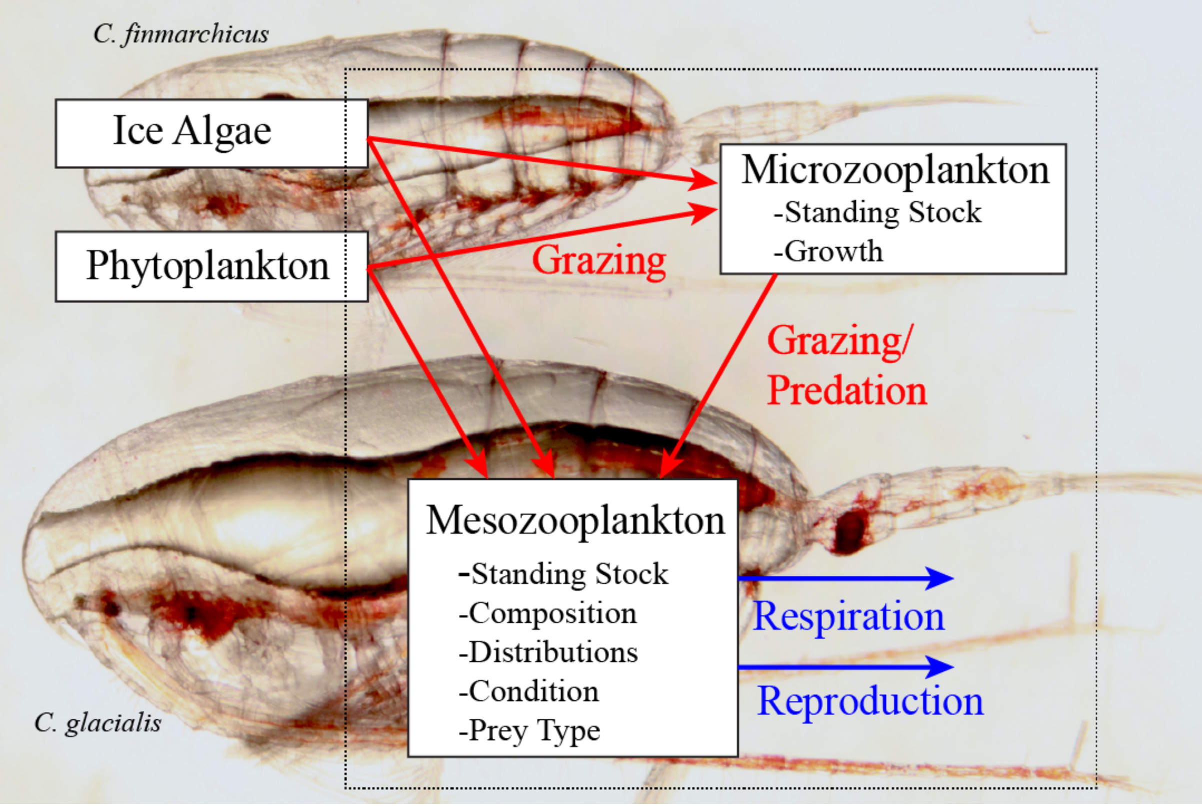

Figure 17. Transformations of energy, carbon and nitrogen by mesozooplankton in the upper water column and near the sea ice-ocean boundary. Arrows indicate transformation rates and component linkages that were quantified; red arrows show incorporation of carbon/nitrogen while blue arrows show export of carbon/nitrogen from the organisms. Characteristics of each ecosystem component that were measured indicated inside boxes.

Supplementary Information

Table S1. Project-specific contributions to the ECO work program. Information on Project Title, PI, involved institutions, funding agencies, and science foci.

Table S2. List of ECO sampling events based on rosette casts and optical particle profiling. Event Operation IDs, date and time, location and bottom depth for PS-CTD rosette, OC-CTD rosette and LISST casts as well as UVP profiles.

Table S3. Overview on sample processing and applied methods. Detailed overview of sampled parameters, applied methods, responsible PIs, coverage, and estimated number of samples. The table represents an extended version of Table 1 from the main document.

Table S4. Overview of quantitively analyzed zooplankton sampling events and collected samples. Samples were collected via LOKI (up to 20 frames sec-1), UVP, multinet (MN), ring nets (RN), Nansen net (NCN) and a net mounted on an ROV (ROVN), from Nov. 2019 to Oct. 2020. For each month, the number of samples is given; depth strata MN: 2000-1000-500-200-50-0 m; depth strata NCN: 1000-200 m & 200 - 0 m.

Table S5. List of ECO sampling events for zooplankton and fish sampling. Event Operation IDs, date and time, location (of *RV Polarstern*), and bottom depth for all zooplankton and fish sampling events for multinets (NM), Light-frame On-sight Key species Investigation system (LOKI), Ring nets, Nansen Nets, long lines, remotely operated vehicle nets (BEAST), finish rods and Gill nets.

Table S6. List of ECO sampling events for first and second year ice. Event Operation IDs, date and time, location and bottom depth for all common time-series ice coring activities at the first and second year ice (FYI and SYI) coring sites.

Table S7. List of ECO sampling events for event driven sampling and intense observation periods (IOPs). Event Operation IDs, date and time, location and bottom depth for event-driven sampling of direct under ice water, leads, melt ponds, new ice formation as well as high frequency IOP sampling.